Hidden symmetries and the structure of hyperbolic knot and link complements

by

Priyadip Mondal

Bachelor of Mathematics (Honours), Indian Statistical Institute, Bangalore Centre, 2013

Master of Mathematics, Indian Statistical Institute, Bangalore Centre, 2015

Submitted to the Graduate Faculty of

the Kenneth P. Dietrich School of Arts and Sciences in partial fulfillment

of the requirements for the degree of

Doctor of Philosophy

University of Pittsburgh

2021

UNIVERSITY OF PITTSBURGH

KENNETH P. DIETRICH SCHOOL OF ARTS AND SCIENCES

This dissertation was presented

by

Priyadip Mondal

It was defended on

July 26th 2021

and approved by

Jason DeBlois, Ph. D., Associate Professor, University of Pittsburgh

Eric Chesebro, Ph. D., Associate Professor, University of Montana

Thomas Hales, Ph. D., Andrew Mellon Professor, University of Pittsburgh

Kiumars Kaveh, Ph. D., Associate Professor, University of Pittsburgh

Hidden symmetries and the structure of hyperbolic knot and link complements

Priyadip Mondal, PhD

University of Pittsburgh, 2021

An isometry h between two finite degree covers of a hyperbolic 3-manifold M is called a hidden symmetry of M if h is not a lift of any self-isometry of M. In 1992, Neumann and Reid [23] asked whether there exists a hyperbolic knot other than the figure eight knot and the two dodecahedral knots of Aitchison and Rubinstein [1] whose complement has hidden symmetries. This thesis aims to study hidden symmetries through the lens of this question.

We study geometrically converging families of hyperbolic knots obtained by Dehn filling all but one cusp of a link complement and investigate the existence of hidden symmetries of the complements of such knots. We first concentrate on Dehn fillings of three 2-component hyperbolic links and use geometric isolation property for cusps of the links for our study. This portion is mostly based on joint work in [8].

We next discuss an effectivization result related to hidden symmetries for one such link and show some relations between the various number fields for these orbifolds. This portion is based on joint work in [7].

Finally, the thesis investigates hidden symmetries through analysis of certain horoball packings of hyperbolic three space $\mathbb{H}^3$ and related circle packings of $\mathbb{C}$. We show that the existence of hidden symmetries in infinitely geometrically converging knots obtained by Dehn filling all but one cusp of a hyperbolic link will necessitate the existence of certain order 3 symmetries of such circle packings. We implement this result into SnapPy/Python code which can rule out cases not having these kind of symmetries. We use this code to study some links (and in the process some potential non-links) in the tetrahedral census of Fominykh, Garoufalidis, Goerner, Tarkaev and Vesnin and show that except for a few cases, these symmetries do not exist, hence proving that for most of the cases we test, geometrically converging families of knots obtained from Dehn fillings all but one cusp can only contain finitely many elements with hidden symmetries.

Table of contents

List of figures

Preface

This thesis could not have been completed without the guidance of my advisor Jason DeBlois. I cannot express my gratitude in words for his countless help and immense amount of support during my time as a PhD student at Pitt. I am very fortunate to have him as my PhD advisor.

I am also grateful to my other committee members Eric Chesebro, Thomas Hales, and Kiumars Kaveh for their many helpful suggestions. Their comments have helped me improve the thesis to a great extent.

I would like to thank the University of Pittsburgh Center for Research Computing for their computational resources, which was used for some of the computations in the thesis. I would like to acknowledge partial support from University of Pittsburgh CRDF through my advisor. I also thank University of Pittsburgh for the support through Andrew Mellon Pre-doctoral Fellowship (2018-19).

Part of this thesis took shape during my visit to American Institute of Mathematics for attending the SQuaRE titled "Which hyperbolic knot complements have hidden symmetries?". I thank American Institute of Mathematics for hosting this SQuaRE. I would like to thank Neil Hoffman for communicating the idea on the horoball packing symmetries and Theorem 6.4 during this SQuaRE. I would also like to thank the other participants of this SQuaRE: Eric Chesebro, Michelle Chu, Jason DeBlois, and Genevieve Walsh. I learned a lot from my discussions with them at AIM as well as afterwards.

I also thank my other co-authors Christian Millichap and William Worden for many helpful conversations.

I express my sincere thanks to the fellow Math PhD students at Pitt for many helpful conversations. I would like to specifically mention Mark, Tyler, Anuradha, Arshia, Manu, Rahul, Thesath and Koundinya's names. I really enjoyed all the math and non-math discussions with them.

The support of my friends was very crucial during my PhD years. I would like to specifically thank Subhadip and Susnata. Thanks to them, life in USA have been very

pleasant and enjoyable.

Last and most importantly, none of these would have been a reality without the constant unwavering support of my parents and my brother. Their confidence in me has kept me motivated all the times. I will be forever grateful to them for all their sacrifices.

1.0 Introduction

The study of geometric structures have a powerful impact on the study of 3-manifolds. Indeed, Thurston's geometrization conjecture ([40]), proven by Gregory Perelman in 2002-2003 ([26], [27], [28]), lays out this intricate relation of geometry and three dimensional topology:

Geometrization Conjecture (Conjecture 1.1, [40]). *Given a compact 3-manifold M, the interior of M can be decomposed into pieces which admit one of the eight geometric structures.*

Each of these eight geometries is rich with its own flavor. This thesis is concerned with the *hyperbolic structure*. Hyperbolic structures on 3-manifolds are built upon the geometry of $\mathbb{H}^3$, the hyperbolic three space. $\mathbb{H}^3$ is the complete, simply connected Riemannian 3-manifold with constant sectional curvature -1 unique up to isometry. 3-manifolds with hyperbolic structures have local copies of $\mathbb{H}^3$ which have them inherit a Riemannian metric with constant sectional curvature -1 as well. We call a 3-manifold a *hyperbolic manifold* if it has a "complete" hyperbolic structure. Hyperbolic 3-manifolds can be realized as the quotient of $\mathbb{H}^3$ by the discrete torsion free subgroups of its isometry group.

The contemporary discipline of hyperbolic 3-manifolds has its roots in Thurston's discovery of the (hyperbolic) tetrahedral decomposition of the figure eight knot complement. This led to the study of hyperbolic knot and link complements (i.e. the knot and link complements which are finite volume (oriented) hyperbolic 3-manifolds). These are often loaded with powerful geometric data obtained from their (geometric) triangulation. These triangulations also allows one to conclude strong results on the hyperbolic knot and link complements based on the behavior of their *cusps*. A cusp of a hyperbolic link complement can be thought of as a neighborhood surrounding a component of the link itself.

This thesis centers around hidden symmetries in hyperbolic 3-manifolds. Hidden symmetries of a hyperbolic 3-manifold M are the symmetries between its finite degree covers which are not lifts of a self-symmetry of M. We are interested in the hidden symmetries of hyperbolic knot complements. It follows from the work of Boileau, Boyer, Cebanu and

Walsh (see [3, Theorem 1.4]) that the study of of hidden symmetries has a very important role to play in the study of the commensurability classes of hyperbolic knot complements. Margulis's arithmeticity theorem (see [19, Theorem 10.3.5], refer to [41] for a proof) implies that a hyperbolic 3-manifold can have infinitely many hidden symmetries if and only if it is an *arithmetic manifold*. On the other hand, Reid [32, Theorem 2] showed that the figure eight knot is the only hyperbolic knot whose complement is arithmetic. An example of how one can construct a hidden symmetry of the figure eight knot complement can be found in Example 3.2 in this thesis. Among the rest of the (non-arithmetic) knots, Neumann and Reid [23] argued that the two dodecahedral knots constructed by Aitchison and Rubinstein [1] have hidden symmetries. No other example of a hyperbolic knot with hidden symmetries have been reported as of yet. The following question of Neumann and Reid (Question 1 in §9 of [23]) from 1992, which conveys this amazing phenomenon, steers the prevailing research on hidden symmetries of hyperbolic knot complements:

Question 3.8 [Question 1, [23]]. *Is there any hyperbolic knot except the figure eight knot and the two dodecahedral knots of Aitchison and Rubinstein [1] whose complement has hidden symmetries?*

In [23], Neumann and Reid also gave a characterization of hyperbolic knot complements with hidden symmetries (Theorem 3.3): A hyperbolic knot complement has hidden symmetries if and only if it non-regularly covers a rigid cusped hyperbolic orbifold. Hyperbolic orbifolds are generalizations of hyperbolic manifolds to spaces with cone points. These cone points come from the fixed points of symmetries that are acting on the hyperbolic three space. The rigidity part in the characterization implies that a hyperbolic knot complement having hidden symmetries must have $\mathbb{Q}(i)$ or $\mathbb{Q}(i\sqrt{3})$ as cusp fields. Cusp field along with (invariant) trace field are number fields associated with a hyperbolic link complement that encodes geometric information about the link complement. Most of the work on hidden symmetries in the literature uses this fact about cusp fields and applying various algebraic methods one shows how different hyperbolic knot complements can not have hidden symmetries.

In this thesis, we investigate a weaker version of Question 3.8. We aim to understand the following question:

Question 4.1 [Conjecture 0.1, [8]]. *Can there exist infinitely many hyperbolic knot complements admitting hidden symmetries all of whose volumes are bounded above by a constant?*

Thanks to Thurston's Dehn surgery theorem, one way of producing infinitely many hyperbolic knots is by Dehn filling all but one component of a given hyperbolic link L. It also follows from Thurston's work that the volumes of these knot complements obtained from Dehn filling are less than the volume of the complement of L. We leverage this fact and study families of knots that *geometrically converge* to a given link L. Such convergence allows us to pass various properties of the knots in the family to the link itself.

In Chapter 2 and 3, we discuss background material and we define the terminology above and illustrate them with examples.

In Chapter 4, most of our discussion is based on the joint work [8] with Eric Chesebro and Jason DeBlois. We study geometrically convergent families of hyperbolic knots obtained from Dehn filling through the lens of deformation variety. In case of a 2-component hyperbolic link L, an infinite family of hyperbolic knots obtained from Dehn filling a fixed component of L always geometrically converge to the complement of L. Corollary 1.8 of [8], which is stated without proof in Theorem 4.6 of this thesis, addresses how existence of hidden symmetries in the elements of such families can be connected to a geometric isolation condition on the components of L. Geometric isolation, a concept defined by Neumann and Reid [24], means that the geometric shape of the non-filled cusp is invariant under Dehn fillings on the other cusp.

Given a hyperbolic link complement and an associated geometric triangulation, one can define an algebraic set (i.e. the zero set of some complex polynomials) called *deformation variety* such the link itself and the hyperbolic knots obtained from Dehn fillings of the components of the link can be thought of as points of this variety. We refer to the point representing the link as the *complete structure*.

Proposition 1.6 from [8] which we state without proof in Proposition 4.5 of this thesis, says that one can define a rational function on the deformation variety whose values record these geometric shapes of cusps of a geometrically triangulated hyperbolic 3-manifold. These rational functions are referred as *cusp parameter functions*. It follows that geometric isolation is equivalent to the cusp parameter functions being locally constant on specific sub-varieties of

the deformation variety near the complete structure. Based on this observation, we show non-geometric isolation for the cusps of 6_2^2 by studying derivatives of cusp parameter functions via implicit function theorem. Theorem 4.6 then gives us to the following theorem:

Theorem 4.11 [Corollary 3.4, [8]]. *A family of hyperbolic knots obtained by Dehn filling a fixed cusp of 6_2^2 can have at most finitely many elements with hidden symmetries.*

The proof of the above result that we present in the thesis is original and different from the one given in the joint work [8].

In section 4.5 (which is taken (almost) verbatim from Example 5.3 of [8]), we focus on the Berge manifold. The Berge manifold is a hyperbolic 3-manifold isometric to the complement of a 2-component hyperbolic link. We show the following using a similar calculus based method as in the case of 6_2^2:

Theorem 4.13 [Example 5.3, [8]]. *Cusps of the Berge manifold are not isolated from each other.*

Section 4.6, the last section of Chapter 4, is new and not part of [8]. In this section, we discuss non-geometric isolation of one of the cusps c from the other cusp c' for the 2-component link $L10n46$. This particular example shows that computing cusp parameter function for this link using Proposition 4.5 is not always as straightforward as in the cases of 6_2^2 and the Berge manifold. We prove the following:

Theorem 4.14. *In the 2-component link $L10n46$, cusp c is not geometrically isolated from cusp c'.*

Our discussion in Chapter 5 is based on contents from joint work [7] with Eric Chesebro, Jason DeBlois, Neil R Hoffman, Christian Millichap and William Worden. We begin by stating Theorem 2.6 from [7] (in Theorem 5.1) which loosely extends Theorem 4.6 for a link with three or more components. The geometric isolation part of Theorem 4.6 can not be extended for hyperbolic links with more than two components. But, it can be shown that the orbifold covering that the Neumann and Reid characterization (see Theorem 3.3) entails to can be passed to an orbifold covering of the link. To be more precise, Theorem 5.1 shows that if we have a family $\mathcal{F}$ of hyperbolic knots obtained from Dehn filling all component but K of a hyperbolic link L which geometrically converge to L such that each element of

$\mathcal{F}$ covers a rigid cusped orbifold, then the complement of L covers an orbifold O which has exactly one rigid cusp which is covered by (only) the cusp corresponding to component K of L.

One might wonder exactly how many of the hyperbolic knots that are obtained from Dehn filling a single cusp of a 2-component hyperbolic link can have hidden symmetries. In Section 5.2 of Chapter 5, we also give some insight to this question on effetivization. In particular, one cay say the following:

Theorem 5.6 [Theorem 1.6, [7]]. *If an orbifold O obtained by Dehn filling a single cusp of 6_2^2 is covered by a hyperbolic knot complement with hidden symmetries, then the Dehn filling coefficient for O is $(2, 0)$.*

We don't present a complete proof of the above result in the thesis. We rather lay out an argument using results that we state from [7] without proof.

In section 5.3, we further study the fillings of one cusp of 6_2^2. We explain how the cusp parameter function helps us understand the relation between the associated number fields of the orbifolds obtained from Dehn filling a cusp of 6_2^2. We prove the following:

Theorem 5.8 [Proposition 6.16, [7]]. *For an orbifold O obtained by Dehn filling a single cusp of 6_2^2, the invariant trace field and trace field are equal.*

The contents of Chapter 6, 7 and 8 are new and original.

In Chapter 6, we show that the orbifold covering criteria from Theorem 5.1 has some strong implications about the horoball packings associated with the link. One can think of the horoballs as portions of the hyperbolic three space that correspond to the cusp ends of a hyperbolic manifold. Given a hyperbolic link, we can talk about different packings of the hyperbolic three space by these horoballs. A hyperbolic link L covering an orbifold in the fashion mentioned in the paragraph above would imply that the horoball packing of hyperbolic three space associated with cusp corresponding to component K of L has order 3 or 6 rotational symmetries. In fact, we have an wallpaper group of symmetries acting on these horoballs. We restrict our attention to the *full sized horoballs*, the ones which have the biggest Euclidean volume. We describe our results in terms of the circle packing of $\mathbb{C}$ obtained from the boundaries of these full sized horoballs corresponding to the cusp

associated with component K. Our next result is the following.

Theorem 6.5. *Given a hyperbolic link L with more than one component and a cusp c of L, if infinitely many elements of a family of geometrically converging hyperbolic knots obtained from Dehn filling all cusps of L but c have hidden symmetries, then the symmetry group of the c-circle packing of $\mathbb{C}$ contains a $(3,3,3)$ wallpaper group W such that the co-area of the translational subgroup of W is*

$$\frac{\textit{cusp area of cusp } c}{4n}$$

for some natural number n. Moreover, no element of W fixes the center of a horoball corresponding to a cusp of L other than c.

Using this area condition and the structure of the $(3,3,3)$ wallpaper group for a given horoball corresponding to component K, we can guarantee the existence of an order 3 symmetry whose center is within a distance of the horoball that is less than a constant solely determined by the associated cusp of the link. This can be turned into an algorithm to find (fixed points of) such order 3 symmetries, if any. We implement this algorithm in SnapPy [9].

In Chapter 7, we apply this SnapPy code for the *tetrahedral links*. A *tetrahedral manifold* is a finite volume hyperbolic 3-manifold whose complement can be triangulated into regular ideal hyperbolic tetrahedra. Such triangulations of the tetrahedral links determines that their cusp fields are $\mathbb{Q}(i\sqrt{3})$ via two results of Neumann and Reid. A result that we state in Chapter 4 then makes the tetrahedral links natural candidates for investigation regarding the existence of hidden symmetries in geometrically convergent families of hyperbolic knots coming from their Dehn fillings. Fominykh et al. in [11] gave a census of tetrahedral manifolds. Their census consists of the orientable tetrahedral manifolds made up of 25 or fewer tetrahedra and non-orientable tetrahedral manifolds made up of 21 or fewer tetrahedra. Since we are interested in oriented hyperbolic manifolds, we will consider their orientable census.

Identifying which of these (orientable) tetrahedral manifolds are actually links is difficult and so we will work with a larger collection of tetrahedral manifolds which are *link complements in integral homology spheres*. Using Proposition 7.1 we write a short SnapPy

code which can find out when a tetrahedral manifold is a link complement in an integral homology sphere and denote the list of such link complements with 24 or fewer (regular ideal) tetrahedra as "K". We test for the existence of order 3 rotational symmetries using the SnapPy code for the first 162 elements of "K" (which in Python notation is "K[0:162]"). If two cusps of a manifold can be exchanged by an isometry of the manifold, we only test the code for one of those cusps. We get a list $Excep_{0,161}$ consisting of pairs (M, i) where M is one of such 162 manifolds and i a cusp of M for which our SnapPy code crashes or the i-circle packing has an order 3 rotational symmetry that our code searches for. Members of $Excep_{0,161}$ are listed in the appendix A. This gives us the following theorem:

Theorem 7.3. *Let L be tetrahedral link in "K[0:162]" and K_0 a component of L. If $(\mathbb{S}^3 - L, c)$ does not belong to $Excep_{0,161}$ for any cusp c of L which is symmetric to the cusp corresponding to K_0, then a family of geometrically convergent hyperbolic knots obtained from Dehn filling all components of L but K_0 can have at most finitely many elements with hidden symmetries.*

Fominykh et al [11] also gives a list of 25 tetrahedral links with more than one component. Using Theorem 7.3 and applying Theorem 6.5 to some additional circle packings corresponding to some of these 25 links we get the following theorem:

Theorem 7.4. *If L is one of 25 tetrahedral links with more than one component that are listed in Fominykh et. al [11], then for any cusp c of L, a family of geometrically convergent hyperbolic knots obtained by Dehn filling all cusps of L but c cannot have infinitely many members with hidden symmetries.*

In Chapter 8, we show that some of the elements of this $Excep_{0,161}$ are actually tetrahedral links. For example, the tetrahedral link $L14n63694$ (which decomposes into 20 regular ideal tetrahedra) belongs to $Excep_{0,161}$. We need different machineries to deal with the tetrahedral links that belongs to $Excep_{0,161}$.

We now summarize the organization of the thesis. We discuss background materials on hyperbolic geometry in Chapter 2 and hidden symmetries in Chapter 3. Chapter 4 contains results regarding geometric isolation and hidden symmetries (mostly) based on joint work with Eric Chesebro and Jason DeBlois [8] and Chapter 5 contains results from joint work with Eric Chesebro, Jason DeBlois, Neil R Hoffman, Christian Millichap and William Worden [7]

discussing the results on the effectivization for 6_2^2, the relation between the trace and cusp fields of the Dehn fillings on a cusp of 6_2^2, and the orbifold covering criteria. We discuss results on horoball packings and hidden symmetries (and the SnapPy code) in Chapter 6. Chapter 7 describes the implementation of the SnapPy code for the elements of the tetrahedral census which are link complements in the integral homology spheres and its output. In Chapter 8, we discuss some examples from the list of exceptional links that we get from our computation and describe the symmetries of associated horoball packings. Contents of Chapter 6, 7 and 8 are from an article in preparation.

2.0 Hyperbolic geometry: the basics

In this chapter, we discuss basics of hyperbolic geometry. Most of the material in this section can be found in introductory textbooks on hyperbolic geometry. For a general reading on introductory topics in hyperbolic geometry, we refer the readers to [39, 30, 2]. In each section, we refer to the sources where detailed discussion on the corresponding topics can be found.

2.1 Geometric structure

We define the notion of a geometric structure following the discussion in Section I.1.1 of [6], which itself goes back to Thurston [39, Chapter 3].

Let X be a real analytic manifold. Let G be a Lie group which acts analytically and faithfully on X. Let M be a topological manifold which has the same dimension as X. We say that M has a (X, G) *structure* if

- M has an (X, G) atlas $\{(U_\alpha, \phi_\alpha)\}_{\alpha \in I}$, i.e., for each $\alpha \in I$, U_α is an open set of M and ϕ_α is a homeomorphism from U_α onto $\phi_\alpha(U_\alpha)$, an open subset of X such that $M = \bigcup_{\alpha \in I} U_\alpha$, and
- for each pair $(\alpha, \beta) \in I \times I$, there exists $g \in G$ such that $\phi_\alpha \phi_\beta^{-1} = g$ on $\phi_\beta(U_\alpha \cap U_\beta)$.

2.1.1 Euclidean structure

An $(\mathbb{R}^n, \mathrm{Isom}(\mathbb{R}^n))$ structure on a smooth manifold of dimension n is called a *Euclidean structure* where $\mathrm{Isom}(\mathbb{R}^n)$ is the group of Euclidean isometries of $\mathbb{R}^n$.

2.1.2 Similarity structure

An $(\mathbb{R}^n, Sim(\mathbb{R}^n))$ structure on a smooth manifold of dimension n is called a *similarity structure* where $Sim(\mathbb{R}^n)$ is the group of similarities of $\mathbb{R}^n$. (A homeomorphism g of $\mathbb{R}^n$ is

said to be a *similarity* of $\mathbb{R}^n$ if $\|g(x)-g(y)\| = s\|x-y\|$ for all $x, y \in \mathbb{R}^n$ where s is a positive constant).

If we identify $\mathbb{R}^2$ with $\mathbb{C}$, then for each $g \in Sim(\mathbb{R}^2)$ there exists $s \in \mathbb{C} - \{0\}$ and $t \in \mathbb{C}$ such that $g(\mathbf{z}) = s\mathbf{z} + t$ for all $\mathbf{z} \in \mathbb{C}$.

2.1.3 Hyperbolic structure

An $(\mathbb{H}^n, \text{Isom}(\mathbb{H}^n))$ structure on an n-dimensional manifold is referred to as a *hyperbolic struture* where $\mathbb{H}^n$ is a Riemannian manifold with *hyperbolic metric* and $\text{Isom}(\mathbb{H}^n)$ is the group of hyperbolic isometries of $\mathbb{H}^n$. In fact, $\mathbb{H}^n$ is the complete simply connected Riemannian manifold of dimension n with constant sectional curvature -1 unique up to isometry. We will focus on hyperbolic structures on 3-manifolds.

Remark 2.1. *A hyperbolic structure on an n-dimensional manifold M induces a Riemannian metric on M which is locally isometric to $\mathbb{H}^n$ but not necessarily complete.*

2.1.4 Isomorphism of geometric structures

Let M_1 and M_2 are two manifolds with (X, G) structures. Let us denote the (X, G) atlas of M_1 by $\{(U_\alpha, \phi_\alpha)\}_{\alpha \in I}$ and of M_2 by $\{(V_\beta, \psi_\beta)\}_{\beta \in J}$. A homeomorphism $f : M_1 \to M_2$ is called an (X, G)-*isomorphism* if $\psi_\beta \circ f \circ \phi_\alpha^{-1}$ and $\phi_\alpha \circ f \circ \psi_\beta^{-1}$ are restrictions of elements of G whenever the maps are defined where $\alpha \in I, \beta \in J$.

2.2 Hyperbolic three space $\mathbb{H}^3$

Hyperbolic three space, denoted as $\mathbb{H}^3$, is the complete, simply connected Riemannian 3-manifold with constant sectional curvature -1. We represent $\mathbb{H}^3$ by four different models: upper half-space model, Poincare Disk model, Klein model and hyperboloid model. We will be using the upper-half space model throughout this thesis. Hence, we discuss this model below.

2.2.1 Upper-half space model

In this model,

$$\mathbb{H}^3 = \{(x, y, z) : (x, y) \in \mathbb{C}, z \in \mathbb{R}_{>0}\} \text{ and } ds^2 = \frac{dx^2 + dy^2 + dz^2}{z^2}. \tag{1}$$

The geodesics of $\mathbb{H}^3$ in the upper half-space model are the vertical lines and semicircular arcs intersecting the complex plane orthogonally. The complex plane along with ∞ is referred as the *sphere at infinity* and is denoted as $\partial_\infty \mathbb{H}^3$.

2.2.2 $\mathbf{Isom}^+(\mathbb{H}^3)$

The group of orientation preserving isometries of $\mathbb{H}^3$ can be identified with $\mathrm{PSL}(2, \mathbb{C}) = \mathrm{SL}(2, \mathbb{C})/\{\pm I\}$. The elements of $\mathrm{PSL}(2, \mathbb{C})$ act as Möbius transformation on $\partial_\infty \mathbb{H}^3$. A formula for the action of the elements of $\mathrm{PSL}(2, \mathbb{C})$ on $\mathbb{H}^3$ can be found in Peter Scott's paper [38, Section 4, p. 448]. We describe this formula here: First one needs to identify an element (x, y, z) of $\mathbb{H}^3$ as the quaternion $x + yi + zj$ and the complex numbers with quaternions of the form $u + vi$. Then for $A = \begin{pmatrix} a & b \\ c & d \end{pmatrix} \in \mathrm{PSL}(2, \mathbb{C})$, the action of A on $\mathbb{H}^3$ can be described as:

$$A(x + yi + zj) = (a(x + yi + zj) + b)\,(c(x + yi + zj) + d)^{-1}. \tag{2}$$

$\mathrm{SL}(2, \mathbb{C})$ inherits a subspace topology as the subspace of the set of 2×2 complex matrices $M(2, \mathbb{C})$ which can be identified with $\mathbb{C}^4$. The topology on $\mathrm{PSL}(2, \mathbb{C})$ is the quotient topology induced from the topology of $\mathrm{SL}(2, \mathbb{C})$.

Given a non-identity element A of $\mathrm{PSL}(2, \mathbb{C})$, either

1. A is elliptic, i.e., A is conjugate to $\begin{pmatrix} e^{i\theta} & 0 \\ 0 & e^{-i\theta} \end{pmatrix}$ for $\theta \in (0, \pi)$, and fixed points of A in $\mathbb{H}^3$ lie in a geodesic γ_A and so A also fixes the end points of γ_A in $\partial_\infty \mathbb{H}^3$, or,
2. A is parabolic, i.e., A is conjugate to $\begin{pmatrix} \pm 1 & c \\ 0 & \pm 1 \end{pmatrix}$ where $c \neq 0$, and has no fixed point in $\mathbb{H}^3$ and exactly one fixed point in $\partial_\infty \mathbb{H}^3$, or,

3. A is hyperbolic, i.e., A is conjugate to $\begin{pmatrix} e^{r+i\theta} & 0 \\ 0 & e^{-r-i\theta} \end{pmatrix}$ where $r \neq 0$, and has exactly two fixed points on $\partial_\infty \mathbb{H}^3$ and A acts as a translation on $\mathbb{H}^3$ along the geodesic joining these two fixed points.

2.3 Hyperbolic manifold and orbifolds

A discrete subgroup of $\mathrm{PSL}(2,\mathbb{C})$ is called a *Kleinian group*. A smooth 3-manifold M is called a *hyperbolic* 3*-manifold* if M is diffeomorphic to $\mathbb{H}^3/\Gamma$ for a torsion free Kleinian group Γ. (This is actually the definition of an *orientable hyperbolic* 3*-manifold*. For the general definition, one would take Γ to be a discrete torsion free subgroup of $\mathrm{Isom}(\mathbb{H}^3)$. Unless otherwise specified, by a hyperbolic 3-manifold we would mean an orientable hyperbolic 3-manifold.) Since $\mathrm{PSL}(2,\mathbb{C})$ acts on $\mathbb{H}^3$ isometrically with respect to the hyperbolic metric, M inherits a Riemannian metric which makes it locally isometric to $\mathbb{H}^3$. Note that, one can identify the fundamental group $\pi_1(M)$ of M with Γ.

Example 2.2. *Let* $\tilde{\Gamma} = \left\langle \begin{pmatrix} 1 & 1 \\ 0 & 1 \end{pmatrix}, \begin{pmatrix} 1 & 0 \\ \frac{1+\sqrt{3}i}{2} & 1 \end{pmatrix} \right\rangle \leq \mathrm{SL}(2,\mathbb{C})$.
If we take Γ *to be the image of* $\tilde{\Gamma}$ *in* $\mathrm{PSL}(2,\mathbb{C})$*, then* Γ *is an example of a torsion free Kleinain group. It was proved by Riley in 1975 in [34]. So, the quotient* $\mathbb{H}^3/\Gamma$ *is hyperbolic* 3*-manifold.*

For two hyperbolic 3-manifolds $M_1 = \mathbb{H}^3/\Gamma_1$ and $M_2 = \mathbb{H}^3/\Gamma_2$, a map g from M_1 to M_2 is called an *isometry* between M_1 and M_2 if it is a Riemannian isometry between the hyperbolic metrics induced on M_1 and M_2 from $\mathbb{H}^3$.

Remark 2.3. *It is easy to see that an isometry between* M_1 *and* M_2 *lifts to an element* g *of* $\mathrm{Isom}^+(\mathbb{H}^3) = \mathrm{PSL}(2,\mathbb{C})$ *such that for each* $\gamma_1 \in \Gamma_1$ *and* $x \in \mathbb{H}^3$*, there exists* $\gamma_2 \in \Gamma_2$ *such that* $g(\gamma_1(x)) = \gamma_2(g(x))$*. Conversely, any such* g *induces an isometry between* M_1 *and* M_2*.*

Remark 2.4. *Note that a hyperbolic* 3*-manifold admits an* $(\mathbb{H}^3, \mathrm{Isom}^+(\mathbb{H}^3))$ *structure which is complete, i.e., the Riemannian metric that it inherits from* $\mathbb{H}^3$ *is complete. Later in Section*

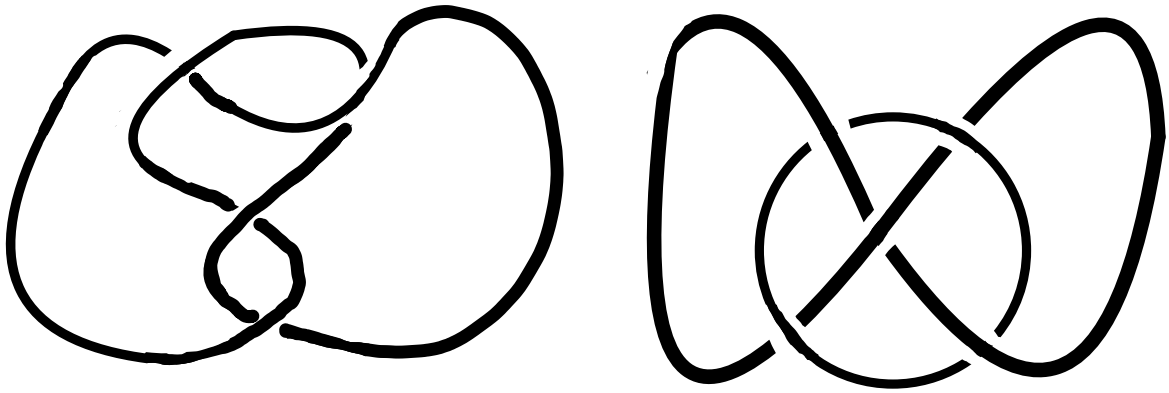

Figure 1: Hyperbolic links - Left: Figure eight knot, Right: Whitehead link

2.7, we will discuss about incomplete structures as well.

An n-component link in $\mathbb{S}^3$ is called a *hyperbolic link* if $\mathbb{S}^3 - L$ is diffeomorphic to a finite volume hyperbolic manifold. When $n = 1$, we say that it is a hyperbolic knot. Figure 1 shows examples of links which are hyperbolic whereas Figure 2 shows some links which are not hyperbolic. The hyperbolic 3-manifold from Example 2.2 is isometric to the figure eight knot complement (see [34, Corollary on p. 284]) .

We can extend the notion of hyperbolic 3-manifolds to *hyperbolic* 3*-orbifolds*: A topological space O is called a hyperbolic 3-orbifold if it is homeomorphic to $\mathbb{H}^3/\Gamma$ where Γ is a Kleinian group (may contain torsion elements). This Γ is referred to as the *orbifold fundamental group* of O and we denote Γ as $\pi_1^{Orb}(O)$.

Remark 2.5. *There is a general definition of orbifolds, morphisms between orbifolds, and (G, X)-orbifolds. We refer the reader to [39, Chapter 13] for the definitions.*

We say a hyperbolic orbifold $O = \mathbb{H}^3/\Gamma$ has *finite volume* (or Γ has *finite co-volume*) if the fundamental domains of Γ in $\mathbb{H}^3$ have finite volume in the hyperbolic metric.

Example 2.6. *We give an example based on [31, Example on p. 349]. We will discuss this*

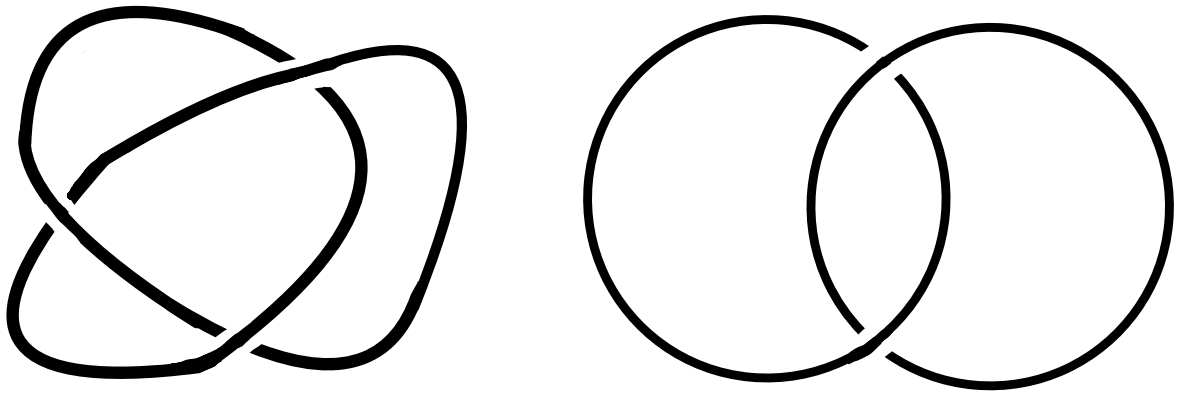

Figure 2: Non-hyperbolic links - Left: Trefoil knot, Right: Hopf link

example again in Example 2.27 in connection with trace fields. Let

$$\tilde{\Gamma}' = \left\langle \begin{pmatrix} 1 & 1 \\ 0 & 1 \end{pmatrix}, \begin{pmatrix} 1 & 0 \\ \frac{1+\sqrt{3}i}{2} & 1 \end{pmatrix}, \begin{pmatrix} i & 0 \\ 0 & -i \end{pmatrix} \right\rangle$$

and Γ' *be the image of* $\tilde{\Gamma}'$ *in* $\mathrm{PSL}(2,\mathbb{C})$. *Note* $\begin{pmatrix} i & 0 \\ 0 & -i \end{pmatrix}$ *has order 2 as an element of* $\mathrm{PSL}(2,\mathbb{C})$ *and normalizes* Γ *from Example 2.2. So,* Γ' *has torsion elements, and* $[\Gamma' : \Gamma] = 2$. *So,* $\mathbb{H}^3/\Gamma'$ *is an orbifold whose two fold cover is the figure eight knot complement.*

2.3.1 Mostow-Prasad rigidity

We now state Mostow-Prasad rigidity theorem which is one of the very important results in the study of hyperbolic manifolds. Here we state a version of the theorem from [19] (the general result is true for all dimension greater than or equal to 3).

Mostow-Prasad rigidity theorem [Theorem 1.6.3, [19]]. *If* Γ_1 *and* Γ_2 *are two isomorphic finite co-volume Kleinian groups, then there is some* g *in* $\mathrm{PSL}(2,\mathbb{C})$ *such that* $\Gamma_2 = g\Gamma_2 g^{-1}$ *and so, two isomorphic finite volume hyperbolic* 3*-orbifolds (see Remark 2.5) are also isometric.*

2.4 Horoballs

A *horoball centered at* ∞ is the region above a horizontal plane in $\mathbb{H}^3$ (the plane is also included in the horoball). For a point $z \in \mathbb{C}$, if B is a Euclidean ball in $\mathbb{H}^3 \cup (\mathbb{C} \times \{0\})$ tangent to the complex plane at z, then we say $B - \{z\}$ is a *horoball centered at* z. The boundary of a horoball B is called the *horosphere* of B and is denoted as ∂B.

Facts 2.7. *i) Let B_∞ and B'_∞ be two horoballs centered at ∞, then there is a hyperbolic element g of the form $\begin{pmatrix} \lambda & 0 \\ 0 & \lambda^{-1} \end{pmatrix}$ in $\mathrm{PSL}(2,\mathbb{C})$ fixing ∞ such that $g(B'_\infty) = B_\infty$.*

Proof. If ∂B_∞ is at height 1 and $\partial B'_\infty$ is at height t, then, $\lambda = \sqrt{t}$ gives such a g. We can use this to construct g for all other cases. □

ii) For horoballs B_∞ and B_z centered at ∞ and z respectively, there is $g \in \mathrm{PSL}(2,\mathbb{C})$ such that $g(B_z) = g(B_\infty)$.

Proof. If $z = 0$, then $g = \begin{pmatrix} 1 & 1 \\ 1 & 0 \end{pmatrix}$ sends 0 to ∞ and so a horoball centered at 0 to a horoball centered at ∞. If $z \neq 0$, then, $g = \begin{pmatrix} z^{-1} & 0 \\ -1 & z \end{pmatrix}$ sends z to ∞ and a horoball centered at z to a horoball centered at ∞. Now, the fact above concludes this fact. □

iii) If $z \in \partial_\infty \mathbb{H}^3$, then, the geodesics through z intersects the horospheres of all the horoballs centered at z orthogonally.

Proof. When z is ∞, it is quite straightforward since the geodesics through ∞ are the vertical lines and the horospheres of the horoballs centered at ∞ are the horizontal planes. Now, an isometry of $\mathbb{H}^3$ sends geodesics to geodesics, the general case follows from the fact above. □

iv) Given a horoball B_z centered at z for some z in $\partial_\infty \mathbb{H}^3$, the restriction of the hyperbolic metric on ∂B_z is actually a Euclidean metric and if for a Kleinian group Γ, $\mathrm{Stab}_\Gamma(z)$ contains a parabolic element, then $\mathrm{Stab}_\Gamma(z)$ acts as Euclidean isometries on ∂B_z.

Proof. We first prove the fact for horoball B_∞ centered at ∞. We note that $\mathrm{Stab}_\Gamma(\infty)$ does not contain any hyperbolic element (see [2, Lemma D.3.6]) and so using the Formula 2 and the description of matrices in 1 and 2, one can check that $\mathrm{Stab}_\Gamma(\infty)$ sends ∂B_∞ to itself. Now, ∂B_∞ is a horizontal plane at some height $t > 0$. From the formula of hyperbolic metric in Equation 1, we see that when the height is constant, the metric becomes a scalar multiple of the standard Euclidean metric, hence, making its restriction on ∂B_∞ a Euclidean metric, which also shows that $\mathrm{Stab}_\Gamma(\infty)$ acts as Euclidean isometries on ∂B_∞ since the elements of $\mathrm{Stab}_\Gamma(\infty)$ are isometries of $\mathbb{H}^3$.

If z is not infinity, we note that there exists $g \in \mathrm{PSL}(2,\mathbb{C})$ sending z to ∞. Now, $g\Gamma g^{-1}$ is also a Kleinian group, $\mathrm{Stab}_{g\Gamma g^{-1}}(\infty) = g\,\mathrm{Stab}_\Gamma(\infty)g^{-1}$ and the conjugate of a parabolic element is a parabolic element as well. It then follows from the $z = \infty$ case. □

2.5 Cusp neighborhood, peripheral subgroup and cusp types

In this section, we will define the cusp ends of a hyperbolic 3-orbifold. Before we begin the definition, we recall from Section 2.1.3 that $\mathbb{H}^n$ is (up to isometry) the unique complete, simply connected Riemannian manifold which has constant sectional curvature equal to -1. The following groundbreaking result of Margulis, which first appeared publicly in Gromov's paper [12], has had a very strong impact on the study of hyperbolic manifolds.

Margulis Lemma (Theorem D.1.1, [2])**.** *There exist $\epsilon > 0$ such that for every discrete subgroup Γ of $\mathrm{Isom}(\mathbb{H}^n)$ and $x \in \mathbb{H}^n$, the group $\Gamma_{x,\epsilon} = \{\gamma \in \Gamma : d_{\mathbb{H}^n}(x, \gamma(x)) < \epsilon\}$ has a finite index subgroup which is nilpotent.*

The supremum of all such ϵ is referred as the *Margulis constant*. In the rest of the section, ϵ is taken to be smaller than the Margulis constant.

Now, let, $O = \mathbb{H}^3/\Gamma$ be a finite volume hyperbolic 3-orbifold. For a given ϵ, the ϵ-thin part of O, denoted as $\mathrm{thin}_\epsilon(O)$, is defined as

$$\{x \in O : x \text{ has distinct pre-images } \tilde{x_1}, \tilde{x_2} \in \mathbb{H}^3 \text{ with } d_{\mathbb{H}^3}(\tilde{x_1}, \tilde{x_2}) \leq \epsilon\}.$$

Cusp neighborhoods of O are one particular type of components of these ϵ-thin parts of O. To proceed further, we need to know the following definition: for $r > 0$ and a geodesic g in $\mathbb{H}^3$, we define $B_r(g)$ as the set $\{x : d_{\mathbb{H}^3}(x, g) \leq r\}$. Using Margulis's lemma, Thurston proved [39, Corollary 5.10.2] that each component of the ϵ-thin part of hyperbolic manifolds are quotients of horoballs and these $B_r(g)$'s. Dunbar and Meyerhoff [10] gave a proof of a more general orbifold version of Thurston's result. We state the Dunbar and Meyerhoff's orbifold version of the result below:

Theorem 2.8 (Dunbar-Meyerhoff, Corollary 2.2, [10])**.** *For any ϵ less than the Margulis constant, each component of* $\text{thin}_\epsilon(O)$ *is either a solid tube, i.e., quotient of $B_r(g)$ by orientation preserving co-compact subgroup of isometries of Γ for some $r > 0$ and geodesic g, or a cusp neighborhood.*

We define a cusp neighborhood of O to be the quotient of the horoball B_z centered some z in $\partial_\infty \mathbb{H}^3$ by a (wallpaper) subgroup W of Γ, the stabilizer of z in Γ, such that the projection of B_z to O factors through an embedding of B_z/W.

Recall from the fourth point in Fact 2.7 that W acts on ∂B_z by Euclidean isometries. We will now review the definition of wallpaper groups (see [37] for details). The set of translational isometries of $\mathbb{R}^2$, V, is two dimensional vector space over $\mathbb{R}$. Let $t_{(a,b)}$ denote the translation on $\mathbb{R}^2$ which maps $\begin{pmatrix} x \\ y \end{pmatrix}$ to $\begin{pmatrix} x+a \\ y+b \end{pmatrix}$ for $\begin{pmatrix} x \\ y \end{pmatrix} \in \mathbb{R}^2$.

A group G of Euclidean isometries of $\mathbb{R}^2$ is said to be a *wallpaper group* if the set of translational isometries in G is generated by a basis for V and

$$\left\{ r \in O_2(\mathbb{R}) : t_{(a,b)} \circ r \in G \text{ for some } \begin{pmatrix} a \\ b \end{pmatrix} \in \mathbb{R}^2 \right\}$$

is finite. The set of translations of $\mathbb{R}^2$ in a wallpaper G form a subgroup of G. We refer this subgroup as the *translational subgroup* of G. We say two wallpaper groups G_1 and G_2 are *equivalent* if there exists a group isomorphism from G_1 onto G_2 which maps the translational subgroup of G_1 onto the translational subgroup of G_2.

A wallpaper group is *oriented* if all its members are orientation preserving as maps of $\mathbb{R}^2$. Note that if a wallpaper group is oriented, so are the groups equivalent to it. There are

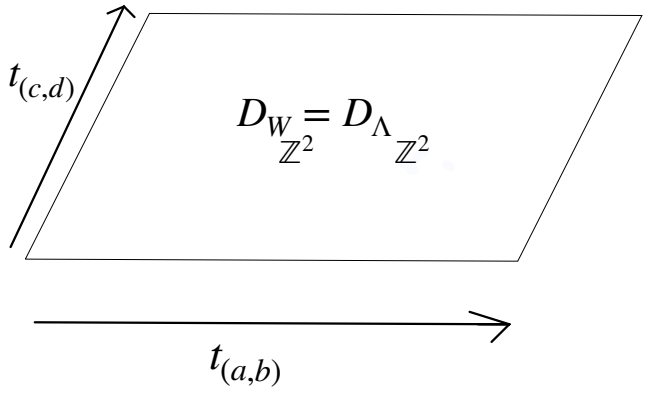

Figure 3: Fundamental domain of a wallpaper group of class $\mathbb{Z}^2$

five equivalence classes of oriented wallpaper groups (see the theorem on p. 127 in [37]). We describe these oriented classes of wallpaper groups below. We write the generating sets of the groups in the line of Hoffman's description of $(2,3,6)$ and $(2,4,4)$ wallpaper groups in §2 of [16]. But, our of choice of rotations in the generating set are counterclockwise as opposed to his clockwise rotations. We will be using $r_{n,(a,b)}$ to denote a counterclockwise rotation of angle $\frac{2\pi}{n}$ around the point (a,b).

Equivalent classes of wallpaper groups:

- $\mathbb{Z}^{\mathbf{2}}$

  A representative of this equivalence class is $W_{\mathbb{Z}^2} = \left\langle t_{(a,b)}, t_{(c,d)} \right\rangle$ where $a,b,c,d \in \mathbb{R}$ such that $ad \neq bc$.

  So, $W_{\mathbb{Z}^2}$ is generated by two linearly independent translations. In this case, the translational subgroup of $W_{\mathbb{Z}^2}$, denoted as $\Lambda_{\mathbb{Z}^2}$, is $W_{\mathbb{Z}^2}$ itself.

  Figure 3 shows a fundamental domain of $W_{\mathbb{Z}^2}$, denoted as $D_{W_{\mathbb{Z}^2}}$, which is also a fundamental domain of $\Lambda_{\mathbb{Z}^2}$ $D_{\Lambda_{\mathbb{Z}^2}}$.

- $(\mathbf{2},\mathbf{2},\mathbf{2},\mathbf{2})$

  A representative of this equivalence class is $W_{2,2,2,2} = \left\langle r_{2,(0,0)},\ r_{2,(\frac{a}{2},\frac{b}{2})},\ r_{2,(\frac{c}{2},\frac{d}{2})} \right\rangle$ where

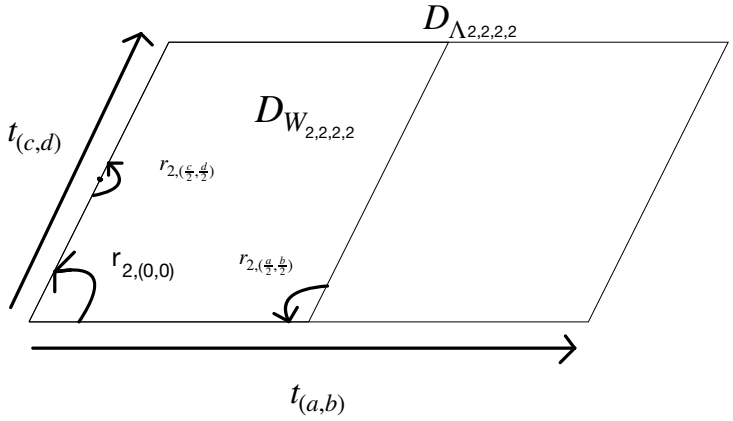

Figure 4: Fundamental domain of a wallpaper group of class $(2, 2, 2, 2)$

$a, b, c, d \in \mathbb{R}$ such that $ad \neq bc$ and

$$r_{2,(0,0)} = \begin{pmatrix} -1 & 0 \\ 0 & -1 \end{pmatrix}, \quad r_{2,(\frac{a}{2},\frac{b}{2})} = t_{(a,b)} \circ r_{2,(0,0)}, \quad r_{2,(\frac{c}{2},\frac{d}{2})} = t_{(c,d)} \circ r_{2,(0,0)}.$$

So, $W_{2,2,2,2}$ is generated by three order 2 rotations. Translation subgroup $\Lambda_{2,2,2,2}$ of $W_{2,2,2,2}$ is generated by the translations $r_{2,(\frac{a}{2},\frac{b}{2})} \circ r_{2,(0,0)}^{-1}$ and $r_{2,(\frac{c}{2},\frac{d}{2})} \circ r_{2,(0,0)}^{-1}$. Note that,

$$r_{2,(\frac{a}{2},\frac{b}{2})} \circ r_{2,(0,0)}^{-1} = t_{(a,b)} \qquad \text{and} \qquad r_{2,(\frac{c}{2},\frac{d}{2})} \circ r_{2,(0,0)}^{-1} = t_{(c,d)}.$$

One can see that $[W_{2,2,2,2} : \Lambda_{2,2,2,2}] = 2$. Figure 4 shows a fundamental domain of $\Lambda_{2,2,2,2}$, denoted as $D_{\Lambda_{2,2,2,2}}$, containing a fundamental domain of $W_{2,2,2,2}$, denoted as $D_{W_{2,2,2,2}}$.

- $(\mathbf{2}, \mathbf{3}, \mathbf{6})$

  A representative of this equivalence class is $W_{2,3,6} = \left\langle r_{6,(0,0)},\ r_{3,(\frac{a}{2},\frac{a}{2\sqrt{3}})} \right\rangle$ where

$$r_{6,(0,0)} = \begin{pmatrix} -\frac{1}{2} & -\frac{\sqrt{3}}{2} \\ \frac{\sqrt{3}}{2} & -\frac{1}{2} \end{pmatrix}, \quad r_{3,(\frac{a}{2},\frac{a}{2\sqrt{3}})} = t_{(a,0)} \circ r_{6,(0,0)}^{2}.$$

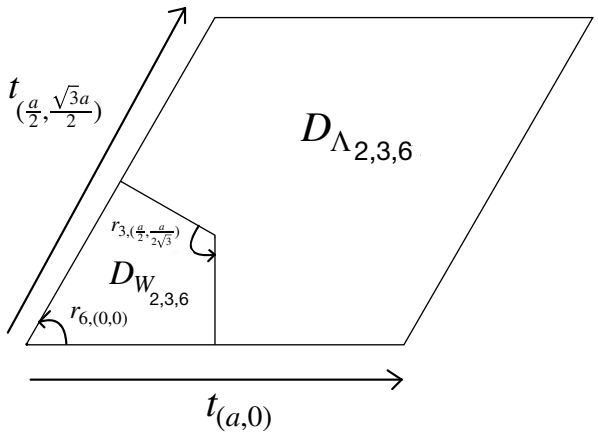

Figure 5: Fundamental domain of a wallpaper group of class $(2, 3, 6)$

So, $W_{2,3,6}$ is generated by an order 6 rotation and an order 3 rotation. Translation subgroup $\Lambda_{2,3,6}$ of $W_{2,3,6}$ is generated by $r_{3,(\frac{a}{2},\frac{a}{2\sqrt{3}})} \circ r^{-2}_{6,(0,0)}$ and $r^{-1}_{3,(\frac{a}{2},\frac{a}{2\sqrt{3}})} \circ r^{2}_{6,(0,0)}$. Note,

$$r_{3,(\frac{a}{2},\frac{a}{2\sqrt{3}})} \circ r^{-2}_{6,(0,0)} = t_{(a,0)} \quad \text{and} \quad r^{-1}_{3,(\frac{a}{2},\frac{a}{2\sqrt{3}})} \circ r^{2}_{6,(0,0)} = t_{(\frac{a}{2},\frac{\sqrt{3}a}{2})}.$$

We have, $[W_{2,3,6} : \Lambda_{2,3,6}] = 6$. Figure 5 shows a fundamental domain of $\Lambda_{2,3,6}$, denoted as $D_{\Lambda_{2,3,6}}$, containing a fundamental domain of $W_{2,3,6}$, denoted as $D_{W_{2,3,6}}$.

- $(\mathbf{3}, \mathbf{3}, \mathbf{3})$

  A representative of this equivalence class is $W_{3,3,3} = \left\langle r_{3,(0,0)},\ r_{3,(\frac{a}{2},\frac{a}{2\sqrt{3}})} \right\rangle$ where

$$r_{3,(0,0)} = \begin{pmatrix} \frac{1}{2} & \frac{-\sqrt{3}}{2} \\ \frac{\sqrt{3}}{2} & \frac{1}{2} \end{pmatrix}, \quad r_{3,(\frac{a}{2},\frac{a}{2\sqrt{3}})} = t_{(a,0)} \circ r_{3,(0,0)}.$$

  So, $W_{3,3,3}$ is generated by two order 3 rotations. Translation subgroup $\Lambda_{3,3,3}$ of $W_{3,3,3}$ is generated by $r_{3,(\frac{a}{2},\frac{a}{2\sqrt{3}})} \circ r^{-1}_{3,(0,0)}$ and $r^{-1}_{3,(\frac{a}{2},\frac{a}{2\sqrt{3}})} \circ r_{3,(0,0)}$. We note,

$$r_{3,(\frac{a}{2},\frac{a}{2\sqrt{3}})} \circ r^{-1}_{3,(0,0)} = t_{(a,0)} \quad \text{and} \quad r^{-1}_{3,(\frac{a}{2},\frac{a}{2\sqrt{3}})} \circ r_{3,(0,0)} = t_{(\frac{a}{2},\frac{\sqrt{3}a}{2})}.$$

  We see that $[W_{3,3,3} : \Lambda_{3,3,3}] = 3$. Figure 6 shows a fundamental domain of $\Lambda_{3,3,3}$, denoted as $D_{\Lambda_{3,3,3}}$ containing a fundamental domain of $W_{3,3,3}$, denoted as $D_{W_{3,3,3}}$.

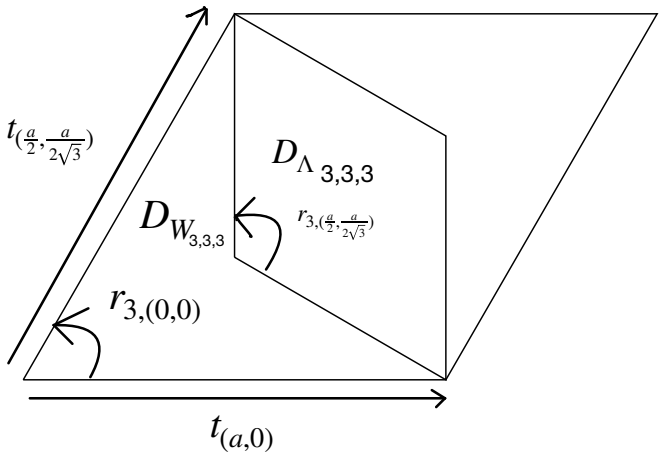

Figure 6: Fundamental domain of a wallpaper group of class $(3, 3, 3)$

- $(\mathbf{2}, \mathbf{4}, \mathbf{4})$

  A representative of this equivalence class is $W_{2,4,4} = \left\langle r_{4,(0,0)},\ r_{4,(\frac{a}{2},\frac{a}{2})} \right\rangle$ where

  $$r_{4,(0,0)} = \begin{pmatrix} 0 & -1 \\ 1 & 0 \end{pmatrix}, \quad r_{4,(\frac{a}{2},\frac{a}{2})} = t_{(a,0)} \circ r_{4,(0,0)}.$$

  So, $W_{2,4,4}$ is generated by two order 4 rotations. Translation subgroup $\Lambda_{2,4,4}$ of $W_{2,4,4}$ is generated by $r_{4,(\frac{a}{2},\frac{a}{2})} \circ r_{4,(0,0)}^{-1}$ and $r_{4,(\frac{a}{2},\frac{a}{2})}^{-1} \circ r_{4,(0,0)}$. Note that

  $$r_{4,(\frac{a}{2},\frac{a}{2})} \circ r_{4,(0,0)}^{-1} = t_{(a,0)} \quad \text{and} \quad r_{4,(\frac{a}{2},\frac{a}{2})}^{-1} \circ r_{4,(0,0)} = t_{(0,a)}.$$

  One can see that $[W_{2,4,4} : \Lambda_{2,4,4}] = 4$. Figure 7 shows a fundamental domain of $\Lambda_{2,4,4}$, denoted as $D_{\Lambda_{2,4,4}}$, containing a fundamental domain of $W_{2,4,4}$, denoted as $D_{W_{2,4,4}}$.

Remark 2.9. *For a hyperbolic link $L = K_1 \sqcup \cdots \sqcup K_n$, each of the components K_i correspond to a cusp end of $\mathbb{S}^3 - L$ for $i = 1, \ldots, n$. Let $h : \mathbb{S}^3 - L \to \mathbb{H}^3/\Gamma$ be the diffeomorphism which makes L a hyperbolic link. Then, there exists a closed tubular neighborhood $N(K_i)$ of K_i such that the image of $N(K_i) - K_i$ under h is a cusp neighborhood corresponding to K_i-component. We will refer to a cusp or cusp neighborhood corresponding to K_i-component as a K_i-cusp or K_i-cusp neighborhood.*

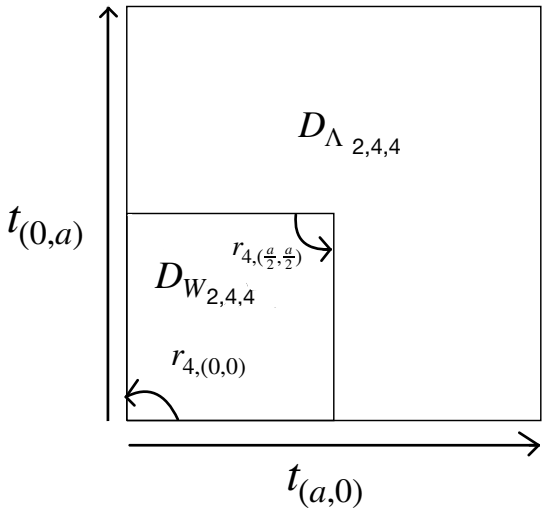

Figure 7: Fundamental domain of a wallpaper group of the class $(2, 4, 4)$

2.5.1 Cusp cross-sections

Let $c = B/W$ be a cusp of an orbifold O where B is a horoball and W is one of the five oriented wallpaper groups. Then $\partial B/W$, the quotient of the horosphere of B by the wallpaper is called the *cusp cross-section* of c.

Note that if for a cusp c, if we denote its cusp cross-section by ∂c, then topologically, c is homeomorphic to $\partial c \times [0, \infty)$.

When W belongs to the $\mathbb{Z}^2$ class, $\partial B/W$ is a torus and so the cusp is called a *torus cusp*. Similarly, when W belong to $(2, 2, 2, 2)$, $(2, 3, 6)$, $(3, 3, 3)$ and $(2, 4, 4)$ equivalence classes, cusp c is referred to as *pillowcase cusp*, $(2, 3, 6)$ *cusp*, $(3, 3, 3)$ *cusp* and $(2, 4, 4)$ *cusp* respectively. We will use the term *smooth cusp* to mean either a torus cusp or a pillowcase cusp, and the term *rigid cusp* to mean either $(2, 3, 6)$ cusp or $(3, 3, 3)$ or $(2, 4, 4)$ cusp (see Figure 8 and 9).

When Γ is torsion free, the cusp cross-sections are all *Euclidean torus*, i.e. a torus with a Euclidean structure inherited from B. The similarity structure of a torus cusp cross-section is referred as the *cusp shape* of the cusp.

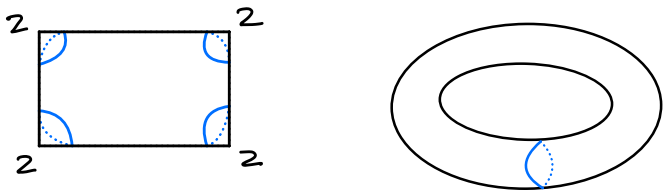

Figure 8: Cross-section of smooth cusps - Left: $(2, 2, 2, 2)$ cusp, Right: torus cusp

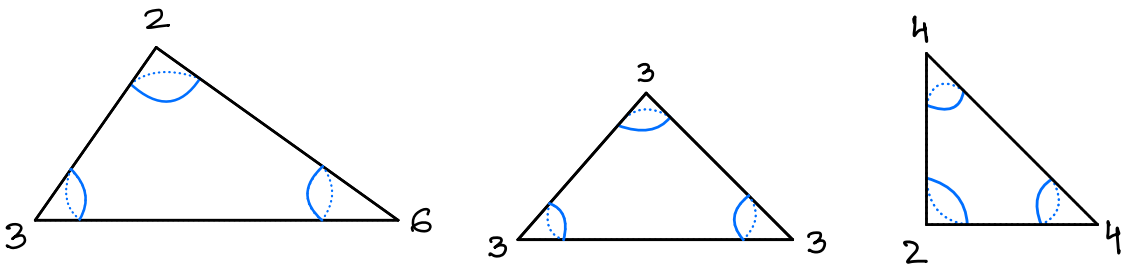

Figure 9: Cross-section of rigid cusps - Left: $(2, 3, 6)$ cusp, Middle: $(3, 3, 3)$ cusp, Right: $(2, 4, 4)$ cusp

2.5.2 Cusp moduli of a torus cusp

Let c be a torus cusp of an orbifold O. Then, $c = B/W_{\mathbb{Z}^2}$ for some horoball B and wallpaper group of $W_{\mathbb{Z}^2} =< t_{(m_1,m_2)}, t_{(l_1,l_2)} >$ as discussed above. We say that $\frac{l_1+l_2 i}{m_1+m_2 i}^{sign(m_1 l_2 - m_2 l_1)}$ is a *cusp moduli* of c. Note that a cusp moduli always belongs to the upper-half plane.

2.6 Dehn filling and geometric convergence

One way of producing new orbifolds out of a given orbifold is the technique of Dehn filling. We first recall from §2.E of [35] that a simple closed curve in $\mathbb{S}^1 \times \mathbb{S}^1$ is called a *meridian* if it bounds a disk in the solid torus $\mathbb{D}^2 \times \mathbb{S}^1$ and it is called a *longitude* if it generates the first homology of $\mathbb{D}^2 \times \mathbb{S}^1$.

For a hyperbolic link L and a component K of L, a K-cusp (which is a torus cusp) is a regular neighborhood of K. A meridian-longitude pair (m, l) in the cusp torus of K-cusp such that l vanishes in the homology of $M - int(c)$, where $M = \mathbb{S}^3 - L$ and $int(c)$ is the interior of c, is referred to as the *preferred meridian-longitude pair*.

Let c be a torus cusp neighborhood of an orbifold O. We choose a meridian-longitude pair (m_c, l_c) in ∂c, which in this context just means a generating pair for $H_1(\partial c)$.

For co-prime integers p and q, the topological space $(O - int(c)) \cup_h \mathbb{D}^2 \times \mathbb{S}^1$ where h is a homeomorphism of $\mathbb{S}^1 \times \mathbb{S}^1$ to ∂c sending the meridian m of $\mathbb{D}^2 \times \mathbb{S}^1$ to the curve $pm_c + ql_c$ is said to be *obtained by* (p, q) *Dehn filling* on c.

To discuss the more general $gcd(p, q) = d \geq 1$ case, we note that, the quotient of the solid torus $\mathbb{D}^2 \times \mathbb{S}^1$ by a $2\pi/d$ rotation around the core curve $\{0\} \times \mathbb{S}^1$ is an orbifold with singular locus $\{0\} \times \mathbb{S}^1$ of order d (when $d = 1$, the singular locus is not singular anymore). Let us denote this orbifold as $(\mathbb{D}^2 \times \mathbb{S}^1)_d$. Topologically, $(\mathbb{D}^2 \times \mathbb{S}^1)_d$ is still a solid torus. We denote the image of the meridian m in $(\mathbb{D}^2 \times \mathbb{S}^1)_d$ as m_d. We now fix a homeomorphism h from the boundary of $(\mathbb{D}^2 \times \mathbb{S}^1)_d$ (which is topologically still a torus) to ∂c sending m_d to the curve $\frac{p}{d} m_c + \frac{q}{d} l_c$. Then, $(O - int(c)) \cup_h (\mathbb{D}^2 \times \mathbb{S}^1)_d$ which has an orbifold structure with its points in (the image of) $\{0\} \times \mathbb{S}^1$ having order d torsion is said to be *obtained by* (p, q)

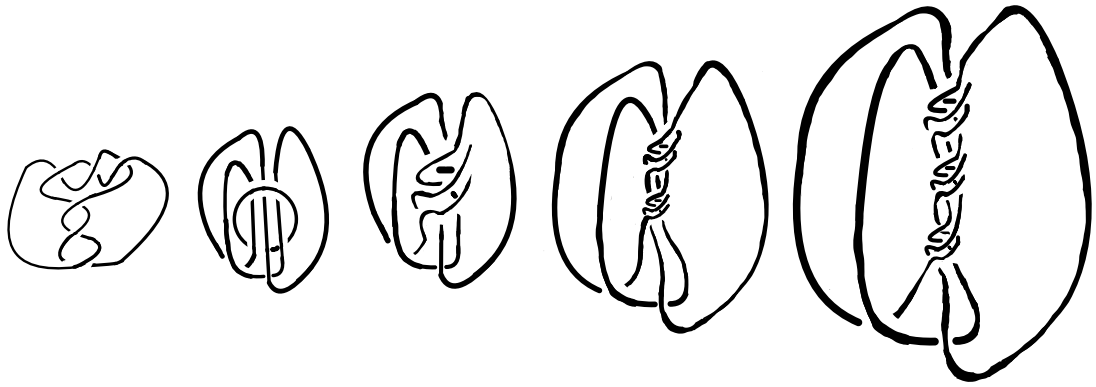

Figure 10: Dehn fillings on a cusp of 6_2^2: First and Second pictures: the link 6_2^2, Third, fourth and fifth pictures: $(1,1)$-filling, $(1,2)$-filling and $(1,3)$-filling respectively

Dehn filling on c.

If the cusps of an orbifold O are $c_1, \ldots, c_n$ then the orbifold obtained by (p_i, q_i) Dehn filling on c_i for each $i \in \{1, \ldots, n\}$ is denoted as $O_{(p_1,q_1),\ldots,(p_n,q_n)}$. If we don't fill a c_i, then we write $(p_i, q_i) = \infty$.

By a $(1, n)$ Dehn filling on the K cusp, we mean a $(1, n)$ Dehn filling using the preferred meridian-longitude pair for K cusp.

Remark 2.10. *Given an n-component link L with an unknotted component K, the manifold M obtained by $(1, n)$ filling on K is homeomorphic to a link with $(n-1)$ components. (See Proposition 2 in §9.H in [35]). Figure 10 shows the $(1, 1)$ and $(1, 2)$ Dehn filling on one cusp of the link 6_2^2.*

The following theorem of Thurston (which was later extended for orbifold fillings of smooth cusps of orbifolds by Dunbar and Meyerhoff in Theorem 5.3 of [10]) makes Dehn filling an intrinsic part of 3-dimensional hyperbolic geometry:

Theorem 2.11 (Thurston, Theorem 5.8.2, [39]). *Let M be a hyperbolic 3-manifold with cusps $c_1, \ldots, c_n$. There exists a compact set K in $\mathbb{R}^2$ such that if integer pairs $(p_1, q_1), \ldots (p_n.q_n)$ lie outside K then the 3-manifold $M_{(p_1,q_1),\ldots,(p_n.q_n)}$ is hyperbolic.*

In fact, one can further say that

Theorem 2.12 (Theorem 6.4, [10]). *Let O be a finite volume hyperbolic 3-orbifold with at-least one smooth cusp and O_{Dehn} be a hyperbolic 3-orbifold obtained by Dehn filling some of the smooth cusps of O. Then O_{Dehn} also has finite volume and the volume of O_{Dehn} is less than the volume of O.*

We now define the notion of a convergence for hyperbolic knots obtained from Dehn filling the components of a hyperbolic link.

Definition 2.13. *Let L be a hyperbolic link with components $K_1, \ldots, K_n$ where $n \geq 2$. Let $\mathcal{F} = \{O_{\infty,(p_2^i,q_2^i),\ldots,(p_n^i,q_n^i)}\}_i$ be a family of hyperbolic 3- orbifolds such that each $O_{\infty,(p_2^i,q_2^i),\ldots,(p_n^i,q_n^i)}$ is obtained by Dehn filling K_j cusp of L with filling coefficient (p_j^i, q_j^i) for $j \in \{2, \ldots, n\}$. If (p_j^i, q_j^i) converges to ∞ (in $\mathbb{S}^2$) as $i \to \infty$ for each $j \in \{2, \ldots, n\}$ for this family $\mathcal{F}$, then we say that the elements of $\mathcal{F}$ geometrically converge to L as $i \to \infty$.*

Remark 2.14. *Note that when L has only two components, for any infinitely family $\mathcal{F}$ of hyperbolic orbifolds obtained from Dehn filling a fixed component of L, the elements of $\mathcal{F}$ geometrically converge to L.*

We make a note of the following important fact:

Fact 2.15. *Let c and c' be two cusps of the complement of a hyperbolic link L which are symmetric, i.e. there is an self-isometry of $\mathbb{S}^3 - L$ exchanging the cusps. Let $\mathcal{F}$ be a geometrically converging family of hyperbolic knots obtained by Dehn filling all cusps of $\mathbb{S}^3 - L$ but c, then there exists a family $\mathcal{F}'$ of geometrically converging family of hyperbolic knots obtained by Dehn filling all cusps of $\mathbb{S}^3 - L$ but c' such that each member of $\mathcal{F}$ is isometric to a member of $\mathcal{F}'$ and vice versa.*

Remark 2.16. *The definition of geometric convergence is more broad. See [20, Section 4.2] for the general definition.*

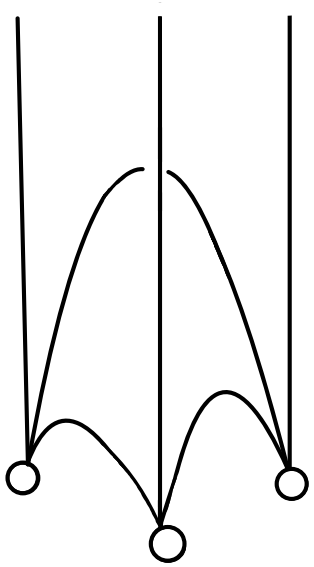

Figure 11: An ideal tetrahedron with an ideal vertex at ∞

2.7 Ideal triangulation and deformation variety

The contents of this section go back to Thurston [39] and Neumann and Zagier [25]. For pinpoint citations of the results and the discussions, we sometimes refer to [2] and [30].

2.7.1 Ideal tetrahedron and shape parameters

Let $\overline{\Delta}$ be a tetrahedron in $\mathbb{H}^3 \cup \partial_\infty \mathbb{H}^3$ whose vertices are in $\partial_\infty \mathbb{H}^3$ and all other simplices are geodesic simplices in $\mathbb{H}^3$. If $\overline{\Delta}^0$ is the set of vertices of $\overline{\Delta}$, then, $\overline{\Delta} - \overline{\Delta}^0$ is called an ideal hyperbolic tetrahedron.

Figure 11 shows the picture of an ideal tetrahedron one of whose ideal vertices is at ∞.

Proposition 2.17. *Let Δ be an ideal tetrahedron with ideal vertices v_0, v_1, v_2 and v_3. Let z be the cross-ratio of the tuple (v_0, v_1, v_2, v_3) defined as $\frac{v_3-v_0}{v_2-v_0}\frac{v_2-v_1}{v_3-v_1}$. We denote this cross ratio as $[v_0, v_1, v_2, v_3]$. Then there exists an isometry $\phi \in \mathrm{PSL}(2,\mathbb{C})$ such that ϕ maps v_0, v_1, v_2 and v_3 to 0, ∞, 1, and z respectively and so, ϕ maps Δ isometrically to the ideal tetrahedron*

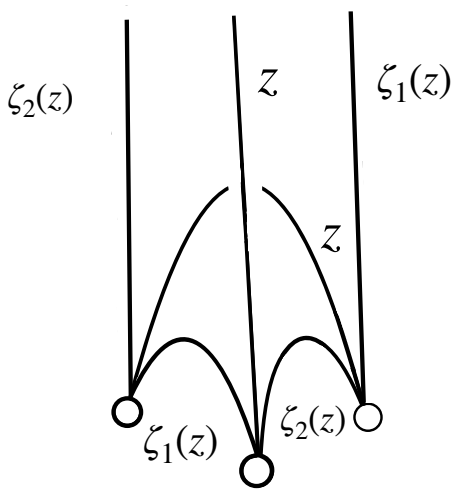

Figure 12: Shape parameters of the ideal tetrahedron

with ideal vertices at 0, ∞, 1, *and* z.

Proof. Let $\phi \in \mathrm{PSL}(2,\mathbb{C})$ be given by the Möbius transformation sending u to $\frac{u-v_0}{u-v_1}.\frac{v_2-v_1}{v_2-v_0}$. One can see that ϕ maps v_0, v_1, v_2 and v_3 respectively to 0, ∞, 1, and z. □

This z is called the *shape parameter* of $[v_0, v_1]$, the edge connecting v_0 to v_1. One can check the following two facts about shape parameters:

Facts 2.18. *1. The shape parameters for two opposite edges of an ideal tetrahedron are same.*

2. For an ideal vertex v of a tetrahedron, if the three edges concurrent at v are written in a counter clockwise order when viewed from v towards to the tetrahedron, then the shape parameters of the three edges read as z, $\frac{1}{1-z}$ and $\frac{z-1}{z}$ where z is the shape parameter of the first edge in the order. From now on, we will use the notation $\zeta_1(z) = \frac{1}{1-z}$ and $\zeta_2(z) = \frac{z-1}{z}$ following [8].

Figure 12 demonstrates these last two facts.

2.7.2 Geometric triangulation, edge equations and holonomy equations

Let M be a 3-manifold with a hyperbolic structure. Let $\mathcal{T} = \{\Delta_i\}_{i=1}^n$ be a collection of ideal hyperbolic tetrahedra and $\mathcal{F} = \{f, f^{-1}\}_{j=1}^{2n}$ be a collection of isometries such that for each $f \in \mathcal{F}$, there exists $i, j \in \{1, \ldots, n\}$ such that f maps a face A of Δ_i onto a face A' of Δ_j and $A' = f(\Delta_i) \cap \Delta_j$. If M is $(\mathbb{H}^3, \mathrm{Isom}^+(\mathbb{H}^3))$ isomorphic to the quotient of $\bigsqcup_{i=1}^n \Delta_i$ by $\mathcal{F}$, then $(\mathcal{T}, \mathcal{F})$ is called a *geometric triangulation* of M.

Each edge of M is an equivalence class of edges of the elements of $\mathcal{T}$. Let's denote the the set of edges of M by $\mathcal{E}$. Now, for M to have hyperbolic structure, the total dihedral angle around each $\mathfrak{e}$ in $\mathcal{E}$ should be 2π. This fact implies (see Equation 16 of [25]) that

$$\prod_{e \in \mathfrak{e}} z_e = 1 \text{ for each } \mathfrak{e} \in \mathcal{E} \text{ where } z_e \text{ is the shape parameter of the edge } e. \tag{3}$$

The equations in Formula 3 are called *edge equations*.

We now assume that M is a hyperbolic 3-manifold and consider a geometric triangulation $(\mathcal{T}, \mathcal{F})$ of the associated hyperbolic structure. Let c be a cusp of M and T_c be a cusp cross-section of c. Recall that T_c is a Euclidean torus. For $[\gamma] \in \pi_1(T_c)$, let γ' be a simplicial curve in the homotopy class of $[\gamma]$. Let l_s denote the number of 1-simplices of γ'. Let $E_{\gamma'}$ denotes the set of edges that γ' meets from the right. Let z_e be the shape parameter of e for each $e \in E$. If one defines the derivative of the holonomy of $[\gamma]$,

$$\mu([\gamma]) = (-1)^{l_s} \prod_{e \in E} z_e$$

then, Neumann and Zagier shows the following:

Proposition 2.19 (Lemma 2.1, [25]). *The map $\mu : \pi_1(T_c) \to \mathbb{C} - \{0\}$ where $\mu([\gamma])$ defined as above is well defined and is a group homomorphism.*

For $i \in \{1, \ldots, k\}$ let $\{m_i, l_i\}$ denote a generating set for the fundamental group of T_{c_i}, a torus cusp cross-section at the c_i cusp of M where k is the number of cusps of M. Since the hyperbolic structure on M is complete, Equations 18 and 19 in [25] establishes

$$\mu(m_i) = \mu(l_i) = 1 \text{ for each } i \in \{1, \ldots, k\}. \tag{4}$$

We refer to the equations in Formula 4 as *holonomy equations*.

2.7.3 Deformation variety, incomplete structures and Dehn filling

For each edge $\mathfrak{e}$ of M, Formula 3 gives a polynomial equation $p_{\mathfrak{e}}(z_1, \ldots, z_n) = 0$ where $z_1, \ldots, z_n$ are the shape parameters of $(\mathcal{T}, \mathcal{F})$. The algebraic set $\mathcal{D}(M) = \{(z_1, \ldots, z_n) \in \mathbb{C}^n : p_{\mathfrak{e}} = 0 \text{ for edge } \mathfrak{e} \text{ of } M\}$ is called the *deformation variety* of M. We note that each $\mathbf{z}$ in $\mathcal{D}(M)$ represents a hyperbolic structure on M.

Let $M_{\mathbf{z}}$ denote the hyperbolic structure of (a homeomorphic copy of) M obtained from the geometric triangulation $(\mathcal{T}_{\mathbf{z}}, \mathcal{F}_{\mathbf{z}})$ for $\mathbf{z} = (z_1, \ldots, z_n) \in \mathcal{D}(M)$. The Riemannian metric that $M_{\mathbf{z}}$ inherits from the structure may not be complete. We say $M_{\mathbf{z}}$ is an *incomplete structure* of M if the corresponding Riemannian metric is not complete. For $\mathbf{z} \in \mathcal{D}(M)$, if $\mu(m_i) = \mu(l_i) = 1$ at $\mathbf{z}$, then, $M_{\mathbf{z}}$ is said to be *complete at the i-th cusp*. Note, if for some $\mathbf{z} \in \mathcal{D}(M)$, $M_{\mathbf{z}}$ is complete at all the cusps, i.e, $\mathbf{z}$ satisfies Equations 3 and 4, then the hyperbolic structure of $M_{\mathbf{z}}$ is that of M. This $\mathbf{z}$ (or $M_{\mathbf{z}}$) is referred as a *complete structure*. Mostow-Prasad rigidity (see Theorem 2.3.1) implies that the number of $\mathbf{z}$ in $\mathcal{D}(M)$ corresponding to the complete hyperbolic manifold M is finite (see [2, Proposition E.6.16]).

Note, $\mathcal{D}(M)$ is in general not irreducible and so not an algebraic variety. Let $\mathcal{D}_0$ be an irreducible component of $\mathcal{D}(M)$ containing a complete structure in $\mathcal{D}(M)$. Let $\mathcal{E} = \{\mathfrak{e}_1, \ldots, \mathfrak{e}_n\}$. By Fact 2, we see that for each $i \in \{1, \ldots, n\}$ the edge equation for edge $\mathfrak{e}_i$ in $\mathcal{E}$ can be written as:

$$\prod_{j=1}^{n} z^{m_{i,j}}(1-z)^{n_{i,j}} = 1, \quad \text{where } m_{i,j}, n_{i,j} \in \{-1, 0, 1\}.$$

We define an $n \times n$ matrix M whose (i,j)th entry is $m_{i,j}$ for $i, j \in \{1, \ldots, n\}$ and matrix N whose (i,j)th entry is $n_{i,j}$ for $i, j \in \{1, \ldots, n\}$. If we define the $n \times 2n$ *edge equation matrix* $P = \begin{pmatrix} M & N \end{pmatrix}$, then the following is true:

Theorem 2.20 (Proposition E.6.19, [2])**.** *The matrix P has rank $n - k$ and the dimension of $\mathcal{D}_0$ is equal to k, where k is the number of cusps of M.*

We define $u_i = log(\mu(m_i))$ and $v_i = log(\mu(l_i))$. Thurston showed that there exists $p_i, q_i \in \mathbb{R}$ such that $p_i u_i + q_i v_i = 2\pi i$. This (p_i, q_i) is called the *generalized Dehn surgery coefficient* at the i-th cusp of M.

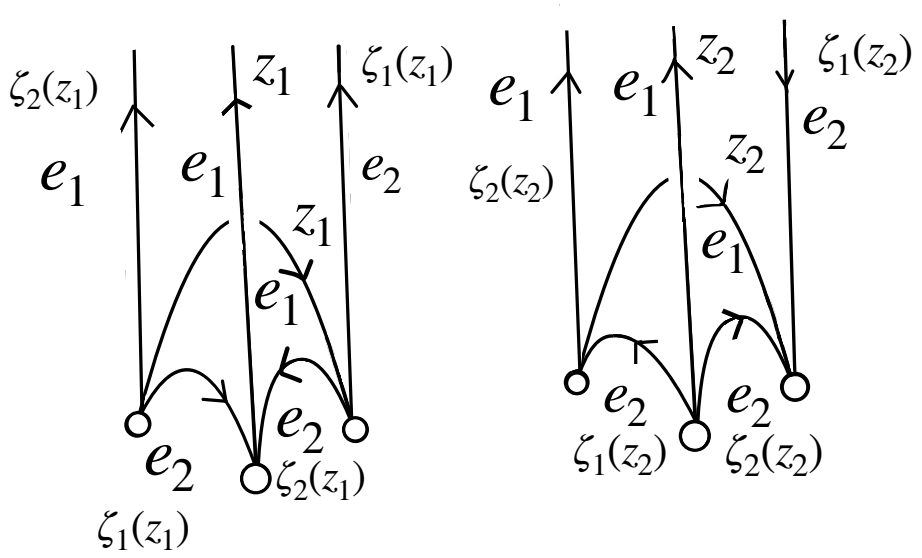

Figure 13: Tetrahedral decomposition of the figure eight knot complement

Theorem 2.21 (Proposition E.6.27, [2])**.** *Let* $\mathbf{z} \in \mathcal{D}_0(M)$ *such that* $M_{\mathbf{z}}$ *is complete at cusps* $c_1, \ldots, c_m$*. Suppose the generalized Dehn surgery coefficients* (p_i, q_i) *of* $M_{\mathbf{z}}$ *are co-prime integers at the* c_i *cusp for* $i \in \{m+1, \ldots, n\}$*. The metric completion of* $M_{\mathbf{z}}$ *is a hyperbolic* 3*-manifold with* m *cusps that is isometric to the hyperbolic manifold obtained by* (p_i, q_i) *Dehn filling on the* c_i *cusp of* M *for* $i \in \{m+1, \ldots, n\}$*.*

2.7.4 Example: figure eight knot

We follow [30] (pp. 485-488) for the discussion below.

The hyperbolic structures of the figure eight knot complement $\mathbb{S}^3 - K$ has geometric triangulations into 2 ideal tetrahedra with face pairing as shown in Figure 13 (cf. Figure 10.5.5 in [30]). One can check that the edge equations in this case are:

$$\frac{z_1 - 1}{z_1} z_2 z_1 \frac{z_2 - 1}{z_2} z_1 z_2 = 1 \tag{5}$$

$$\frac{1}{1 - z_1} \frac{z_2 - 1}{z_2} \frac{z_1 - 1}{z_1} \frac{1}{1 - z_2} \frac{1}{1 - z_2} \frac{1}{1 - z_1} = 1. \tag{6}$$

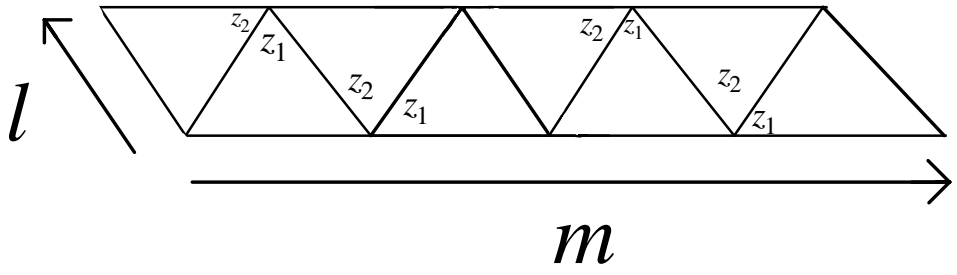

Figure 14: Cusp triangulation the figure eight knot complement

Simplifying the expressions above, one finds that Equations 5 and 6 are equivalent to the polynomial equation $z_1(z_1-1)z_2(z_2-1)-1=0$. So, $\mathcal{D}(\mathbb{S}^3-K)$, the deformation variety of $\mathbb{S}^3-K$, is $\{(z_1,z_2) : z_1(z_1-1)z_2(z_2-1)-1=0\}$.

To understand the map μ, we look at Figure 14 (cf. Figure 10.5.7 in [30]), which represents the cusp cross section $\mathbb{S}^3-K$. Triangles in Figure 14 are the horospherical cross sections of the tetrahedra around the ideal vertices.

The two generators for the fundamental group of this cross section are denoted by m and l here. One can see that

$$\mu(m) = (-1)^4 \frac{1}{1-z_1} z_2 z_1 \frac{z_1-1}{z_1} \frac{1}{1-z_1} \frac{z_1-1}{z_1} \frac{1}{1-z_1} z_2 z_1 \frac{z_2-1}{z_2} \frac{1}{1-z_1} \frac{z_2-1}{z_2} = \frac{(z_2-1)^2}{(z_1-1)^2} \quad (7)$$

$$\mu(l) = (-1) \frac{1}{1-z_1} \frac{1}{1-z_2} \frac{z_2-1}{z_2} = \frac{1}{z_2(1-z_1)}. \quad (8)$$

Solving for $\mathbf{z}=(z_1,z_2)$ in Equations 5 and 6 and $\mu(m)=\mu(l)=1$ gives us $z_1=z_2=\frac{1+\sqrt{3}i}{2}$. So, the complete structure corresponds to $\mathbf{z}=(\frac{1+\sqrt{3}i}{2},\frac{1+\sqrt{3}i}{2})$. This $\mathbf{z}=(\frac{1+\sqrt{3}i}{2},\frac{1+\sqrt{3}i}{2})$ corresponds to the hyperbolic structure of $\mathbb{S}^3-K$ which makes K a hyperbolic knot.

2.8 Trace fields vs. cusp fields

For this section, we assume that Γ is a Kleinian group with finite co-volume, i.e. fundamental domains of Γ in $\mathbb{H}^3$ have finite volume.

Definition 2.22. *$\mathbb{Q}(\{trace(\gamma) : \gamma \in \Gamma\})$, the field generated by the traces of the elements of Γ over $\mathbb{Q}$ is said to be the trace field of Γ. We denote this field as $Tr(\Gamma)$.*

We define another closely related field called the *invariant trace field* as follows:

Definition 2.23. *$\mathbb{Q}(\{trace(\gamma^2) : \gamma \in \Gamma\})$, the field generated by the traces of the squares of the elements of Γ over $\mathbb{Q}$ is called the invariant trace field. We denote this field as $k\Gamma$.*

The following theorem shows that trace fields and invariant trace fields are in fact number fields.

Theorem 2.24 (Theorem 3.1.2, [19])**.** *The trace field of a finite co-volume Kleinian group is a finite degree extension of $\mathbb{Q}$.*

Example 2.25. *Let's take Γ from Example 2.2. Then since Γ is generated by $A = \begin{pmatrix} 1 & 1 \\ 0 & 1 \end{pmatrix}$ and $B = \begin{pmatrix} 1 & 0 \\ \omega & 1 \end{pmatrix}$ (where $\omega = \frac{1+\sqrt{3}i}{2}$), $Tr(\Gamma)$ is generated by $trace(A)$, $trace(B)$ and $trace(AB)$ (see Equation 3.25 in [19]). Now, $AB = \begin{pmatrix} \omega+1 & 1 \\ \omega & 1 \end{pmatrix}$. $trace(A) = trace(B) = 2$ and $trace(AB) = \omega+2$. So, $Tr(\Gamma) = \mathbb{Q}(\sqrt{3}i)$. On the other hand, $(AB)^2 = \begin{pmatrix} 2\omega & \omega+2 \\ \omega-1 & \omega+1 \end{pmatrix}$ and so, $trace((AB)^2) = 3\omega + 1$. So, $\omega \in k\Gamma$ meaning $k\Gamma = \mathbb{Q}(\sqrt{3}i)$ as well.*

Reid established the following interesting fact:

Theorem 2.26 (Theorem 2, [31])**.** *If Γ_1 and Γ_2 are commensurable (i.e., $\Gamma_1 \cap \Gamma_2$ has finite index in both Γ_1 and Γ_2), then, $k\Gamma_1 = k\Gamma_2$.*

In general, $k\Gamma$ could be smaller than $Tr(\Gamma)$. An example of such a scenario is given by Reid in [31]:

Example 2.27 (Example, §1, [31]). *Let* Γ *and* Γ' *be from Example 2.2 and Example 2.6 respectively. By Theorem 2.26,* $k\Gamma = k\Gamma'$*. From Equation 3.26 of [19], it follows that* $Tr(\Gamma')$ *is generated by the set*

$$\{trace(A), trace(B), trace(C), trace(AB), trace(AC), trace(BC), trace(ABC)\}$$

where

$$A = \begin{pmatrix} 1 & 1 \\ 0 & 1 \end{pmatrix}, \quad B = \begin{pmatrix} 1 & 0 \\ \omega & 1 \end{pmatrix}, \quad C = \begin{pmatrix} i & 0 \\ 0 & -i \end{pmatrix}.$$

If we compute these traces, we see, $trace(A) = trace(B) = 2, trace(C) = trace(AC) = trace(BC) = 0, trace(AB) = \omega + 2, trace(ABC) = i\omega$*. So,* $Tr(\Gamma') = \mathbb{Q}(i, \sqrt{3})$*, which strictly contains* $k\Gamma' = \mathbb{Q}(\sqrt{3}i)$*.*

But, Neumann and Reid proved the following:

Theorem 2.28 (Neumann-Reid, Corollary 2.3, [23]). $k\Gamma = Tr(\Gamma)$ *when* Γ *is the fundamental group of a hyperbolic link complement.*

When M is a hyperbolic 3-manifold, then the trace field and the invariant trace field of the fundamental group of M are referred as the trace field and the invariant trace field of M respectively.

Definition 2.29. *Let* M *be a hyperbolic three manifold with geometric triangulation* $(\mathcal{T}, \mathcal{F})$*. If* $\{z_1, \ldots, z_n\}$ *denote the shape parameters of this triangulation* $(\mathcal{T}, \mathcal{F})$*, then* $\mathbb{Q}(\{z_1, \ldots, z_n\})$ *is called the shape field of* M*.*

Neumann and Reid proved,

Theorem 2.30 (Neumann-Reid, Theorem 2.4, [23]). *For a hyperbolic* 3*-manifold* M*, the shape field of* M *is equal to the invariant trace field of* M*.*

The field generated by the cusp moduli of the cusps of M over $\mathbb{Q}$ is called the *cusp field* of M. Neumann and Reid also proved that

Theorem 2.31 (Neumann-Reid, Proposition 2.7, [23]). *Cusp field of* M *is a subfield of* $k\Gamma$*.*

3.0 Hidden symmetry of hyperbolic knot complements

In this chapter, we describe the background material in hidden symmetries. Margulis's arithmeticity theorem (see [19, Theorem 10.3.5], refer to [41] for a proof) implies that a hyperbolic 3-manifold has infinitely many hidden symmetries if and only if it is arithmetic. This makes the study of hidden symmetries in hyperbolic knot complements quite interesting since by a result of Reid, figure eight knot is the only arithmetic knot. Our exposition of the introductory topics on hidden symmetries here closely follow Neumann and Reid's seminal paper [23] from 1992. We also discuss some recent results on research on hidden symmetries.

3.1 Hidden symmetry

For a hyperbolic 3-manifold M, if there exists an isometry g between two finite index coverings of M such that g is not a lift of any self-isometry of M, then g is said to be a *hidden symmetry* of M.

Facts 3.1. • *The group of self-isometries of* $M = \mathbb{H}^3/\Gamma$ *can be identified with* $N(\Gamma)/\Gamma$ *where* Γ *is the fundamental group of* M *and* $N(\Gamma)$ *is the normalizer of* Γ *in* $\mathrm{PSL}(2,\mathbb{C})$ *(see Remark 2.3).*

• *On the other hand, the isometries between finite index covers of* M *can be identified with* $Comm(\Gamma) = \{g \in \mathrm{PSL}(2,\mathbb{C}) : [\Gamma : \Gamma \cap g\Gamma g^{-1}] < \infty, [g\Gamma g^{-1} : \Gamma \cap g\Gamma g^{-1}] < \infty\}$. *So, the hidden symmetries of* M *are in one-to-one correspondence with the cosets of* $N(\Gamma)$ *in* $Comm(\Gamma)$ *(see p. 274 of [23]).*

Example 3.2. *Let* M *the figure eight knot complement. Then, we know from Example 2.2 that* M *is isometric to* $\mathbb{H}^3/\Gamma$ *where* $\Gamma = \left\langle \begin{pmatrix} 1 & 1 \\ 0 & 1 \end{pmatrix}, \begin{pmatrix} 1 & 0 \\ \omega & 1 \end{pmatrix} \right\rangle$. *Let* $g = \begin{pmatrix} 0 & \sqrt{-3} \\ 1 & 0 \end{pmatrix}$. *Let* $\Gamma_1 = (g\Gamma g^{-1}) \cap \Gamma$. *Let* $T = \left\{ \begin{pmatrix} a & b\sqrt{-3} \\ c & d \end{pmatrix} : a, b, c, d \in O_3 \right\}$ *where* O_3 *is the ring of integers of the number field* $\mathbb{Q}(\sqrt{-3})$. *We note that* g *normalizes* T. *We will write* $\mathrm{PGL}(2, O_3)$

to mean $\mathrm{GL}(2,O_3)/Z(\mathrm{GL}(2,O_3))$ *where* $\mathrm{GL}(2,O_3)$ *is the set of* 2×2 *matrices whose elements and whose matrix inverses' elements belong to* O_3 *and* $Z(\mathrm{GL}(2,O_3))$ *is the center of* $\mathrm{GL}(2,O_3)$. *We note that* T *is index* 4 *and* Γ *is index* 24 *subgroup of* $\mathrm{PGL}(2,O_3)$ *(see Remark 2 in Section 2 of [13]). So,* $\Gamma\cap T$ *has finite index in* Γ *and in turn, in* $\mathrm{PGL}(2,O_3)$. *This means* $g(\Gamma\cap T)g^{-1}$ *is also finite index in* $\mathrm{PGL}(2,O_3)$. *So,* $\Gamma\cap g(\Gamma\cap T)g^{-1}$ *has finite index in* Γ. *This implies* Γ_1 *is also finite index in* Γ. *So,* $\mathbb{H}^3/\Gamma_1$ *is finite index cover of* $\mathbb{H}^3/\Gamma$. *Now,* $g^{-1}\begin{pmatrix}1 & 1\\ 0 & 1\end{pmatrix}g=\begin{pmatrix}1 & 0\\ \frac{1}{\sqrt{-3}} & 1\end{pmatrix}$, *which does not belong to* $\mathrm{PGL}_2(O_3)$. *So,* $g\notin N(\Gamma)$. *So,* g *cannot induce a self-isometry of* $\mathbb{H}^3/\Gamma$. *On the other hand,* $g\Gamma_1 g^{-1}=\Gamma_1$ *since* g^2 *is identity matrix. So,* g *induces a self-isometry of* $\mathbb{H}^3/\Gamma_1$ *implying* g *induces a hidden symmetry of* $\mathbb{H}^3/\Gamma$, *the figure eight knot complement.*

g in the above example is in $Comm(\Gamma)$. Since the fundamental group Γ of the figure eight knot complement is arithmetic, $Comm(\Gamma)$ is dense in $\mathrm{PSL}(2,\mathbb{C})$ by Margulis's arithmeticity theorem (see [19, Theorem 10.3.5]). So, we can produce infinitely many such g's and so hidden symmetries of the figure eight knot complement. Note that this way of constructing hidden symmetries would also hold for more general arithmetic hyperbolic manifolds. Neumann and Reid gave the following characterization of knots with hidden symmetries:

Theorem 3.3 (Neumann-Reid, Proposition 9.1, [23])**.** *A hyperbolic knot complement has hidden symmetries if and only if it non-regularly covers an orbifold with a rigid cusp.*

In their proof of the above theorem, Neumann and Reid constructed this orbifold by taking a quotient of $\mathbb{H}^3$ by $Comm(\Gamma)$ where Γ is the fundamental group of the hyperbolic knot complement with hidden symmetries. Recall from Subsection 2.5.1 that a rigid cusp refers to $(2,3,6)$, $(3,3,3)$ or $(2,4,4)$ cusp. So, as a consequence of the above theorem, one can say the following:

Fact 3.4 (Corollary 2.2, [33])**.** *If a hyperbolic knot complement has hidden symmetries, then its cusp field is either* $\mathbb{Q}(i)$ *or* $\mathbb{Q}(i\sqrt{3})$.

In fact a relatively recent result of Hoffman [16] implies a stronger fact. Hoffman [16] showed:

Theorem 3.5 (Hoffman, Theorem 1.1, [16])**.** *A hyperbolic knot complement cannot cover*

an orbifold with a $(2, 4, 4)$ *cusp.*

This above theorem together with Theorem 3.3 yields the following:

Fact 3.6. *The cusp field of a hyperbolic knot complement with hidden symmetries is* $\mathbb{Q}(i\sqrt{3})$.

Going forward, we will often say hyperbolic knot with hidden symmetry to mean that the complement of the hyperbolic knot has hidden symmetries.

3.2 The Neumann-Reid question

Airthmetic knots admit infinitely many hidden symmetries by Margulis's result, but, the following seminal theorem of Reid shows figure eight knot is the only such knot:

Theorem 3.7 (Theorem 2, [32])**.** *The figure eight knot knot complement is the only hyperbolic knot complement which is arithmetic.*

Aitchison and Rubinstein [1, Example 5 and 6] constructed two hyperbolic knot complements by identifying faces of a regular ideal dodecahedron both of which cover an orbifold with $(2, 3, 6)$ cusp (for details see the explanation before Question 1 on p. 307 of [23]) thus implying via Theorem 3.3 that they have hidden symmetries. We don't know any other example of a hyperbolic knot with hidden symmetries. The following open question of Neumann and Reid is a testimony of this dearth of examples:

Question 3.8 (Neumann-Reid, Question 1, [23])**.** *Is there any hyperbolic knot except the figure eight knot and the two dodecahedral knots of Aitchison and Rubinstein [1] whose complement has hidden symmetries?*

3.2.1 Literature survey

1. Picture of a general 2-bridge link is shown in Figure 15. For a detailed discussion on 2-bridge links, we refer the readers to [29, Chapter 10]. The term 2-bridge refers to the fact that the link can be put in a position such that the y-coordinate of the projection has exactly two local maxima. One can associate a rational number corresponding

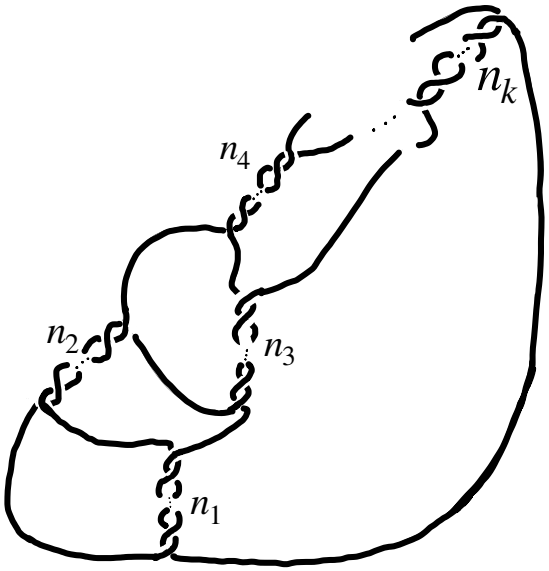

Figure 15: The general form of a 2-bridge link

to the 2-bridge link that is shown in Figure 15 by the continued fraction expression: $[n_1, n_2 \ldots, n_{k-1}, n_k]$ where $[n_1, n_2] = \frac{1}{n_1 + \frac{1}{n_2}}$ and $[n_1, n_2, \ldots, n_k] = [n_1, [n_2, \ldots, n_k]]$ defined inductively. When the denominator is odd, the 2-bridge link has only one component, i.e. it is a "2-bridge knot". Note that figure eight knot drawn in Figure 1 is a 2-bridge knot corresponding to the rational number $\frac{2}{5}$. Reid and Walsh proved the following:

Theorem 3.9 (Reid-Walsh, Theorem 3.1, [33])**.** *No hyperbolic* 2*-bridge knot except the figure eight knot can admit hideden symmetries.*

2. Macasieb and Mattman [18] discussed the family of hyperbolic $(-2, 3, 2m + 1)$ pretzel knots where $m \in \mathbb{Z} - \{0, 1, 2\}$ and m negative means $|m|$ number of right handed crossings (see Figure 1 in their paper for a picture). They showed the following:

   Theorem 3.10 (Macasieb-Mattman, Theorem 1.4, [18])**.** *Hyperbolic* $(-2, 3, 2m + 1)$ *pretzel knots do not have hidden symmetries.*

3. Berge manifold is the complement of a 2-component hyperbolic link (see Figure 1 in [14]). Hoffman [14] showed the following:

Theorem 3.11 (Hoffman, Proof of Theorem 1.1, [14]). *No hyperbolic knots except at-most finitely many of the ones obtained by* $(1, n)$ *Dehn fillings of the unknot of Berge Manifold has hidden symmetries.*

4. Millichap [21] investigated the hidden symmetries of hyperbolic $(q_1, q_2, \ldots, q_{2n+1})$ pretzel knots (see Figure 5 in [21] for a picture). He proved the following:

   Theorem 3.12 (Millichap, Proposition 7.5, [21]). *If for all* i *in* $\{1, \ldots, 2n+1\}$ q_i *is sufficiently large, then the hyperbolic* $(q_1, q_2, \ldots, q_{2n+1})$ *pretzel knots do not have hidden symmetries where* q_i *is even only for* $i = 1$ *and* $q_i \neq q_j$ *when* $1 \leq i \neq j \leq 2n+1$.

In the rest of the thesis, Question 3.8 will be our center of attention. We will discuss different approaches, techniques and corresponding results that shed some light in our understanding of the study of hidden symmetries of hyperbolic knot complements that stem from Question 3.8.

4.0 Dehn filling, geometric isolation and hidden symmetry

Most of the contents in this chapter are based on joint work [8] with Eric Chesebro and Jason DeBlois. We here state three results from [8] without proof: Proposition 4.5, Theorem 4.6 and Theorem 4.7. The results in Section 4.4 are already in [8], but, the proof that we present in this section is different from that in [8]. The discussion in Section 4.5 is (almost) verbatim from Example 5.3 of [8]. The content and the result in Section 4.6 is new and not part of [8]. All proofs presented in Section 4.6 are original. Figure 17 is taken directly and Figure 20 almost directly from [8].

4.1 A weaker question

It is hard to decipher what approach and machineries one should apply to directly attack Question 3.8. Thus, we restrict our attention to the following weaker question:

Question 4.1 (Conjecture 0.1, [8])**.** *Can there exist infinitely many hyperbolic knot complements admitting hidden symmetries all of whose volumes are bounded above by a constant?*

We know from Theorem 2.11 and Theorem 2.12 that one could produce a family of infinitely many hyperbolic 3-manifolds of bounded volume by Dehn filling all but one cusp of a given cusped hyperbolic 3-manifold. So, we focus on understanding Question 4.1 in regards to the families of hyperbolic knots obtained by Dehn filling all but one component of hyperbolic links.

4.2 Geometric isolation

Let O be an orbifold with torus cusps $c_1, \ldots, c_n$. As defined in [24], the set of cusps $\{c_1, \ldots, c_m\}$ is said to be *geometrically isolated* from the set of remaining cusps $\{c_{m+1}, \ldots, c_n\}$

if the shapes of the cusps $c_1, \ldots, c_m$ do not change under all but finitely many Dehn fillings on c_i cusp for each $i \in \{m+1, \ldots, n\}$.

Remark 4.2. *Neumann and Reid's actual definition does not allow the finitely many exceptions part that we do.*

Neumann and Reid showed the existence of hyperbolic manifold with geometrically isolated cusps:

Theorem 4.3 (Neumann-Reid, Theorem 2, [24])**.** *There exists a 2-cusped arithmetic manifold whose cusps are geometrically isolated.*

Its worth stating that geometric isolation is not a symmetric property, i.e, the fact that the set $\{c_1, \ldots, c_m\}$ is geometrically isolated from $\{c_{m+1}, \ldots, c_n\}$ does not imply that the set $\{c_{m+1}, \ldots, c_n\}$ is geometrically isolated from $\{c_1, \ldots, c_m\}$ (see Section 5 of [24]). But the following fact is true (the manifold version of the fact is mentioned as Fact 2.2 in [8]):

Fact 4.4. *Given a 2-cusped hyperbolic orbifold O if the cusps of O are symmetric, i.e, there is a self-isometry of O which exchanges the cusps, then geometrically isolation is a symmetric property.*

The fact above follows from Fact 2.15.

4.3 Dehn fillings, hidden symmetry and cusp fields

In this section, given a 2-cusped hyperbolic 3-manifold M, we relate the existence of hidden symmetries in infinitely many hyperbolic knots obtained from Dehn filling a fixed cusp of M to a geometric isolation of the cusps of M. We first describe Proposition 4.5 which helps us in our study of geometric isolation. We recall from Subsection 2.7.3 that $\mathcal{D}_0(M)$ is the irreducible component containing the complete structure of M in the deformation variety $\mathcal{D}(M)$ of M. We first define rational functions τ on $\mathcal{D}_0(M)$ whose values will give us the cusp moduli, as we will see in Proposition 4.5, which we need to understand geometric isolation.

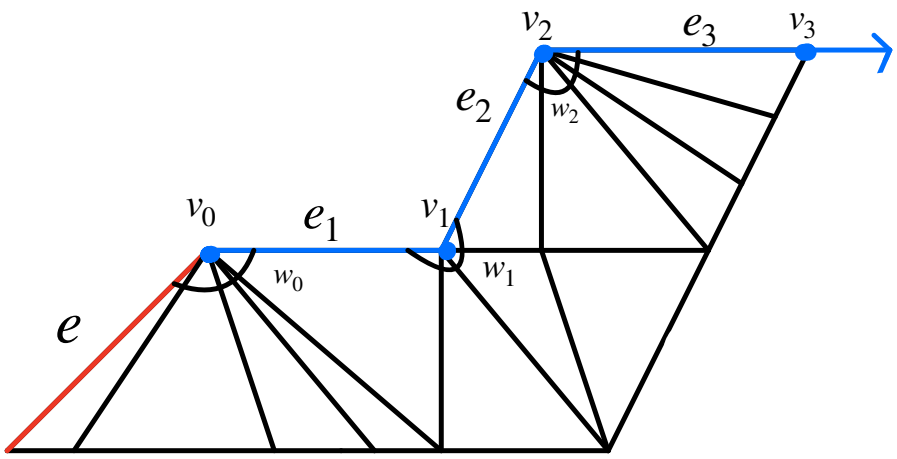

Figure 16: Construction of the cusp parameter function τ

Let M be a cusped hyperbolic 3-manifold with geometric triangulation $(\mathcal{T}, \mathcal{F})$. Let ∂c be a cusp cross section of the cusp c of M. We have seen in Subsection 2.7.2 that $(\mathcal{T}, \mathcal{F})$ introduces a triangulation $\mathfrak{T}_c$ of ∂c (into triangles). We fix a vertex v and an edge e of $\mathfrak{T}_c$ incident to v. Let γ be an oriented simplicial closed curve in ∂c passing through v. Let $\gamma = e_1 * e_2 * \cdots * e_n$, the concatenation of edges $e_1, \ldots, e_n \in \mathfrak{T}_c$ where e_i joins vertices v_{i-1} to v_i for each $i \in \{1, \ldots, n\}$. We may further assume that $v_0 = v_n = v$.

Let $\mathbf{z} \in \mathcal{D}_0(M)$. We have triangulation $(\mathcal{T}_\mathbf{z}, \mathcal{F}_\mathbf{z})$ associated with the hyperbolic structure $M_\mathbf{z}$ (which is in general, incomplete). If e is e_1, we define $w_0(\mathbf{z})$ to be 1, otherwise, $w_0(\mathbf{z})$ is defined to be the product of the shape parameters of all the edges of $\mathcal{T}$ that passes through v_0 between e and e_1 on the right of γ. For $j \in \{1, \ldots, n-1\}$, we define $w_j(\mathbf{z})$ as the product of the shape parameters of all the edges of $\mathcal{T}$ that passes through v_i on the right of γ. We define

$$\tau(\gamma)(\mathbf{z}) = \sum_{i=0}^{n-1} (-1)^i \prod_{j=0}^{i} w_j(\mathbf{z}). \tag{9}$$

Figure 16 (cf. Figure 2 of [8]) explains the construction of τ pictorially. Note that $\tau(\gamma)$ is a rational function on $\mathcal{D}_0(M)$ as are w_j's being the product of shape parameters. The following proposition describes the important properties of $\tau(\gamma)$.

Proposition 4.5 (Chesebro-DeBlois-Mondal, Proposition 1.6, [8]). *Given a closed oriented simplicial curve γ in ∂c containing v, the rational function $\tau(\gamma)$ defined on $\mathcal{D}_0$ as above satisfies the following properties:*

1. *$\tau(\gamma)$ is analytic near $\mathbf{z}^0$, the point representing the complete structure.*
2. *If γ is not null homotopic, then, $\tau(\gamma)(\mathbf{z}^0) \neq 0$.*
3. *If $\mathfrak{m}$ and $\mathfrak{l}$, both containing v, represent a generating pair for $\pi_1(\partial c)$, then on a neighborhood U of $\mathbf{z}^0$, for all $\mathbf{z} \in U$ such that $\mu(\mathfrak{m})(\mathbf{z}) = 1$, the value of $\frac{\tau(\mathfrak{l})}{\tau(\mathfrak{m})}$ at $\mathbf{z}$ is a cusp moduli of the complete geometrized cusp.*

Given a cusp c of a hyperbolic 3-manifold with an associated geometric triangulation and a choice of generators $\mathfrak{m}$ and $\mathfrak{l}$ in $\pi_1(\partial c)$, we will refer to $\frac{\tau(\mathfrak{l})}{\tau(\mathfrak{m})}$ as the *cusp parameter function* of cusp c. We will use τ_c to denote this cusp parameter function of c.

We now state the theorem that connects hidden symmetries with geometric isolation.

Theorem 4.6 (Chesebro-DeBlois-Mondal, Corollary 1.8, [8]). *Let M be a complete, oriented hyperbolic 3-manifold with two cusps c and c', and an ideal triangulation decorated by the choice of an edge of each simplex. Fix a cross section ∂c of the cusp c and simplicial curves $\mathfrak{m}$ and $\mathfrak{l}$ representing a generating pair for $H_1(\partial c)$, and let $\tau_c = \tau(\mathfrak{l})/\tau(\mathfrak{m})$ be a cusp parameter function for c. If infinitely many 1-cusped orbifolds produced by hyperbolic Dehn filling on c' cover orbifolds with rigid cusps then for $\mathbf{z}^0 \in \mathcal{D}_0$ corresponding to the complete hyperbolic structure on M:*

1. *$\tau_c(\mathbf{z}^0) \in \mathbb{Q}(i)$ or $\tau_c(\mathbf{z}^0) \in \mathbb{Q}(\sqrt{-3})$ and*
2. *τ_c is constant on the irreducible component of $\{\mathbf{z} \in \mathcal{D}_0(M) \,|\, \mu(\mathfrak{m})(\mathbf{z}) = 1\}$ containing $\mathbf{z}^0$, i.e., c is geometrically isolated from c'.*

In particular, this holds if infinitely many hyperbolic knot complements in $\mathbb{S}^3$ with hidden symmetries can be produced from M by Dehn filling c'.

When M has more than one cusps and we study the existence of hidden symmetries in infinitely many hyperbolic knots obtained from Dehn filling all but one cusp of M, we no longer have any geometric isolation implications. Nevertheless, we can conclude the following:

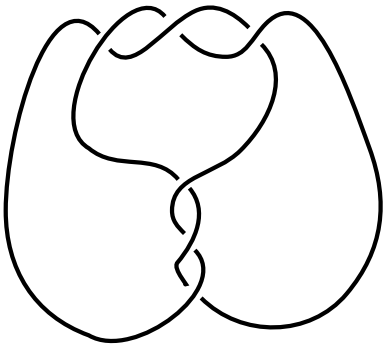

Figure 17: The 2-bridge link 6_2^2

Theorem 4.7 (Chesebro-DeBlois-Mondal, Corollary 1.4, [8]). *Let $L = K \sqcup L'$ be a hyperbolic link where L' is a link and K is a knot. Let $\mathcal{F}$ be a family of hyperbolic knots obtained by Dehn filling the components of L' such that elements of $\mathcal{F}$ geometrically converge to L. If infinitely many elements of $\mathcal{F}$ have hidden symmetries, then, the cusp field of K cusp in L is $\mathbb{Q}(i)$ or $\mathbb{Q}(i\sqrt{3})$.*

4.4 The link 6_2^2

In this section, our goal is to study the complement of the link 6_2^2 in $\mathbb{S}^3$ in Figure 17. We prove in Proposition 4.10 that the cusps of 6_2^2 are not geometrically isolated. It then implies Theorem 4.11 which says that a family of geometrically converging hyperbolic knots obtained from Dehn filling a cusp of 6_2^2 can not have infinitely many elements with hidden symmetries. We first note from Figure 17 that 6_2^2 is a 2-component two bridge link associated with the rational number $\frac{1}{3+\frac{1}{3}} = \frac{3}{10}$ (see part 1 of Subsection 3.2.1). Sakuma and Weeks in [36] laid out a process of finding a *canonical triangulation* for the hyperbolic two bridge link complements.

We will use this Sakuma-Weeks triangulation for 6_2^2 for our investigation of whether the cusps of 6_2^2 are geometrically isolated. We first briefly review this triangulation for 6_2^2.

We begin by noting the following fact:

Fact 4.8 (Section II.1, [36]). *For a 3-tuple u of distinct rational numbers (r_1, r_2, r_3) such that $r_i = \frac{p_i}{q_i}$ for each $i = 1, 2, 3$ and up to reordering, $p_3 = p_1 + p_2$ and $q_3 = q_1 + q_2$, the lines passing through points in $\mathbb{Z}^2$ with slopes r_1, r_2 and r_3 determine a triangulation of $(\mathbb{R}^2, \mathbb{Z}^2)$.*

Let us denote this triangulation as T_u. Now, consider the following 3-tuples of rational numbers $t_1 = (0, 1, \frac{1}{2})$, $t_2 = (0, \frac{1}{2}, \frac{1}{3})$, $t_3 = (0, \frac{1}{3}, \frac{1}{4})$ and $t_4 = (\frac{1}{3}, \frac{1}{4}, \frac{2}{7})$. Note that T_{t_i} and $T_{t_{i+1}}$ share the edges of exactly two slopes - 0 and $\frac{1}{i+1}$ for $i = 1, 2$; $\frac{1}{3}$ and $\frac{1}{4}$ for $i = 3$. If we put a copy of $\mathbb{R}^2$ with triangulation $T_{t_{i+1}}$ above a copy of $\mathbb{R}^2$ with triangulation T_{t_i} so that the edges shared by T_{t_i} and $T_{t_{i+1}}$ are identified, it will produce a sheet of tetrahedra with 2-simplices of $T_{t_{i+1}}$ as top faces and 2-simplices of T_{t_i} as bottom faces. For each i, the edges shared by T_{t_i} and $T_{t_{i+1}}$ divide the plane up into a tiling by quadrilaterals, and the remaining edges of T_{t_i} and $T_{t_{i+1}}$ are opposite diagonals of these quadrilaterals. Therefore if we identify two copies of $\mathbb{R}^2$ along the edges shared by $T_{t_i}$and $T_{t_{i+1}}$, each quadrilateral doubles to a copy of $\mathbb{S}^2$ that is triangulated by edges of T_{t_i} and $T_{t_{i+1}}$ as the boundary of a tetrahedron. We fill each such $\mathbb{S}^2$ with a tetrahedron. Note that the vertices of the tetrahedra come from the points of $\mathbb{Z}^2$. We consider these tetrahedra with their vertices removed. Let us call this sheet of (vertices removed) tetrahedra $\mathcal{S}_i$. The top faces of $\mathcal{S}_i$ and the bottom faces of $\mathcal{S}_{i+1}$ can be identified with 2-simplices of triangulation $T_{t_{i+1}}$ of $\mathbb{R}^2$. This will give face pairing identifications between the top faces of $\mathcal{S}_i$ and the bottom faces of $\mathcal{S}_{i+1}$.

Let W be the group of Euclidean isometries of $\mathbb{R}^2$ generated by the rotations of angle π around points in $\mathbb{Z}^2$. W preserves the points of $\mathbb{Z}^2$ as well as the slopes of the lines. Consequently, W preserves each T_{t_i}. For each $\mathcal{S}_i$, the action of W on $\mathbb{R}^2$ can be extended to an action on $\mathcal{S}_i$ by identifying W with the group generated by rotations of angle π around the vertical axes through the points of $\mathbb{Z}^2$. The fundamental domains of each of these actions consist of two tetrahedra. From each $\mathcal{S}_i$, if we choose two such tetrahedra Δ_i and Δ_{i+1}, we get a total of 6 tetrahedra. Now, note that each face F of either of these 6 tetrahedra except the bottom faces of S_1 and the top faces of S_3 can be identified with another face F' of one of these 6 tetrahedra (which is not a bottom face of S_1 and top face of S_3) via the face pairing identifications from last paragraph and action of W. Let's call the set of face pairings given

by these identifications $\mathcal{F}_{stack}$.

Now note that the bottom faces of $\mathcal{S}_1$ correspond to 2-simplices in T_{t_1} and top faces of $\mathcal{S}_3$ correspond to 2-simplices in T_{t_3}. For any 2 simplex *tri* of T_{t_1} (respectively, T_{t_3}) there is a unique 2 simplex *tri*′ of T_{t_1}(respectively, T_{t_3}) sharing the edge of slope $\frac{1}{2}$ (respectively, $\frac{1}{4}$). We identify *tri* with *tri*′ via a linear map which fixes the vertices on the common edge and exchanges the third vertices. These identifications are equivariant under the action of W and so gives a face pairing amongst the bottom faces of $\mathcal{S}_1$ and amongst the top faces of $\mathcal{S}_3$. Let's call the set of these face pairings $\mathcal{F}_{linear}$. Let $\mathcal{T}$ be the set of tetrahedra $\{\Delta_i\}_{i=1,2,3}$ and $\mathcal{F} = \mathcal{F}_{stack} \cup \mathcal{F}_{linear}$. Sakuma and Weeks prove that

Theorem 4.9 (Theorem II.2.4, [36])**.** $(\mathcal{T}, \mathcal{F})$ *is a geometric triangulation of* $\mathbb{S}^3 - 6_2^2$.

We show the tetrahedra of the Sakuma-Weeks triangulation of 6_2^2 complement in Figure 18. Pairs of consecutive triangulations of $\mathbb{R}^2$ are shown in the left of Figure 18 (cf. Figure II.2.5 in [36], Figure 3 in [22]). We straighten up these pairs in the right of Figure 18 to see three pairs of ideal tetrahedra (Δ_i, Δ_{i+1}) for i in $\{1, 2, 3\}$. We denote the faces of tetrahedra by F_i and F_i' for $i \in \{1, \ldots, 8\}$ and by $F_{b_1}, F_{b_1}', F_{b_2}, F_{b_2}', F_{t_1}, F_{t_1}', F_{t_2}$ and F_{t_2}'. We use [36]'s face pairings to see that F_i is identified with F_i' for i in $\{1, \ldots, 8\}$, F_{b_i} with F_{b_i}' for $i = 1, 2$ and F_{t_i} with F_{t_i}' for $i = 1, 2$ via the linear maps as follows:

$$
\begin{aligned}
F_1 &: && ((0,0),(2,1),(3,1)) \leftrightarrow ((2,0),(4,1),(5,1)) && : F_1' \\
F_2 &: && ((0,0),(3,1),(1,0)) \leftrightarrow ((0,0),(3,1),(1,0)) && : F_2' \\
F_3 &: && ((1,0),(3,1),(4,1)) \leftrightarrow ((1,0),(3,1),(4,1)) && : F_3' \\
F_4 &: && ((1,0),(4,1),(2,0)) \leftrightarrow ((1,0),(4,1),(2,0)) && : F_4' \\
F_5 &: && ((0,0),(3,1),(4,1)) \leftrightarrow ((0,0),(3,1),(4,1)) && : F_5' \\
F_6 &: && ((0,0),(4,1),(1,0)) \leftrightarrow ((6,2),(10,3),(7,2)) && : F_6' \\
F_7 &: && ((1,0),(4,1),(5,1)) \leftrightarrow ((7,2),(4,1),(3,1)) && : F_7' \\
F_8 &: && ((1,0),(5,1),(2,0)) \leftrightarrow ((7,2),(3,1),(6,2)) && : F_8' \\
F_{b_1} &: && ((0,0),(2,1),(1,0)) \leftrightarrow ((2,0),(4,1),(3,1)) && : F_{b_1}' \\
F_{b_2} &: && ((1,0),(2,1),(3,1)) \leftrightarrow ((1,0),(2,0),(3,1)) && : F_{b_2}' \\
F_{t_1} &: && ((0,0),(7,2),(4,1)) \leftrightarrow ((6,2),(3,1),(10,3)) && : F_{t_1}' \\
F_{t_2} &: && ((0,0),(3,1),(7,2)) \leftrightarrow ((10,3),(3,1),(7,2)) && : F_{t_2}'
\end{aligned}
$$

We note that the identifications above partition the vertices into two equivalence classes: one consisting of $(0,0)$, $(2,0)$, $(6,0)$, $(2,1)$, $(4,1)$ and $(10,3)$, and the second consisting of $(1,0)$, $(3,1)$, $(5,1)$ and $(7,2)$. Each of this equivalence class corresponds to a cusp of $\mathbb{S}^3 - 6_2^2$. We will denote the first class by $[(0,0)]$ and the second by $[(1,0)]$.

We now choose one edge from each Δ_i and denote its shape parameters by z_i. The shape parameters of other edges of Δ_i will then be determined as described in Fact 2. We recall from Subsection 2.7.2 that since $(\mathcal{T}, \mathcal{F})$ is a geometric triangulation, these shape parameters satisfy the edge equations and the holonomy equations. For each edge of $\mathbb{S}^3 - 6_2^2$ as shown

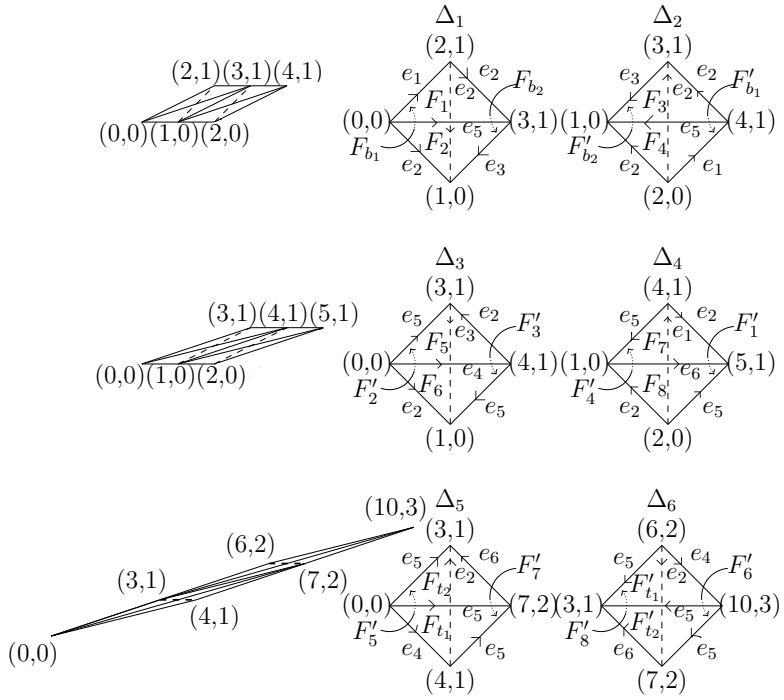

Figure 18: Sakuma-Weeks triangulation of $\mathbb{S}^3 \setminus 6_2^2$

in Figure 18 the corresponding edge equation is determined as follows:

$$\text{edge } e_1 : \zeta_1(z_1)z_4\zeta_1(z_2) = 1 \tag{10}$$

$$\text{edge } e_2 : z_1z_2z_5z_6(\zeta_2(z_1)\zeta_2(z_3)\zeta_2(z_4)\zeta_2(z_2))^2 = 1 \tag{11}$$

$$\text{edge } e_3 : \zeta_1(z_1)z_3\zeta_1(z_2) = 1 \tag{12}$$

$$\text{edge } e_4 : z_3\zeta_2(z_5)\zeta_2(z_6) = 1 \tag{13}$$

$$\text{edge } e_5 : z_1z_2z_5z_6(\zeta_1(z_3)\zeta_1(z_4)\zeta_1(z_5)\zeta_1(z_6))^2 = 1 \tag{14}$$

$$\text{edge } e_6 : z_4\zeta_2(z_5)\zeta_2(z_6) = 1. \tag{15}$$

Equations 10 and 12 imply that

$$z_3 = z_4 = \frac{1}{\zeta_1(z_1)\zeta_1(z_2)}. \tag{16}$$

Similarly from Equations 13 and 15, we get

$$z_3 = z_4 = \frac{1}{\zeta_2(z_5)\zeta_2(z_6)}. \tag{17}$$

Using Equations 16 and 17, we get

$$\zeta_1(z_1)\zeta_1(z_2) = \zeta_2(z_5)\zeta_2(z_6). \tag{18}$$

Note that Equation 14 can be derived from Equation 11, Equation 16 and Equation 17.

So, the deformation variety $\mathcal{D}(\mathbb{S}^3 - 6_2^2)$ is the set of tuples (z_1, z_2, z_5, z_6) of complex numbers satisfying Equation 11 and 18.

In Section II.4, [36] also shows how one can find the cusp triangulation for a two bridge link complement from its canonical decomposition. We follow their procedure to obtain the cusp triangulation picture of a cusp of 6_2^2. Figure 19 (cf. figure II.4.1 of [36]) shows the cusp triangulation of the cusp corresponding to $(0, 0)$. In Figure 19, we choose two generators $m_{(0,0)}$ (the blue edge) and $l_{(0,0)}$ (the red edge) for the homology of the cusp torus of the cusp at $(0, 0)$.

We assume that the cusp at [(0,0)] is complete. Following Equation 4, we find the holonomy equation at the cusp at $[(0, 0)]$ as below:

$$\mu(m_{(0,0)}) = -\zeta_2(z_4)\zeta_2(z_2)z_2\zeta_2(z_1)\zeta_2(z_3)z_6 = 1. \tag{19}$$

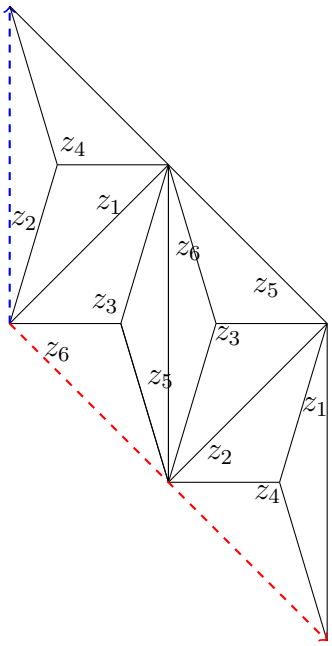

Figure 19: Sakuma-Weeks cusp triangulation of 6_2^2 at $[(0,0)]$

We use the help of [17] for the calculations below.

We see that Equation 19 gives us,

$$z_6 = \frac{\zeta_1(z_2)}{\zeta_2(z_1)\zeta_2(z_3)^2} = -\frac{(-1+z_1)z_1(-1+z_2)}{(z_1+z_2-z_1z_2)^2}. \tag{20}$$

Using the above equation with Equation 11 and Equation 16 we get,

$$z_5 = \frac{\zeta_1(z_1)}{\zeta_2(z_2)\zeta_2(z_3)^2} = -\frac{(-1+z_1)(-1+z_2)z_2}{(z_1+z_2-z_1z_2)^2}. \tag{21}$$

If we denote the algebraic subset of $\mathcal{D}(\mathbb{S}^3 - 6_2^2)$ where the cusp at $[(0,0)]$ is complete as V_0, then, $V_0 = \{(z_1, z_2) : p(z_1, z_2) = 0\}$ where

$$\begin{aligned} p(z_1,z_2) =& z_1^3 + 2z_1^2z_2 - z_1^3z_2 - z_1^4z_2 + 2z_1z_2^2 - z_1^2z_2^2 - \\ & 4z_1^3z_2^2 + 3z_1^4z_2^2 + z_2^3 - z_1z_2^3 - 4z_1^2z_2^3 + \\ & 7z_1^3z_2^3 - 3z_1^4z_2^3 - z_1z_2^4 + 3z_1^2z_2^4 - 3z_1^3z_2^4 + \\ & z_1^4z_2^4. \end{aligned} \tag{22}$$

We get this polynomial from Equation 18 by replacing z_5 and z_6 in terms of z_1 and z_2 with the help of Equations 20 and 21.

We will now write the cusp parameter function for the cusp at $[(0,0)]$ using Equation 9. We choose $m_{(0,0)}$ as the reference edge. This gives us $\tau(m_{(0,0)}) = 1$. From Figure 19, we see that $\tau(l_{(0,0)}) = \zeta_2(z_2)\zeta_2(z_4) - \zeta_2(z_2)\zeta_2(z_4)\zeta_1(z_4)z_1\zeta_1(z_3)\zeta_1(z_5)z_6\zeta_1(z_5)$. On V_0, using Equations 16, 21 and 20, one can write all of z_3, z_4, z_5 and z_6 in terms of z_1 and z_2. Then, on V_0, the cusp parameter function τ have the formula:

$$\begin{aligned}\tau =&((z_1(-1+z_2)-z_2)(z_1^4(-1+z_2)^4+z_2^2-2z_1(-1+z_2)z_2^2+\\ &z_1^2(1+z_2-3z_2^2+z_2^4)+\\ &z_1^3(-1+z_2(3-2z_2(3+(-3+z_2)z_2))))))/\\ &((-1+z_1)z_2(z_1(z_1(-1+z_2)-z_2)(-1+z_2)+z_2)^2). \qquad (23)\end{aligned}$$

In Theorem II.3.2 of their paper [36], Sakuma and Weeks described the (orientation preserving) combinatorial symmetries of the canonical triangulation of the (hyperbolic) two bridge links. They [36, p. 415] provide elements of this symmetry group, which for our discussion on 6_2^2, exchanges Δ_i and Δ_{i+1} for $i = 1, 3, 5$. Using Mostow-Prasad rigidity (see Theorem 2.3.1) one can see these combinatorial symmetries are hyperbolic isometries as well, implying $z_i = z_{i+1}$ for $i = 1, 3, 5$.

So, solving for $z_1 = z_2$ in $p(z_1, z_2) = 0$ we see that, $z_1 = z_2 = \frac{3+\sqrt{3}i}{2}$ is the only solution with positive imaginary part. So, $z_1 = z_2 = \frac{3+\sqrt{3}i}{2}$ corresponds to the complete structure. Now at the complete structure, i.e. at $z_1 = z_2 = \frac{3+\sqrt{3}i}{2}$, we have $\frac{\partial p}{\partial z_1} = \frac{\partial p}{\partial z_2} = \frac{9+9\sqrt{3}i}{2}$. So, by implicit function theorem, both z_1 and z_2 can be taken as a parameter for V_0 and $\frac{dz_2}{dz_1} = \frac{dz_1}{dz_2} = -1$ around the complete structure. We use z_1 as the parameter for V_0 near the complete structure. Using this information, we can now apply chain rule repeatedly to write the derivatives of z_2 (with respect to z_1) in terms of z_1 and z_2. We compute, $\frac{d\tau}{dz_1} = 0$ and $\frac{d^2\tau}{dz_1^2} = \frac{-3-\sqrt{3}i}{9}$. Since $\frac{d^2\tau}{dz_1^2}$ is non-zero at the complete structure, we conclude that τ is not constant near the complete structure in V_0. This together with Fact 4.4 (re)prove the following:

Proposition 4.10 (Corollary 3.3, [8]). *The cusps of 6_2^2 are not geometrically isolated from each other.*

We can now use Theorem 4.6 to conclude the following:

Theorem 4.11 (Corollary 3.4, [8]). *A family of hyperbolic knots obtained by Dehn filling a fixed cusp of 6_2^2 can have at most finitely many elements with hidden symmetries.*

Remark 4.12. *Even though the proof of Proposition 4.10 in [8] uses deformation variety, it is somewhat different. Instead using the calculus based approach, the proof there uses algebraic geometric nature of V_0 and the cusp parameter function. Also, the Sakuma-Weeks triangulation there is obtained by stacking down the $\mathbb{R}^2$ triangulations T_{t_i} one after another in contrast with what we do here, which is stacking up the T_{t_i}'s.*

4.5 Berge manifold

Here we will apply Theorem 4.6 to (re-)prove that Dehn filling one cusp of the *Berge manifold* $M = \mathbb{S}^3 - L$, where L is a certain 2-component link in $\mathbb{S}^3$ (see [14, Fig. 1]), produces at most finitely many hyperbolic knot complements with hidden symmetries. This was first established in the proof of [14, Theorem 1.1] by Hoffman, whose later result [15, Theorem 6.1] implies that in fact no hyperbolic knot complement with hidden symmetries is produced by Dehn filling a cusp of M. This stronger assertion is out of reach of Theorem 4.6.

M is triangulated by four regular ideal tetrahedra (see eg. [11]). It therefore covers the Bianchi orbifold $\mathrm{PSL}(2, O_3)$ and thus satisfies condition (1) of Theorem 4.6, so we will use condition (2). SnapPy finds an involution of M exchanging the two cusps. As only one component of L is unknotted, this involution does not extend to $\mathbb{S}^3$; nor does it preserve the triangulation by regular ideal tetrahedra, since this induces different triangulations of the cusps' cross sections. Nonetheless, by appealing to Fact 4.4 we may conclude that neither cusp is geometrically isolated from the other after checking this for only one of them.

We check the cusp c corresponding to the unknotted component of L. A cross section inherits the triangulation pictured in Figure 20, with parallel sides identified by translations.

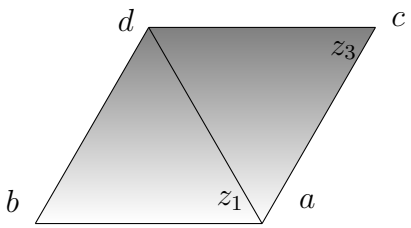

Figure 20: The induced triangulation of a cusp cross section of the Berge manifold

(The triangulation may be extracted from Regina [5] after entering its isomorphism signature "jLLzzQQccdffihhiiqffofafoaa". The *isomorphism signature* is a combinatorial invariant of a triangulation introduced by Burton [4]; this particular one is the *isometry signature* of M as defined in [11], an isometry invariant which can be computed by SnapPy.) Taking $\mathfrak{m}$ to be the projection of the horizontal sides of the parallelogram, equation (9) yields:

$$\mu(\mathfrak{m}) = -\zeta_1(z_1)\zeta_1(z_3)z_3 = \frac{-z_3}{(1-z_1)(1-z_3)}.$$

The triangulation's edge equations are:

$$f_1 = 0, \text{ where } f_1(z_1, z_2, z_3, z_4) = z_4(1-z_3) - z_3z_2(1-z_4)(1-z_1) \tag{24}$$

$$f_2 = 0, \text{ where } f_2(z_1, z_2, z_3, z_4) = z_4(1-z_3) - z_1(1-z_2). \tag{25}$$

Equations (24) and (25) cut out $\mathcal{D}_0(M)$ in $\mathbb{C}^4$. To show that c is not geometrically isolated from the other cusp of M, we need to show that the cusp parameter function τ_c is non-constant on the irreducible component V_0 that contains the discrete, faithful representation, of the algebraic subset of $\mathcal{D}_0(M)$ where $\mu(\mathfrak{m}) = 1$. By the above, this subset is cut out by

$$f_3 = 0, \text{ where } f_3(z_1, z_2, z_3, z_4) = z_3 + (1-z_1)(1-z_3) = 1 - z_1(1-z_3).$$

To compute τ_c we take $\mathfrak{l}$ to be the projection of the diagonal sides of the parallelogram in Figure 20, oriented from b to d, and appeal to Proposition 4.5. Letting the reference edge f of the Proposition equal $\mathfrak{m}$, we obtain $\tau_c = \zeta_2(z_1)$, which is constant on V_0 if and only if z_1 is.

As in Section 4.4, we will use a calculus-based approach to show that z_1 is non-constant on V_0. Specifically, we will use the implicit function theorem to show that z_2 is a parameter for V_0 near the point $\vec{\eta} \doteq (\eta, \eta, \eta, \eta)$, for $\eta = \frac{1+\sqrt{-3}}{2}$, corresponding to the complete hyperbolic structure, and that $\frac{d^2 z_1}{dz_2^2} \neq 0$ at $\vec{\eta}$. (As the given triangulation of the complete hyperbolic manifold M is by regular ideal tetrahedra, $\vec{\eta}$, which we note is a fixed point of ζ_1 and ζ_2, corresponds to the complete structure. And since τ_c is an even function of $\log z_2$ [25, Lemma 4.1(b)], we have $\frac{dz_1}{dz_2} = 0$.)

By the implicit function theorem, z_2 is a parameter for V_0 (and hence non-constant on it) in a neighborhood of $\vec{\eta}$ if and only if the partial derivative matrix

$$M_2 = \left(\frac{\partial f_i}{\partial z_j}(\vec{\eta}) \right)_{j=1,3,4}^{i=1,2,3}$$

is non-singular. A straightforward computation shows that it is. Implicit function theorem also implies that $(\frac{dz_1}{dz_2}, \frac{dz_3}{dz_2}, \frac{dz_4}{dz_2})^T = -M_2^{-1}\vec{v}$ around $\vec{\eta}$, where $\vec{v} = (\frac{\partial f_1}{\partial z_2}, \frac{\partial f_2}{\partial z_2}, \frac{\partial f_3}{\partial z_2})^T$. Using this formula and chain rule repeatedly, one can write all higher power derivatives of z_i with respect to z_2 in terms of all the z_i's. From [17] we see that, $\frac{d^2 z_1}{dz_2^2} = \frac{i}{\sqrt{3}} \neq 0$ at $\vec{\eta}$ so z_1 is non-constant around $\vec{\eta}$ inside V_0. This together with Fact 4.4 proves,

Theorem 4.13 (Example 5.3, [8])**.** *Cusps of the Berge manifold are not isolated from each other.*

Now using Theorem 4.6, we see that a given family of hyperbolic knots obtained from Dehn filling a cusp of the Berge manifold has at-most finite elements admitting hidden symmetries.

4.6 The link $L10n46$

$L10n46$, also known as $otet08_{00002}$ from [11], (see Figure 3 in [11]), is a 2-component tetrahedral link, i.e. it decomposes into regular ideal tetrahedra. Similarly as in the last two sections, we will investigate a geometric isolation property for this link and comment on its relation with hidden symmetries. We denote $\mathbb{S}^3 - L10n46$ by M. M decomposes into 8

regular ideal tetrahedra. As in the case of Berge manifold, we find the isometry signature of this link in SnapPy [9], which turns out to be "mvLLwMAQQdfeihgjlkkjlloafaofoqfofaq". We use this as the isomorphism signature in Regina [5] to get a SnapPy triangulation for this link which consists of regular ideal tetrahedra. We use this triangulation to find the following edge equations:

$$z_0 z_1 z_7 z_6 \zeta_2(z_4)\zeta_1(z_5) = 1 \tag{26}$$

$$\zeta_1(z_0) z_5 z_2 z_1 z_4 \zeta_2(z_6) = 1 \tag{27}$$

$$\zeta_2(z_0)\zeta_1(z_6)\zeta_2(z_7)\zeta_1(z_3)\zeta_2(z_2)\zeta_1(z_1) = 1 \tag{28}$$

$$\zeta_2(z_0)\zeta_1(z_3)\zeta_2(z_4)\zeta_1(z_1)\zeta_2(z_7)\zeta_2(z_5) = 1 \tag{29}$$

$$\zeta_1(z_0)\zeta_2(z_1)\zeta_1(z_4)\zeta_2(z_5)\zeta_1(z_2)\zeta_2(z_3) = 1 \tag{30}$$

$$z_0 z_3 z_7 \zeta_1(z_5)\zeta_2(z_2) z_6 = 1 \tag{31}$$

$$\zeta_2(z_1)\zeta_1(z_2)\zeta_1(z_6)\zeta_1(z_4)\zeta_2(z_3)\zeta_1(z_7) = 1 \tag{32}$$

$$z_2 z_3 z_4 z_5 \zeta_1(z_7)\zeta_2(z_6) = 1. \tag{33}$$

Since $L10n46$ is a 2-component link, $\mathcal{D}_0(\mathbb{S}^3 - L10n46)$ has dimension 2 and one can write down the deformation variety by finding out which rows of the edge equation matrix P form the basis for the row space (see Theorem 2.20 and the related discussion in Subsection 2.7.3). Using Mathematica [17], we see that the first six rows of R is the basis for the row space of R. So, $\mathcal{D}(M)$ is the set of tuples $(z_0, z_1, \ldots, z_7)$ satisfying equations 26 through 31. Figure 21 represents the cusp triangulation from [5] of the cusp with 8 2-simplices in its triangulation (the other cusp has 24 2-simplices in its triangulation). Let's denote the cusp with 8 2-simplices as c and the cusp with 24 2-simplices as c'. The red and blue edges in Figure 21, denoted by m and l respectively, are two chosen generators of the cusp torus for c. So, the derivative of the holonomy of the longitude is

$$\mu(l) = \frac{\zeta_1(z_5)\zeta_1(z_1)}{z_2\zeta_2(z_7)}. \tag{34}$$

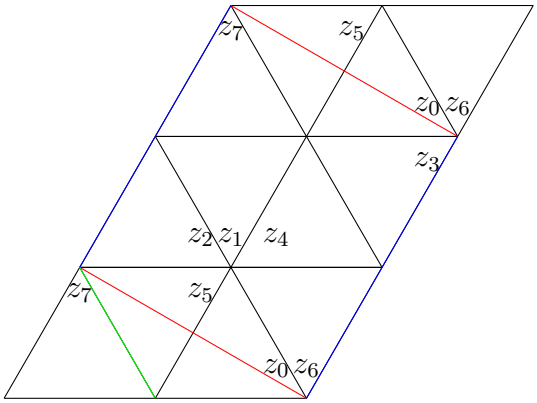

Figure 21: Cusp triangulation of $\mathbb{S}^3 - L10n46$

So, V_0 is the algebraic subset of $\mathcal{D}(M)$ cut out by setting $\mu(l) = 1$. (In the rest of the section, we use the help of [17] for the calculations.) Note that from Equations 26, 34 and 31, we get,

$$z_7 = \frac{z_4 z_5 - z_4}{z_0 z_1 z_6 - z_0 z_1 z_4 z_6} \tag{35}$$

$$z_2 = \frac{z_4 - z_1 z_4}{z_1(z_4(z_5 - 1) + z_0 z_1(z_4 - 1) z_6)} \tag{36}$$

$$z_3 = \frac{(z_1 - 1) z_1 (z_4 - 1)}{z_4(z_1 z_5 - 1) + z_0 z_1^2 (z_4 - 1) z_6}. \tag{37}$$

We write $\mathbf{z}$ for the tuple $(z_0, z_1, z_4, z_5, z_6)$. Substituting z_7, z_2 and z_3 from above formulae we get polynomial equations $p_1(\mathbf{z}) = 0$, $p_2(\mathbf{z}) = 0$, $p_3(\mathbf{z}) = 0$ and $p_4(\mathbf{z}) = 0$ from Equations

27, 28, 29 and 30 respectively, where,

$$\begin{aligned}
p_1(\mathbf{z}) =&(-1+z_1)z_4^2z_5(-1+z_6)-\\
&(-1+z_0)z_6(z_4(-1+z_5)+z_0z_1(-1+z_4)z_6)\\
p_2(\mathbf{z}) =&(-1+z_0)(z_4(-1+z_5)+z_0z_1(-1+z_4)z_6)(z_4(-1+z_1z_5)+\\
&z_0z_1^2(-1+z_4)z_6)^2-\\
&z_0(-1+z_1)^2z_4^2(-1+z_5)(-1+z_6)(-z_4+\\
&z_1(-1+z_4+z_4z_5+z_1(-1+z_4)(-1+z_0z_6)))\\
p_3(\mathbf{z}) =&(-1+z_0)(-1+z_4)(z_4(-1+z_5)+\\
&z_0z_1(-1+z_4)z_6)(z_4(-1+z_1z_5)+z_0z_1^2(-1+z_4)z_6)+\\
&z_0(-1+z_1)z_4^2z_5(-z_4+\\
&z_1(-1+z_4+z_4z_5+z_1(-1+z_4)(-1+z_0z_6)))\\
p_4(\mathbf{z}) =&(-1+z_5)(z_4(-1+z_5)+z_0z_1(-1+z_4)z_6)(-z_4+\\
&z_1(-1+z_4+z_4z_5+z_1(-1+z_4)(-1+z_0z_6)))+(-1+\\
&z_0)z_1(-1+z_4)^2z_5(z_4(-1+z_1z_5)+z_0z_1^2(-1+z_4)z_6). \qquad (38)
\end{aligned}$$

Let $p:\mathbb{C}^5\to\mathbb{C}^4$ be the function defined as $p=(p_1,p_2,p_3,p_4)$. So, $V_0=\{\mathbf{z}=(z_0,z_1,z_4,z_5,z_6):p(\mathbf{z})=0\}$.

Now, in Figure 21, in order to apply Proposition 4.5, we choose the green edge as the reference edge e. So, by Equation 9 and Proposition 4.5, we get, $\tau(\mathbf{z})=\frac{\tau(m)(\mathbf{z})}{\tau(l)(\mathbf{z})}$ where $\tau(m)(\mathbf{z})=-\frac{z_0+z_5-1}{(z_0-1)(z_5-1)}$ and $\tau(l)(\mathbf{z})=\frac{z_4+z_0z_1z_6-z_1z_4(z_5+z_0z_6)}{(z_1-1)z_4(z_5-1)}$.

At the complete structure (and so in a neighborhood around the complete structure), rank of the derivative matrix of p, Dp, is $Rank(\mathfrak{M})$ where $\mathfrak{M}$ is the minor of Dp which excludes the last column (i.e. the column consisting the partials of components of p with respect to z_6). But, $Rank(\mathfrak{M})$ is 4. So, by implicit function theorem, in a neighborhood around the complete structure, z_6 is a parameter for V_0 and

$$\begin{pmatrix}\frac{dz_0}{dz_6}\\ \frac{dz_1}{dz_6}\\ \frac{dz_4}{dz_6}\\ \frac{dz_5}{dz_6}\end{pmatrix}=-\mathfrak{M}^{-1}\begin{pmatrix}\frac{\partial p_1}{\partial z_6}\\ \frac{\partial p_2}{\partial z_6}\\ \frac{\partial p_3}{\partial z_6}\\ \frac{\partial p_4}{\partial z_6}\end{pmatrix}. \qquad (39)$$

Using the above equation, we write the derivatives of z_0, z_1, z_4 and z_5 with respect to z_6 in terms of z_0, z_1, z_4, z_5 and z_6. We finally find $\frac{d\tau}{dz_6} = 0$ and $\frac{d^2\tau}{dz_6^2} = \frac{4i}{3\sqrt{3}} \neq 0$. This proves the following:

Proposition 4.14. *In the* 2*-component link* $L10n46$*, cusp* c *is not geometrically isolated from cusp* c'*.*

Using Theorem 4.6, we can now conclude that a family of hyperbolic knots obtained from Dehn filling c' can not contain infinitely many elements with hidden symmetries.

5.0 Hidden symmetry and orbifold covering

The contents of this chapter are from joint work [7] with Eric Chesebro, Jason DeBlois, Neil R Hoffman, Christian Millichap and William Worden. The following results from [7] are stated here without proof: Theorem 5.1, Theorem 5.3, Proposition 5.4 and Lemma 5.5. We include proofs (using some of these stated results) of the following results from [7]: Theorem 5.6, Proposition 5.7, Theorem 5.8 and Corollary 5.9. One argument in the proof of Theorem 5.6 slightly differs from that in [7]. The language in the proofs of Proposition 5.7, Theorem 5.8 and Corollary 5.9 are (almost) verbatim from respectively the proofs of Corollary 6.15, Proposition 6.16 and Corollary 6.17 of [7]. Figure 24 is taken directly from [7].

5.1 The orbifold covering result

The geometric isolation criteria (see Theorem 4.6 in the last chapter) that came in handy in our study of hidden symmetries for hyperbolic knots coming from Dehn fillings of 2-component hyperbolic links do not extend for our study of (Dehn fillings on cusps of) hyperbolic links with more than two components. In the same theorem in the last chapter we have also seen that for a family $\mathcal{F}$ of hyperbolic knots originating from Dehn filling a cusp of 2-component link, how the cusp fields being $\mathbb{Q}(i)$ (or $\mathbb{Q}(i\sqrt{3})$) for infinitely many members of $\mathcal{F}$ would imply that the cusp field of the non-filled cusp to also be $\mathbb{Q}(i)$ (or $\mathbb{Q}(i\sqrt{3})$). In this chapter, we state a result that says that this kind of passing of properties to the geometric limit also holds for the property of covering rigid cusped orbifolds. But, before doing that, we will need to define what Dehn filling on pillowcase cusp means.

Let (p, q) be a pair of integers with $gcd(p, q) = d$. Recall from Section 2.6 that the orbifold $(\mathbb{D}^2 \times \mathbb{S}^1)_d$ is the quotient of $\mathbb{D}^2 \times \mathbb{S}^1$ by order d rotation around $\{0\} \times \mathbb{S}^1$ and the image of meridian m in $(\mathbb{D}^2 \times \mathbb{S}^1)_d$ is denoted as m_d. There is order 2 rotational symmetry r of $(\mathbb{D}^2 \times \mathbb{S}^1)_d$ with its rotational axis intersecting the boundary of $(\mathbb{D}^2 \times \mathbb{S}^1)_d$ in four points. The quotient of $(\mathbb{D}^2 \times \mathbb{S}^1)_d$ by this order 2 rotation is an orbifold which we refer as *orbi-pillow*

and denote as P_d. The singular loci of the orbi-pillow P_d has cone points of order d and order 2. The boundary of P_d is the pillowcase orbifold, i.e. $\mathbb{S}^2(2,2,2,2)$ and it is the quotient of the boundary of $(\mathbb{D}^2 \times \mathbb{S}^1)_d$ (which is a torus) by r. We will denote the image of the meridian m_d in ∂P_d as m_d^{pillow}.

Note that since ∂c is pillowcase, it could be thought of as a quotient of $\mathbb{S}^1 \times \mathbb{S}^1$ (by r described above) via a map $\phi : \mathbb{S}^1 \times \mathbb{S}^1 \to \partial c$. Let's choose two generators m and l of $H_1(\mathbb{S}^1 \times \mathbb{S}^1)$ and denote the image of $\frac{p}{d}m + \frac{q}{d}l$ via ϕ in ∂c as γ.

The orbifold $(O - int(c)) \cup_h P_d$ where h is a homeomorphism from ∂P_d to ∂c sending m_d^{pillow} to γ is said to be *obtained by (p,q) Dehn filling* on c.

Now we can state the orbifold covering result:

Theorem 5.1 (Theorem 2.6, [7]). *Let $L = K_1 \sqcup K_2 \sqcup \cdots \sqcup K_n$ be a hyperbolic link where $n \geq 2$. If for the family of hyperbolic knots $\mathcal{F} = \{L_{(\infty,(p_2^i,q_2^i)\ldots,(p_n^i,q_n^i))}\}$ geometrically converging to L as $i \to \infty$, $\mathbb{S}^3$ complement of each $L_{(\infty,(p_2^i,q_2^i)\ldots,(p_n^i,q_n^i))}$ in $\mathcal{F}$ covers a rigid cusped orbifold O_i, then after passing to a subsequence, we can say, $\mathbb{S}^3 - L$ covers an orbifold O with exactly one rigid cusp c_{rigid} and one or more smooth cusps, such that*

1. *Only the cusp corresponding to component K_1 of L covers c_{rigid},*
2. *Each O_i is obtained by some Dehn fillings on the smooth cusps of O,*
3. *If ϕ denotes the covering from $\mathbb{S}^3 - L$ to O and ϕ_i the covering from $\mathbb{S}^3 - L_{(\infty,(p_2^i,q_2^i)\ldots,(p_n^i,q_n^i))}$ to O_i, then degree of ϕ_i does not depend on i, and* $\text{degree}(\phi) = \text{degree}(\phi_i)$.

Remark 5.2. *The last part of Theorem 2.6 in [7] is technical. So, here we stated the consequence of that last part that we will use in future.*

In the last chapter, we have seen that the cusps of 6_2^2 are not geometrically isolated (see Proposition 4.10) which by Theorem 4.6 implies Theorem 4.11 stating that only finitely many of the hyperbolic knots obtained from Dehn filling a single cusp of 6_2^2 can have hidden symmetries. One can ask whether similar results follow for other hyperbolic two bridge links. One very interesting application of Theorem 5.1 is that we used it in [7] to give a positive answer to this question:

Theorem 5.3 (Theorem 1.5, [7]). *Let L be a hyperbolic 2-bridge link and $\mathcal{F}$ be a sequence of hyperbolic knots obtained by Dehn filling a fixed cusp of L. Then at-most finitely many*

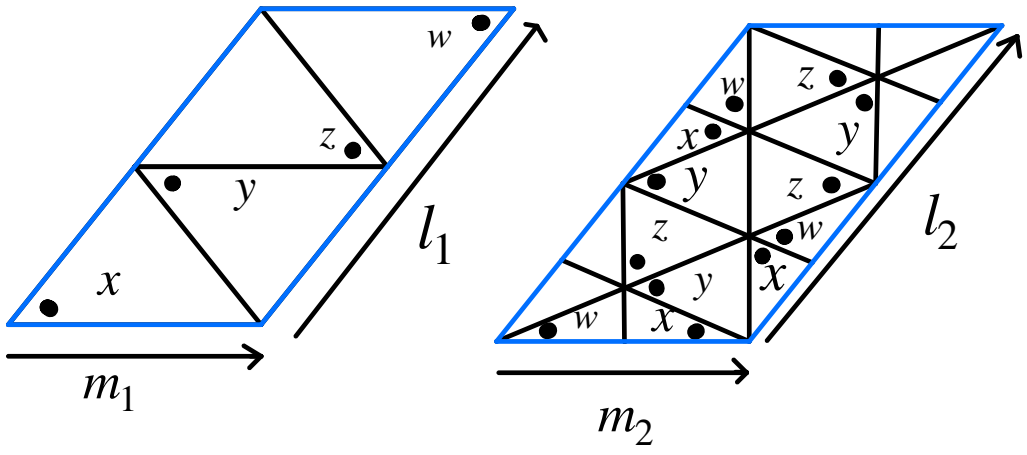

Figure 22: Cusp triangulations for the regular ideal triangulation of 6_2^2 - Left: Cusp c_1, Right: Cusp c_2

elements in $\mathcal{F}$ can have hidden symmetries.

5.2 Exploring fillings on a single cusp of 6_2^2 further

We recall from Section 4.4 that the complement of 6_2^2 decomposes into 6 ideal tetrahedra given by the Sakuma-Weeks traingulation. The discussion in this section will be based on a different triangulation of $\mathbb{S}^3 - 6_2^2$ consisting of 4 regular ideal tetrahedra. It is explained in Section 5.1 of [7] how one can obtain this regular ideal triangulation from the Sakuma-Weeks triangulation. The discussion below follows from Section 6 of [7].

The cusp triangulation induced by this regular ideal triangulation has 4 triangles for one cusp, which we will refer as c_1, and 12 triangles for the other cusp, which we will refer as c_2. In Figure 22, we show the pictures of these cusp triangulations from [7, Figure 8]. The deformation variety, $\mathcal{D}$, associated with the regular ideal triangulation is given by $\{(x, y, z, w) \in \mathbb{C}^4 : (1-x)(1-y)(1-z)(1-w) = xw = yz\}$.

It turns out that on the subvariety V_0 of $\mathcal{D}$ where cusp c_1 is complete,

$$y = xw(1-w) \quad \text{and } z = \frac{1}{1-w}. \tag{40}$$

Using this one can write V_0 as the set $\{(x, w) : 1 - x(1-x)w(1-w) = 0\}$. We write σ_1 and σ_2 to denote $x + w$ and xw respectively. Then we can check that the equation $1 - x(1-x)w(1-w) = 0$ implies

$$1 + \sigma_1\sigma_2 - \sigma_2 - \sigma_2^2 = 0. \tag{41}$$

So, on V_0, σ_1 and σ_2 satisfy the equation above. One can also find that after choosing generators m_1 and l_1 of the fundamental group of the cusp torus for cusp c_1 (see Figure 22) and m_1 as the reference edge, the cusp parameter function for cusp c_1 is given by $\tau(x, w) = x + w = \sigma_1$. We now state two results from [7] (without proof):

Proposition 5.4 (Proposition 6.10, [7])**.** *If (x, w) in V_0 corresponds to a (p, q) Dehn filling (on cusp c_2) for non-negative integers p, q such that $(p, q) \neq (1, 1)$ and $q \neq 0$, then, $\mathbb{Q}(\sigma_1) = \mathbb{Q}(\sigma_2)$.*

Lemma 5.5 (Corollary 6.14, [7])**.** *If the cusp field of an orbifold O obtained by Dehn filling a single cusp of 6_2^2 is quadratic imaginary, then the filling coefficient for O is either $(2, 0)$ (with the corresponding cusp field $\mathbb{Q}(i\sqrt{3})$) or $(3, 0)$ (with the corresponding cusp field $\mathbb{Q}(i)$).*

These imply the following strengthening of Theorem 4.11.

Theorem 5.6 (Theorem 1.6, [7])**.** *If an orbifold O obtained by Dehn filling a single cusp of 6_2^2 is covered by a hyperbolic knot complement with hidden symmetries, then the Dehn filling coefficient for O is $(2, 0)$.*

Proof. Let M be a hyperbolic knot complement with hidden symmetries which covers a filling of a cusp of $\mathbb{S}^3 - 6_2^2$. $\mathbb{S}^3 - 6_2^2$ has an involution which exchanges its cusps. So, without loss of generality, we may assume that M overs a filling of the cusp c_2. We know from Fact 3.6 that the cusp field of M is $\mathbb{Q}(i\sqrt{3})$. This would mean that the filling on c_2 that M covers should also have cusp field $\mathbb{Q}(i\sqrt{3})$. Lemma 5.5 then implies that the filling is the $(2, 0)$ filling and one can see from Figure 25 that the figure eight knot complement is a 2-fold cover of the $(2, 0)$-filling of c_2. This proves the theorem.

□

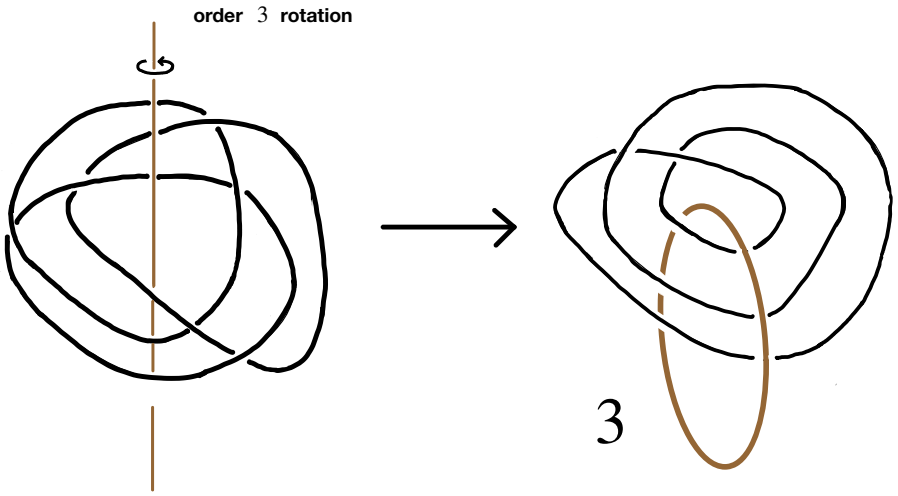

Figure 23: Borromean rings complement is a 3-fold cover of the $(3,0)$ filling on a cusp of 6_2^2

5.3 Trace field and cusp field

Proposition 5.7 (Corollary 6.15, [7]). *If O is an arithmetic orbifold obtained by Dehn filling a single cusp of 6_2^2, then, the filling coefficient for O is either $(2,0)$ or $(3,0)$.*

Proof. If (p,q) filling of c_2 produces an arithmetic orbifold then by Proposition 4.4(a) of [23], the invariant trace field of the orbifold is quadratic imaginary. Since the cusp field can't be $\mathbb{Q}$, Theorem 2.31 implies $\mathbb{Q}(\sigma_1)$ is quadratic imaginary as well. So, Lemma 5.5 implies that $(2,0)$ and $(3,0)$ are the only possible candidates for arithmeticity. The figure eight knot complement is a 2-fold cyclic cover of the $(2,0)$-filling of c_2, and as shown in Figure 23 (cf. Figure 11 of [7]), the Borromean rings complement is a three-fold cyclic cover of the $(3,0)$-filling. It follows that these fillings are arithmetic, as the covering knot and link complements are. □

We will now see a result which will relate the invariant trace field and trace field of an orbifold obtained by Dehn filling a fixed cusp of 6_2^2. Our approach here follows that of

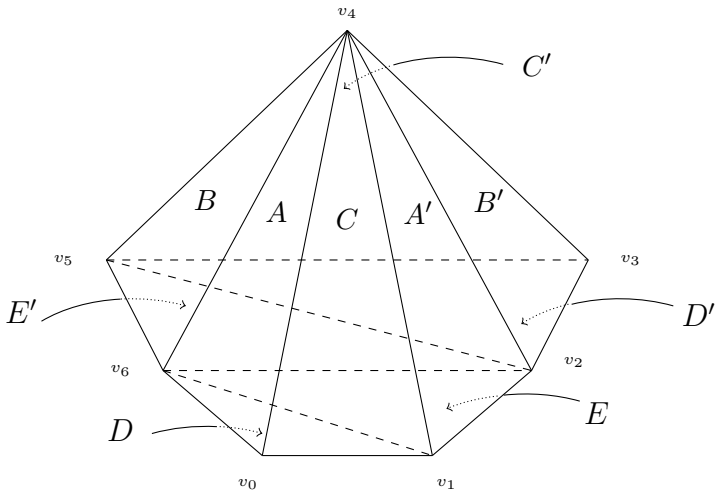

Figure 24: 6_2^2 complement as a quotient of an ideal decahedron

Theorem 6.2 of [23].

Theorem 5.8 (Proposition 6.16, [7])**.** *For an orbifold O obtained by Dehn filling a single cusp of 6_2^2, its invariant trace field and trace field are equal.*

Proof. We may recover the face pairings of the triangulation $\mathcal{T}_4$ of $\mathbb{S}^3 - 6_2^2$ from the cusp triangulation pictures in Figure 22. Assembling its four ideal tetrahedra so that they share an ideal vertex corresponding to the cusp c_1, with a horospherical cross-section around this ideal vertex as on the left side of Figure 22, produces the ideal decahedron of Figure 24. We produce $\mathbb{S}^3 - 6_2^2$ by identifying faces in pairs: A with A' and so on, so that pairings of faces containing the ideal vertex v_4 take it to itself, the pairing of D with D' takes v_0 to v_3, and that of E with E' takes v_1 to v_6. Then v_4 corresponds to c_1 and all other vertices to c_2.

For any $(x, w) \in V_0$, the shape parameters x, y, z and w labeled in Figure 22 determine the tetrahedra comprising the decagon up to isometry, where $z = 1/(1-w)$ and $y = xw(1-w) = 1/(1-x)$ (see Equation 40). Embedding the resulting decahedron in $\mathbb{H}^3$ with $v_0 = 0$, $v_1 = 1$ and $v_4 = \infty$ thus yields $v_3 = 1 + x + w$, $v_5 = x + w$, and $v_6 = x$. This in turn determines isometries a, b, c, d, and e realizing the face pairings sending A to A', B to B', C to C', D to D', and E to E', respectively. In particular, we have the matrix representatives

below in $\mathrm{SL}(2,\mathbb{C})$. (We have used Mathematica [17] to assist with some computations here.)

$$a = \begin{pmatrix} 1 & 1 \\ 0 & 1 \end{pmatrix}, \quad e = \begin{pmatrix} w + wx + x^2 - wx^2 & -w - wx - x^3 + wx^3 \\ w + x - wx & -w - x^2 + wx^2 \end{pmatrix}. \tag{42}$$

For each such $(x, w) \in V_0$, the face-pairing isometries generate the image of $\Gamma \doteq \pi_1(\mathbb{S}^3 - 6_2^2)$ under the holonomy representation determined by the hyperbolic structure on $\mathbb{S}^3 - 6_2^2$ corresponding to (x, w). At the complete structure $x = w = \frac{1}{2}(1 + \sqrt{-3})$, the Poincaré polyhedron theorem yields a presentation for Γ:

$$\Gamma \cong \langle a, e \,|\, ae^2a^{-1}e^{-1}a^{-1}e^2 = e^2a^{-1}e^{-1}a^{-1}e^2a \rangle.$$

(Specifically, it gives $b = a$, $[a, c] = 1$, $d = e^2$, and $c = db^{-1}e^{-1}a^{-1}d$.)

Now fix $(x, w) \in V_0$ corresponding to a (p, q)-hyperbolic Dehn filling of c_2, and let $\Gamma_{p,q}$ be the orbifold fundamental group of the resulting hyperbolic orbifold M. The corresponding holonomy representation factors through a surjection $\Gamma \to \Gamma_{p,q}$, so as a Kleinian group in $\mathrm{PSL}(2,\mathbb{C})$, $\Gamma_{p,q}$ is generated by the cosets of the matrices a and e described above. The traces of a, e, and ae thus generate the trace field of $\Gamma_{p,q}$ as an extension of $\mathbb{Q}$ (see equation 3.25 in [19]). These are respectively 2, $wx = \sigma_2$, and $w + x = \sigma_1$, so since $\sigma_1 \in \mathbb{Q}(\sigma_2)$ this is the trace field of $\Gamma_{p,q}$.

The invariant trace field of $\Gamma_{p,q}$ contains the trace of e^2 by definition. As this is $\sigma_2^2 - 2$, the invariant trace field contains σ_2^2. By Theorem 2.31 the cusp field of M, which here is $\mathbb{Q}(\sigma_1)$, is a subfield of the invariant trace field of M. So, $\sigma_2 = \frac{\sigma_2^2 - 1}{\sigma_1 - 1}$ is contained in the invariant trace field. Since the invariant trace field is contained in the trace field, it is also $\mathbb{Q}(\sigma_2)$. □

Corollary 5.9 (Corollary 6.17, [7]). *Let O be an orbifold obtained by (p, q)-Dehn filling on a single cusp of $\mathbb{S}^3 - 6_2^2$ such that $q \neq 0$, then, the invariant trace field of O equals its cusp field.*

Proof. If O is the hyperbolic orbifold obtained by (p, q) Dehn filling on one cusp of 6_2^2, where $q \neq 0$, then by Proposition 5.4, $\mathbb{Q}(\sigma_1) = \mathbb{Q}(\sigma_2)$. Now, since the cusp field of M is $\mathbb{Q}(\sigma_1)$, and by Theorem 5.8 above the invariant trace field of M is $\mathbb{Q}(\sigma_2)$, we conclude that the invariant trace field is equal to the cusp field for M. □

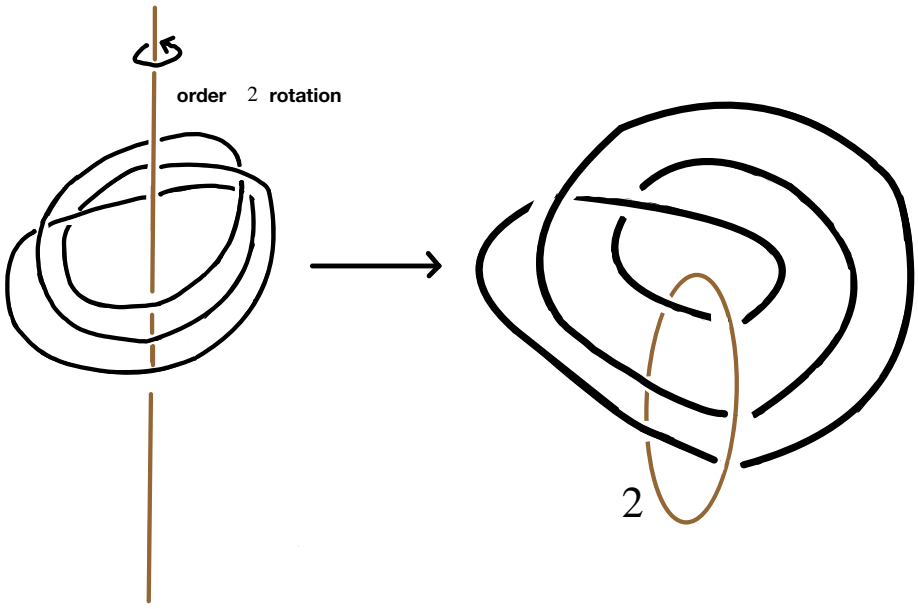

Figure 25: Figure eight knot complement is a 2-fold cover of the $(2, 0)$ filling on a cusp of 6_2^2

6.0 Hidden symmetry and horoball packing

The contents of this chapter and the next two chapters are from a solo project which has not been put in a preprint yet. The theme of this project is to study hidden symmetries in terms of certain symmetries of the horoball packings.

6.1 Horoball packings and circle packings associated with an orbifold

Let $O = \mathbb{H}^3/\Gamma$ be a hyperbolic 3-orbifold with cusps. Let c be a cusp of O (see Section 2.5 for the definition). A *horoball packing of* $\mathbb{H}^3$ is a union of horoballs such that no two such horoballs intersect each other in the interior. We note the following fact:

Fact 6.1. *The pre-image of a disjoint union of cusp neighborhoods of* O *in* $\mathbb{H}^3$ *is a* Γ *invariant horoball packing of* $\mathbb{H}^3$.

Proof. We have seen that c is of the form B/W where B is a horoball and W the stabilizer of the horocenter of B. Then, all the horoballs obtained by translating B by the elements of Γ project down to c as well and their union is the pre-image of c. The fact that the projection of B to O factors through an embedding of B/W implies that distinct Γ translations of B are disjoint from B, and hence that no two translates intersect unless they are equal. So, the pre-image of c becomes a horoball packing of $\mathbb{H}^3$ and this collection of horoballs is Γ invariant since they are all Γ translates of B. Now, if we take other cusp neighborhoods of O disjoint from c in similar manner, then, the pre-image of this disjoint union is also a horoball packing of $\mathbb{H}^3$, which is Γ invariant. This proves the fact. □

The *c-maximal horoball packing of* $\mathbb{H}^3$ is a horoball packing of $\mathbb{H}^3$ which map to a maximal cusp neighborhood for cusp c. An *O-horoball packing of* $\mathbb{H}^3$ is a horoball packing of $\mathbb{H}^3$ which map to a union of cusp neighborhoods of all the cusps of O. We will refer a horoball in an O-horoball packing as a *c-horoball* if it maps to a cusp neighborhood of c. An *O-maximal horoball packing of* $\mathbb{H}^3$ is an O-horoball packing of $\mathbb{H}^3$ which is not contained in a bigger

O-horoball packing of $\mathbb{H}^3$. A (c, O)-*maximal horoball packing of* $\mathbb{H}^3$ is a O-maximal horoball packing of $\mathbb{H}^3$ which contains the c-maximal horoball packing of $\mathbb{H}^3$.

Given an O-horoball packing $\mathcal{H}$ for an orbifold $O = \mathbb{H}^3/\Gamma$, there is a hyperbolic element g in $\mathrm{PSL}(2, \mathbb{C})$ such that $g(H_\infty)$ is the horoball centered at ∞ at height 1 (see the first point in Fact 2.7). Now, $g(\mathcal{H})$ is an O_g-horoball packing of $\mathbb{H}^3$ where $O_g = \mathbb{H}^3/g\Gamma g^{-1}$ and O and O_g are isometric. So, in light of this fact we will always assume that for an orbifold O, the horoball centered at ∞ of an O-horoball packing is at height 1. We will use the term full sized horoballs to refer to the horoballs centered at points in $\mathbb{C}$ that have diameter 1. So, the full sized horoballs are tangent to the horoball at height 1.

Let H be a horoball packing of $\mathbb{H}^3$ contained an O-maximal horoball packing of $\mathbb{H}^3$. The circle packing of $\mathbb{C}$ obtained by projecting down the boundaries of the full-sized horoballs of H, an O-horoball packing of $\mathbb{H}^3$, onto $\mathbb{C}$ is called the H-circle packing of $\mathbb{C}$. For a given cusp c of O, a circle C in the H-circle packing is called a *c-circle* if the horoball in H which projects down to the disk bounded by C maps to a cusp neighborhood of c in O. If H_c is the c-maximal horoball packing of $\mathbb{H}^3$ such that horoball centered at ∞ projects down to a cusp neighborhood of cusp c, then, we will refer the H_c-circle packing as *c-circle packing of* $\mathbb{C}$.

Remark 6.2. *We recall from Remark 2.9 that for a hyperbolic link L with components $K_1, \ldots, K_n$, K_i-cusp of $\mathbb{S}^3 - L$ is the cusp corresponding to the K_i-component. We will use the term K_i-circle packing to mean the K_i-cusp circle packing.*

Let us consider the c-maximal horoball packing of O such that the horoball centered at ∞ projects to a cusp neighborhood of cusp c. The volume of this cusp neighborhood is called the *(maximal) cusp volume* of c. $\mathrm{Stab}(\infty)$ in $\pi_1(M)$ acts on the c-circle packing as a wallpaper group W. The area of the fundamental domains of W is called the *cusp area* of c. Recall from Subsection 2.5.1 that when O is a hyperbolic manifold, W is lattice wallpaper group. A fundamental domain of such a W is called a *cusp parallelogram* of c. We will use the following fact later:

Fact 6.3. *For a cusp c of an orbifold O, the cusp area of $c = 2$ (maximal cusp volume of c).*

Proof. Using the first point in Facts 2.7, we can assume $c = B_\infty/W$ where B_∞ is horizontal

centered ∞ at height 1. Let D be a fundamental domain of W. Note since D lies on the plane at height 1, the hyperbolic metric on B_∞ is the standard Euclidean metric on B_∞. So, cusp area of c is the area of D in the standard Euclidean metric. Then the cusp volume of c is

$$\iint_D \int_1^\infty \sqrt{\frac{1}{z^6}}\, dz\, dA = \iint_D \int_1^\infty \frac{1}{z^3}\, dz\, dA = \iint_D \frac{1}{2}\, dA = \frac{\text{cusp area of } c}{2}.$$

□

6.1.1 SnapPy

SnapPy [9] is a 3-manifold software written by Marc Culler, Nathan Dunfield and Matthias Goerner built upon the SnapPea kernel written by Jeffrey Weeks. SnapPy can compute several geometric information about a hyperbolic 3-manifold. SnapPy treats a hyperbolic 3-manifold as a geometric triangulation and it computes geometric data based on that triangulation. For example, one can find edge equations or tetrahedral shapes for a hyperbolic 3-manifold from SnapPy. SnapPy also provides information about cusp neighborhood, which we briefly describe below.

SnapPy denotes the cusps of hyperbolic 3-manifold by indices staring from 0. On SnapPy, one can view the horoball packing of $\mathbb{H}^3$ that come from the cusp neighborhoods of a hyperbolic 3-manifold. This view of horoball packing is from ∞ above and one has the option to select which cusp of the hyperbolic 3-manifold is to be arranged at ∞. The SnapPy horoballs are labelled different colors. Each color corresponds to a cusp. For example, if a hyperbolic 3-manifold has four cusps, then the horoballs projecting down to cusp 0 is labelled red, cusp 1 blue, cusp 2 green and cusp 3 light blue. One can also (equivariantly) maximize the horoballs of a single cusp until they touch one of their own tangentially. Maximizing (horoballs of) different cusps gives us different pictures of horoball packing. Now, we will discuss some examples of horoball packings using pictures from SnapPy.

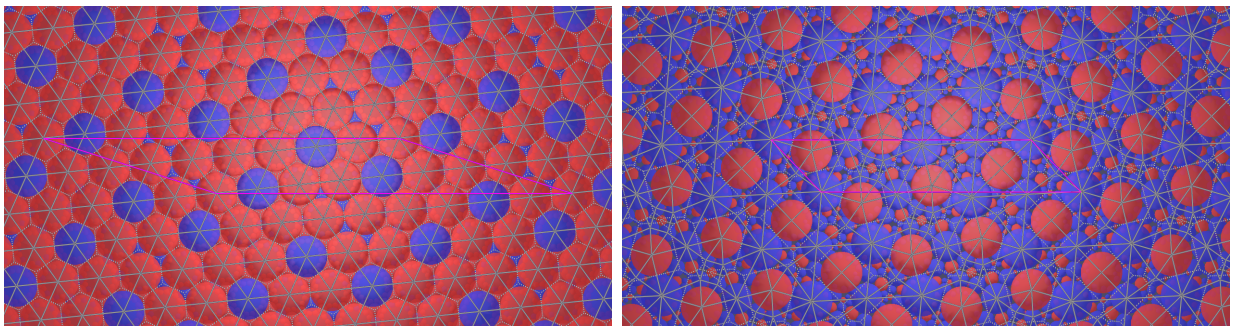

Figure 26: Left: (Red cusp, $\mathbb{S}^3 - L14n24613$)-maximal horoball packing of $\mathbb{H}^3$, Right: (Blue cusp, $\mathbb{S}^3 - L14n24613$)-maximal horoball packing of $\mathbb{H}^3$ (pictures are obtained from SnapPy [9])

6.1.2 Examples

Figure 26 shows two ($\mathbb{S}^3 - L14n24613$)-maximal horoball packings of $\mathbb{H}^3$. $L14n24613$ is a 2-component hyperbolic link (refer to Figure 3 in [11] for a picture of the link). The cusp of $L14n24613$ are labelled in red and blue in Figure 26. Left of Figure 26 shows how the (red cusp, $\mathbb{S}^3 - L14n24613$)-maximal horoball packing of $\mathbb{H}^3$ looks like from ∞, where ∞ corresponds to the red cusp, i.e. the horoball centered at ∞ maps down to a cusp neighborhood of the red cusp. Here the horoball centered at ∞ (the horizontal plane) is at Euclidean height 1. We obtained this maximal horoball packing of $\mathbb{H}^3$ by first maximizing the horoballs corresponding to the red cusp, and then, maximizing the horoballs corresponding to the blue cusp. Similarly, the picture in the right of Figure 26 shows how the (blue cusp, $\mathbb{S}^3 - L14n24613$)-maximal horoball packing of $\mathbb{H}^3$ looks like from ∞, where ∞ corresponds to the blue cusp. This is obtained by first maximizing the blue horoballs and then the red horoballs. The parallelograms drawn in pink in both pictures are cusp parallelograms.

Note that if we only consider the full sized red (respectively, blue) horoballs in the picture in the left (respectively, right) of Figure 26, it will give us the red cusp (respectively, blue cusp)-circle packing of $\mathbb{C}$.

6.2 Hidden symmetry and symmetries of c-circle packing

6.2.1 Hoffman's observation

The following result was communicated by Neil Hoffman in an AIM SQuaRE program in 2019. It builds on an approach taken by Millichap [21]. We include a proof below.

Theorem 6.4. *Let L be a 2-component hyperbolic link with components K_1 and K_2. Let $\mathfrak{F} = \{K_{\infty,(p^i,q^i)}\}_i$ be a family of hyperbolic knots geometrically converging to L as $i \to \infty$. If infinitely many elements of $\mathfrak{F}$ have hidden symmetries then for any $(\mathbb{S}^3 - L)$-maximal horoball packing H of $\mathbb{H}^3$, the H-circle packing of $\mathbb{C}$ has a rotational symmetry of order 3 or 6 whose fixed point cannot be the center of a K_2 horoball.*

Proof. By Theorem 3.3, each $K_{\infty,(p^i,q^i)}$ having hidden symmetry will cover an orbifold O_i with a rigid cusp. Now, Theorem 5.1 implies that $\mathbb{S}^3 - L$ covers a 2-cusped orbifold O with a single rigid cusp c such that c is covered only by cusp K_1 of $\mathbb{S}^3 - L$ and after taking a subsequence, we may assume that O_i are obtained by Dehn filling the smooth cusp of O.

Since K_1 covers c and K_2 covers the smooth cusp of O, H is also an O-maximal horoball packing of $\mathbb{H}^3$. The elements of $\pi_1^{Orb}(O)$ act as symmetries of any O-maximal horoball packing of $\mathbb{H}^3$ and so of H. We assume that the cusp at ∞ is c, then the elements of $\mathrm{Stab}(\infty)$ in $\pi_1^{Orb}(O)$ act as Euclidean isometries of $\mathbb{C}$. So, since $\mathrm{Stab}(\infty)$, a subgroup of $\pi_1^{Orb}(O)$, acts as symmetries of H, $\mathrm{Stab}(\infty)$ acts as symmetries of H-circle packing of $\mathbb{C}$. Now, O_i is covered by $K_{\infty,(p^i,q^i)}$; by Theorem 3.5, we see that c is $(3,3,3)$ or $(2,3,6)$. So, $\mathrm{Stab}(\infty)$ in π_1^{Orb} is a $(3,3,3)$ or $(2,3,6)$ wallpaper group. So, there is an order 3 or 6 rotational symmetry r of the H-circle packing. Now, r is an elliptic element in $\pi_1^{Orb}(O)$ of order 3 or 6. So, if the fixed point of r is the center of a K_2-horoball, then that would imply that K_2 cusp cross-section has a cone point of order 3 or 6 which contradicts that the K_2-cusp is smooth. This completes the proof. □

6.2.2 Hyperbolic link with three or more components

In general, when a hyperbolic 3-manifold M covers a hyperbolic three orbiold O and two or more cusps of M map to the same cusp of O, the M-maximal horoball packing of $\mathbb{H}^3$ might not be an O-maximal packing of $\mathbb{H}^3$. This obstructs us in extending Theorem 6.4 for links with three components as in the current form. We therefore use the one-to-one nature between the un-filled cusps in the orbifold covering provided by Theorem 5.1 and prove the following:

Theorem 6.5. *Let L be a hyperbolic link with n components $K_1, K_2, \ldots, K_n$, where $n \geq 2$. If there is an infinite family of hyperbolic knots $\mathfrak{F} = \{K_{\infty,(p_2^i,q_2^i),\ldots,(p_n^i,q_n^i)}\}_i$ with hidden symmetries which geometrically converge to L as $i \to \infty$, then the following results hold:*

1. *Symmetry group of the K_1-circle packing contains a $(2,3,6)$ or a $(3,3,3)$ wallpaper group W. Consequently, K_1-circle packing has an order 3 or 6 rotational symmetry whose fixed point can not be the center of a K_j-horoball for $j \in \{2,\ldots,n\}$.*
2. *Co-area of the translation subgroup of W =*

$$\frac{\textit{maximal cusp area of } K_1}{4n}$$

for some $n \in \mathbb{N}$.

Proof. Proof of Part 1 is similar to the proof of Theorem 6.4. The only difference is that unlike $n = 2$ case, for general $n \geq 2$ case an $(\mathbb{S}^3 - L)$-maximal horoball packing might not be an O-maximal horoball packing since more than one cusps of L might map to a single smooth cusp of O. But, since only the K_1-cusp of L covers the rigid cusp, say c_{rigid}, of O, the K_1-maximal horoball packing is also a c_{rigid}-maximal horoball packing. So, arranging the cusp at ∞ to be c_{rigid}, similarly as in proof of Theorem 6.4, one can see that, $\mathrm{Stab}(\infty)$ in $\pi_1^{Orb}(O)$ which is either the $(3,3,3)$ wallpaper group or the $(2,3,6)$ wallpaper group acts as symmetries of K_1-circle packing of $\mathbb{C}$ and the order 3 or 6 rotational symmetries in $\mathrm{Stab}(\infty)$ can't fix the center of a K_j-horoball for $j = 2,\ldots,n$. This proves Part 1.

Before we prove Part 2, we recall the following two degree formulae of Hoffman which we will use in the proof:

Theorem 6.6 (Hoffman, Part 1 of Lemma 5.5, [15]). *If ϕ is an orbifold covering from a manifold M to a $(3,3,3)$-cusped orbifold O such that M is covered by a hyperbolic knot complement , then the index of ϕ is $12n$ for some $n \in \mathbb{N}$.*

Theorem 6.7 (Hoffman, Theorem 1.2, [16]). *For an orbifold covering ϕ from a manifold M to a $(2,3,6)$-cusped orbifold O where M is covered by a hyperbolic knot complement, the index of ϕ is $24n$ for some $n \in \mathbb{N}$.*

Denote the wallpaper group from part 1 as W. Let Λ_W denote the translation subgroup of W. If c_{rigid} is $(3,3,3)$, then using the degree formula in Theorem 5.1 and applying Theorem 6.6 we get, degree$(\mathbb{S}^3 - L \to O) = 12n$ for $n \in \mathbb{N}$. So, the maximal area of c_{rigid} is

$$\frac{\text{maximal cusp area of } K_1}{12n}.$$

But, this is same as $\frac{\text{co-area of } L}{3}$. This implies

$$\text{co-area of } L = \frac{\text{maximal cusp area of } K_1}{4n}.$$

If the rigid cusp of O is $(2,3,6)$, then the degree formula in Theorem 5.1 and Theorem 6.7 implies degree$(\mathbb{S}^3 - L \to O) = 24n$ for $n \in \mathbb{N}$. So,

$$\frac{\text{maximal cusp area of } K_1}{24n} = \text{maximal area of } c_{rigid} = \frac{\text{co-area of L}}{6}.$$

Thus, co-area of $L = \frac{\text{maximal cusp area of } K_1}{4n}$ in this case as well. This ends the proof. □

We emphasize the following crucial fact,

Fact 6.8. *We note from the proof of Theorem 6.5 that the elements of the $(2,3,6)$ or $(3,3,3)$ wallpaper group of symmetries of the K_1-circle packing are also symmetries of any K_1-horoball packing of $\mathbb{H}^3$. So, they must send a non-full sized K_1-horoball to another K_1-horoball of the same size.*

We describe Theorem 6.5 in terms of the K_1-circle packing since it will be easier for us to code the theorem into an algorithm and use the code for a large collection of links. We develop the coding mechanism in the next section (Section 6.3).

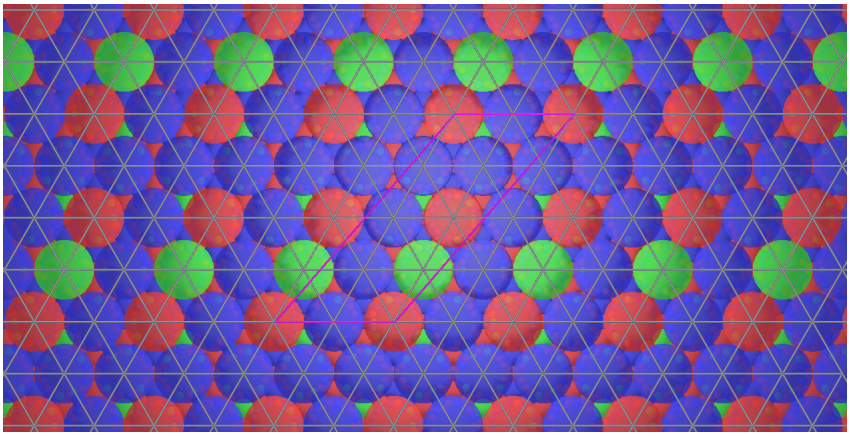

Figure 27: (Red cusp, $\mathbb{S}^3 - L11n354$)-horoball packing has no order 3 or 6 rotational symmetry (picture obtained from SnapPy [9])

6.2.3 Examples

Figure 27 shows a (red cusp, $\mathbb{S}^3 - L11n354$)-horoball packing of $\mathbb{H}^3$ where ∞ corresponds to the red cusp. We can see that red cusp circle packing of $\mathbb{C}$ in Figure 27 has no order 3 or 6 rotational symmetry.

A (green cusp, $\mathbb{S}^3 - L10a157$)-horoball packing of $\mathbb{H}^3$ is shown in Figure 28 where ∞ is at the green cusp. The green cusp circle packing in Figure 28 has order 6 (and so order 3 as well) rotational symmetry. But, note that these symmetries fix the centers of red or blue horoballs.

If we analyze Figure 29, which depicts the view of a (red cusp, $\mathbb{S}^3 - L8a20$)-horoball packing of $\mathbb{H}^3$ from the red cusp at ∞, we see red cusp circle packing of $\mathbb{C}$ has order 3 as well as order 6 rotational symmetry which does not fix centers of horoballs corresponding to the blue cusp. One can see that the cusp area of the red cusp in $L8a20$ is $16a$ where $a = \frac{\sqrt{3}}{4}$. But, the red cusp circle packing does a have hexagonal lattice symmetry of co-area less than or equal to $4a$ and cannot have a hexagonal lattice symmetry of co-area of the form $\frac{16a}{4n}$ for some $n \in \mathbb{N}$.

If we consider the horoball packings that we have seen in Figure 26, we see that neither

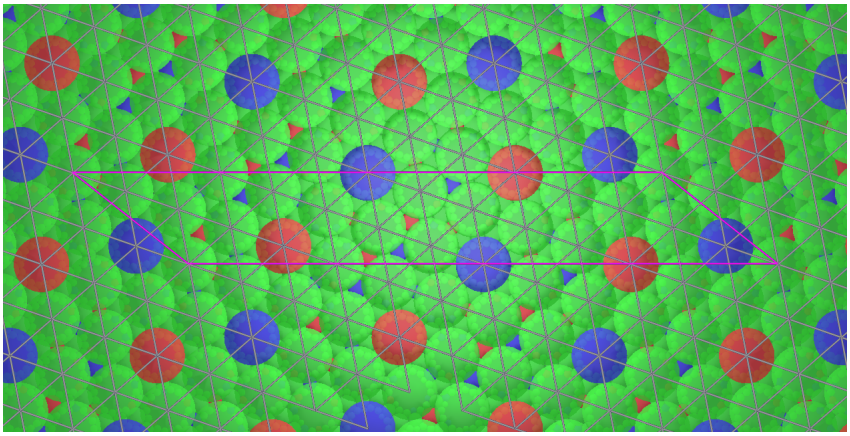

Figure 28: Order 3 or 6 rotational symmetries of (green cusp, $\mathbb{S}^3 - L10a157$)-horoball packing fixes centers of red or blue horoballs (picture obtained from SnapPy [9])

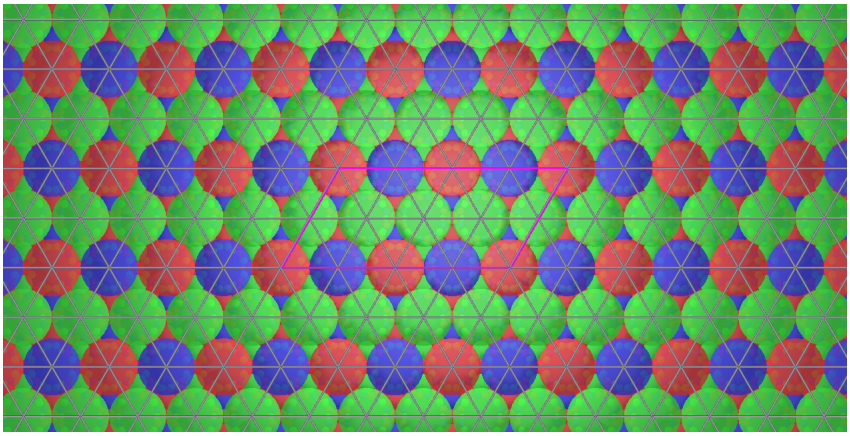

Figure 29: (Red cusp, $\mathbb{S}^3 - L8a20$)-horoball packing has order 3 or 6 rotational symmetries (picture obtained from SnapPy [9])

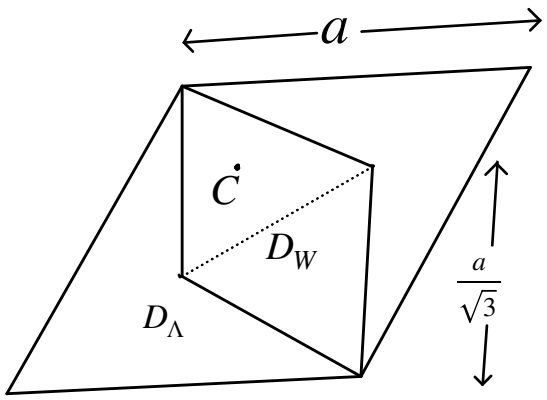

Figure 30: Order 3 rotational symmetry with fixed point near C

the red cusp circle packing of $\mathbb{C}$ in left of Figure 26 nor the blue cusp circle packing of $\mathbb{C}$ has any order 3 rotational symmetry.

6.2.4 A corollary

Corollary 6.9. *Let $L = K_1 \sqcup K_2 \ldots \sqcup K_n$ be an n-component hyperbolic link where $n \geq 2$. Let $\mathcal{F} = \{K_{\infty,(p_2^i,q_2^i),\ldots,(p_n^i,q_n^i)}\}_i$ be an infinite family of hyperbolic knots with hidden symmetries geometrically converging to L as $i \to \infty$. Then for each C in the K_1-circle packing, there is an order 3 or 6 rotational symmetry r which does not fix the center of a K_j-horoball for $j \in \{2, \ldots, n\}$ such that the distance between the center of C and the fixed point of r is less than or equal to $\frac{\sqrt{\text{maximal cusp area of } K_1}}{\sqrt{2}3^{\frac{5}{4}}}$.*

Proof. Since $(2, 3, 6)$ wallpaper group also contains a $(3, 3, 3)$ wallpaper group, by Theorem 6.5, K_1-circle packing has a $(3, 3, 3)$ wallpaper group of symmetries, say W. Let Λ be the translation subgroup of W. Then $C \in D_W \subset D_\Lambda$ where D_Λ and D_W are fundamental domains of L and W respectively. D_Λ is the region bounded by a hexagonal rhombus. If the length of the sides of D_Λ is a, then by Part 2 of Theorem 6.5,

$$\frac{\sqrt{3}a^2}{2} = 2\left(\frac{\sqrt{3}a^2}{4}\right) \leq \frac{\text{maximal cusp area of } K_1}{4}. \tag{43}$$

This means $a \leq \frac{\sqrt{\text{maximal cusp area of } K_1}}{\sqrt{2}3^{\frac{1}{4}}}$. Now, the region D_W is also bounded by a hexagonal rhombus such that the length of the sides of D_W is $\frac{2}{3}\frac{\sqrt{3}a}{2} = \frac{a}{\sqrt{3}}$ (see Figure 30). So, given any point in D_W, there is at-least one vertex of D_W whose distance from that point is less than or equal to $\frac{2}{3}\frac{\sqrt{3}}{2}\frac{a}{\sqrt{3}} = \frac{a}{3}$ since this given point would belong to one of the equilateral triangles divided by one of D_W's diagonal as shown in Figure 30. But, $\frac{a}{3} \leq \frac{\sqrt{\text{maximal cusp area of } K_1}}{\sqrt{2}3^{\frac{5}{4}}}$ and each vertex of D_W is the center of an order 3 rotation r which does not fix the center of a K_j-horoball for $j \in \{2, \ldots, n\}$. That completes the proof. □

6.3 An algorithm for testing symmetries

We are interested in understanding whether there exist a hyperbolic link (with two or more components) such that Dehn fillings on all but one component of the link produces infinitely many hyperbolic knots with hidden symmetries geometrically converging to the link. Our approach in this pursuit is to use Theorem 6.5 to exclude as many hyperbolic links as possible until we find a probable candidate for such phenomenon. In this section, we describe an algorithm which can be implemented in SnapPy [9] to determine the cusps whose corresponding circle packings of $\mathbb{C}$ do not have the required symmetry for such existence as prescribed by Theorem 6.5.

Let L be a hyperbolic link with components $K_1, \ldots, K_n$ where $n \geq 2$. Now, note that a rotational symmetry of $\mathbb{C}$ is a symmetry of the K_1-circle packing if and only if it is a symmetry of the centers of the circles in the K_1-circle packing. Let $\mathcal{C}$ denote the centers of the circles in the K_1-circle packing and P denote a cusp parallelogram of the K_1-cusp. We recall from Section 2.5 that $r_{O,3}$ denotes the order 3 counter clockwise rotation of $\mathbb{R}^2$ around O. Now, for an order 3 rotational symmetry $r_{O,3}$ of $\mathcal{C}$, there exists $g \in \text{Stab}(\infty)$ such that $g(O) \in P$. Now, since g is also symmetry of $\mathcal{C}$, so is $gr_{O,3}g^{-1} = r_{g(O),3}$, which has order 3. This proves the following fact:

Fact 6.10. *If the K_1-circle packing has some order 3 or 6 rotational symmetry, it has one such whose fixed point lies inside each cusp parallelogram of K_1.*

We assume that two parallel sides of P are horizontal. Our assumption comes from the fact that the cusp parallelograms that SnapPy [9] determines always have horizontal sides and we will implement our following results in a SnapPy/Python code. Let $\mathbf{l}$ be the complex number (with imaginary part 0) representing the vector these horizontal sides determine from left to right and let $\mathbf{m}$ be the complex number representing the vector the other two parallel sides determine from bottom left to top left. Note that $\mathbf{l}$ is the length of the horizontal side.

Let $\mathcal{C}_P$ be the set of points in $\mathcal{C}$ which lies in P. We fix $C_0 \in \mathcal{C}_P$. We denote the angle between $\mathbf{m}$ and $\mathbf{l}$ by θ. Let $d = max\{\|\mathbf{m}\|, \|\mathbf{l}\|, \|\mathbf{m}+\mathbf{l}\|, \|\mathbf{m}-\mathbf{l}\|\}$. We define the following quantities:

- $k'_{\mathbf{h}} = \left\lceil \frac{\frac{4d}{3}+1}{\|\mathbf{m}\||\sin\theta|} \right\rceil$,
- $k' = \left\lceil \frac{k'_{\mathbf{h}}\|\mathbf{m}\||\cos\theta|}{\|\mathbf{l}\|} \right\rceil$,
- $k'_{\mathbf{l}} = \left\lceil \frac{\frac{4d}{3}+1}{\|\mathbf{l}\|} \right\rceil$,
- $k''_{\mathbf{h}} = \left\lceil \frac{d(\frac{12}{5}+k'_{\mathbf{h}}+k'+k'_{\mathbf{l}})+1}{\|\mathbf{m}\||\sin\theta|} \right\rceil$,
- $k'' = \left\lceil \frac{k''_{\mathbf{h}}\|\mathbf{m}\||\cos\theta|}{\|\mathbf{l}\|} \right\rceil$,
- $k''_{\mathbf{l}} = \left\lceil \frac{d(\frac{12}{5}+k'_{\mathbf{h}}+k'+k'_{\mathbf{l}})+1}{\|\mathbf{l}\|} \right\rceil$.

We define

$$\mathcal{C}'_P = \{C + p\,\mathbf{m} + q\,\mathbf{l} : C \in \mathcal{C}_P, p, q \in \mathbb{Z} \text{ and } |p| \leq k'_{\mathbf{h}}, |q| \leq k' + k'_{\mathbf{l}}\}$$
$$\mathcal{C}''_P = \{C + p\,\mathbf{m} + q\,\mathbf{l} : C \in \mathcal{C}_P, p, q \in \mathbb{Z}, |p| \leq k''_{\mathbf{h}}, |q| \leq k'' + k''_{\mathbf{l}}\}.$$

Elements of $\mathcal{C}'_P$ and $\mathcal{C}'_P$ are certain translations of the elements of $\mathcal{C}_P$. The following lemma will be crucial in the succeeding results:

Lemma 6.11. *$\mathcal{C}'_P$ contains all elements of $\mathcal{C}$ which are within distance $\frac{d}{3}$ from C_0 and $\mathcal{C}''_P$ contains all elements of $\mathcal{C}$ within distance $d\left(\frac{7}{5} + k'_{\mathbf{h}} + k' + k'_{\mathbf{l}}\right)$ from C_0.*

Proof. Let v_0 denote the left bottom vertex of P. Let us denote the disk of radius s centered v_0 by D_s. First note that the distance between any two points in P is less than or equal to d. So, $\|C_0 - v_0\| \leq d$.

We first prove the case regarding $\mathcal{C}'_P$. Let $C \in \mathcal{C}$ such that $\|C - C_0\| \leq \frac{d}{3}$. We have,

$$\|C - v_0\| \leq \|C - C_0\| + \|C_0 - v_0\| \leq \frac{d}{3} + d = \frac{4d}{3}.$$

So, if we prove $\mathcal{C}'_P$ contains $\mathcal{C} \cap D_{\frac{4d}{3}}$, it will imply $\mathcal{C}'_P$ contains all elements of $\mathcal{C}$ which are within distance $\frac{d}{3}$ from C_0.

We define $\mathbf{h}$ to be the vector equal to $\|\mathbf{m}\||\sin\theta|\,\mathbf{i}$ with initial point v_o. Note that $\mathbf{h}$ is the vector starting from v_o determined by the height of P. Let R be the rectangle determined by $\mathbf{h}$ and $\mathbf{l}$ with the bottom left vertex as v_0. We define,

$$R^+_{\frac{4d}{3}} = \bigcup_{j=0}^{k'_{\mathbf{h}}-1} R + j\,\mathbf{h} \quad \text{and} \quad R^-_{\frac{4d}{3}} = \bigcup_{j=-k'_{\mathbf{h}}}^{-1} R + j\,\mathbf{h}.$$

Note that $R^+_{\frac{4d}{3}}$ and $R^-_{\frac{4d}{3}}$ respectively are the vertical strips (and so in the direction of $\mathbf{h}$) over and below R.

We similarly define,

$$P^+_{\frac{4d}{3}} = \bigcup_{j=0}^{k'_{\mathbf{h}}-1} P + j\,\mathbf{m} \quad \text{and} \quad P^-_{\frac{4d}{3}} = \bigcup_{j=-k'_{\mathbf{h}}}^{-1} P + j\,\mathbf{m}.$$

Note that $P^+_{\frac{4d}{3}}$ (respectively, $P^-_{\frac{4d}{3}}$) is the slanted strip (in the direction of $\mathbf{m}$) based over (respectively below) P.

Now,

$$R^+_{\frac{4d}{3}} \subset \bigcup_{j=-k'}^{k'} P^+_{\frac{4d}{3}} + j\,\mathbf{l} \quad \text{and} \quad R^-_{\frac{4d}{3}} \subset \bigcup_{j=-k'}^{k'} P^-_{\frac{4d}{3}} + j\,\mathbf{l}.$$

(See Figures 31 and 32 for a pictorial explanation.)

If we define, $P_{\frac{4d}{3}} = P^+_{\frac{4d}{3}} \cup P^-_{\frac{4d}{3}}$, then, $P_{\frac{4d}{3}} = \bigcup_{j=-k'_{\mathbf{h}}}^{k'_{\mathbf{h}}-1} P + j\,\mathbf{m}$. This would mean that both $R^+_{\frac{4d}{3}}$ and $R^-_{\frac{4d}{3}}$ are contained in $\bigcup_{j=-k'}^{k'} P_{\frac{4d}{3}} + j\,\mathbf{l}$. So, $R_{\frac{4d}{3}} = R^+_{\frac{4d}{3}} \cup R^-_{\frac{4d}{3}}$ is also contained in $\bigcup_{j=-k'}^{k'} P_{\frac{4d}{3}} + j\,\mathbf{l}$.

Now, we note that $D_{\frac{4d}{3}} \subset \bigcup_{n=-k'_{\mathbf{l}}}^{k'_{\mathbf{l}}} R_{\frac{4d}{3}} + n\,\mathbf{l}$ (See Figures 31 and 32). This means

$$D_{\frac{4d}{3}} \subset \bigcup_{n=-k'_{\mathbf{l}}}^{k'_{\mathbf{l}}} \left(\bigcup_{j=-k'}^{k'} P_{\frac{4d}{3}} + j\,\mathbf{l} \right) + n\,\mathbf{l} = \bigcup_{n=-(k'+k'_{\mathbf{l}})}^{k'+k'_{\mathbf{l}}} P_{\frac{4d}{3}} + n\,\mathbf{l} = \bigcup_{n=-(k+'k'_{\mathbf{l}})}^{k+'k'_{\mathbf{l}}} \left(\bigcup_{j=-k'_{\mathbf{h}}}^{k'_{\mathbf{h}}-1} P + j\,\mathbf{m} \right) + n\,\mathbf{l}$$
$$\subset \bigcup_{n=-(k'+k'_{\mathbf{l}})}^{k'+k'_{\mathbf{l}}} \bigcup_{j=-k'_{\mathbf{h}}}^{k'_{\mathbf{h}}} P + j\,\mathbf{m} + n\,\mathbf{l}.$$

The intersection of the right most union above with $\mathcal{C}$ is $\mathcal{C}'_P$. Therefore, $\mathcal{C} \cap D_{\frac{4d}{3}}$ is contained in $\mathcal{C}'_P$.

For second case which concerns $\mathcal{C}''_P$, we note that if $C \in \mathcal{C}$ such that $\|C - C_0\| \leq d\left(\frac{7}{5} + k'_{\mathbf{h}} + k' + k'_l\right)$, then

$$\|C - v_0\| \leq \|C - C_0\| + \|C_0 - v_0\| \leq d\left(\frac{7}{5} + k'_{\mathbf{h}} + k' + k'_l\right) + d = d\left(\frac{12}{5} + k'_{\mathbf{h}} + k' + k'_l\right).$$

Now, proceeding similarly as the first case, we can show that $\mathcal{C}''_P$ contains $\mathcal{C} \cap D_{(\frac{12}{5} + k'_{\mathbf{h}} + k' + k'_{\mathbf{l}})}$ which would then prove $\mathcal{C}''_P$ contains all elements of $\mathcal{C}$ within distance $d\left(\frac{7}{5} + k'_{\mathbf{h}} + k' + k'_{\mathbf{l}}\right)$ from C_0. □

We note the following fact:

Fact 6.12. *Let r be an order 3 symmetry of $\mathcal{C}$. Then the orbits of the action of the group $\{1, r, r^2\}$ on $\mathcal{C}$ have either 1 element or 3 elements. If this action has an orbit with one element, then it is unique and the element in the orbit is the fixed point of r. On the other hand, the elements in an orbit with 3 elements form an equilateral triangle.*

Now, if x, y and z are the vertices of an equilateral triangle tri, then the barycenter of tri is fixed by any symmetry of the tri. With this in mind, we define the set

$$\mathcal{E} = \{C_0\} \bigcup \left\{ \frac{X + Y + C_0}{3} : X, Y \in \mathcal{C}'_P, 0 < \|X - C_0\| = \|Y - C_0\| \leq \frac{\sqrt{\text{area of } P}}{\sqrt{2}3^{\frac{3}{4}}}, \right.$$
$$\left. \frac{\|(X - C_0).(Y - C_0)\|}{\|X - C_0\|\|Y - C_0\|} = \frac{1}{2} \right\}.$$

$\mathcal{E}$ consists of the point C_0 and the centers of the equilateral triangles with a fixed vertex at C_0 and two other vertices from $\mathcal{C}'_P$ such that length of its sides is less than or equal to $\frac{\sqrt{\text{area of } P}}{\sqrt{2}3^{\frac{3}{4}}}$.

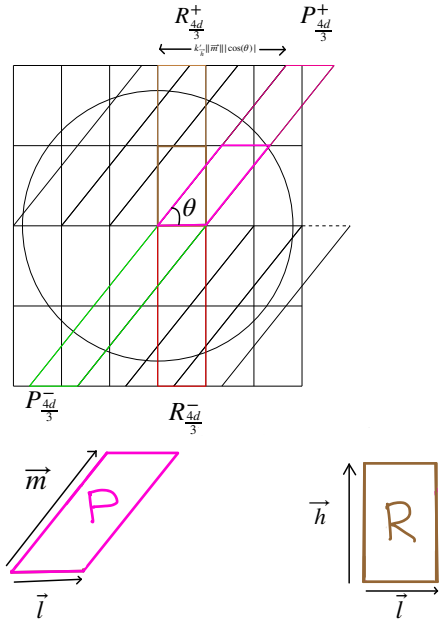

Figure 31: $\mathcal{C}'_P$ contains $\mathcal{C} \cap D_{\frac{4d}{3}}$: θ acute case

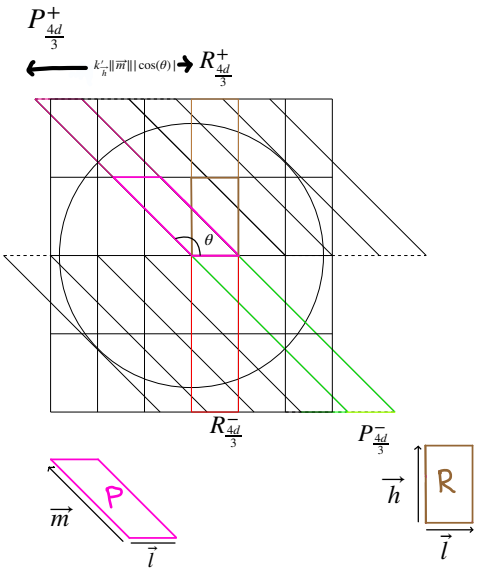

Figure 32: $\mathcal{C}'_P$ contains $\mathcal{C} \cap D_{\frac{4d}{3}}$: θ obtuse case

If $r_{X,n}$ denotes the $\frac{2\pi}{n}$ counterclockwise rotation around X as in Section 2.5, we can say the following:

Proposition 6.13. *If there exists an infinite family of hyperbolic knots with hidden symmetries $\mathcal{F} = \{K_{\infty,(p_2^i,q_2^i),\ldots,(p_n^i,q_n^i)}\}_i$ which geometrically converge to L as $i \to \infty$, then, there exists $E \in \mathcal{E}$ such that $\|E - C_0\| < \frac{d}{5}$ and $\mathcal{C}''_P$ contains $r_{E,3}(\mathcal{C}'_P)$ and $r^2_{E,3}(\mathcal{C}'_P)$.*

Proof. By Corollary 6.9, there exists $r_{E,3}$ such that $\|E - C_0\| \leq \frac{\sqrt{\text{area of } P}}{\sqrt{2}3^{\frac{5}{4}}}$ for some E in $\mathbb{C}$. Now, C_0, $r_{E,3}(C_0)$ and $r^2_{E,3}(C_0)$ are the vertices of an equilateral triangle with E as the center. So,

$$\|r_{E,3}(C_0) - C_0\| = \|r^2_{E,3}(C_0) - C_0\| = \sqrt{3}\|E - C_0.\| \leq \frac{\sqrt{\text{area of } P}}{\sqrt{2}3^{\frac{3}{4}}} \leq \frac{\sqrt{\|m\|\|l\|}}{\sqrt{2}3^{\frac{3}{4}}} < \frac{d}{3}.$$

Now by Lemma 6.11, we have, $r_{E,3}(C_0)$ and $r^2_{E,3}(C_0)$ lie in $\mathcal{C}'_P$. So, $E \in \mathcal{E}$.

For any $C' \in \mathcal{C}'_P$, $C' = C + p\,\mathbf{m} + q\,\mathbf{l}$ for some $C \in \mathcal{C}_P$ and p and q such that $|p| \leq k'_{\mathbf{h}}$ and $|q| \leq k' + k'_l$. So, we have,

$$\begin{aligned}\|C' - E\| \leq \|C' - C_0\| + \|C_0 - E\| &\leq \|C - C_0\| + |p|\|\mathbf{m}\| + |q|\|\mathbf{l}\| + \|C_0 - E\| \\ &\leq d + k'_{\mathbf{h}}d + (k' + k'_l)\,d + \frac{d}{5} = d\left(\frac{6}{5} + k'_{\mathbf{h}} + k' + k'_l\right).\end{aligned}$$

Here, note that $\|E - C_0\| \leq \frac{\sqrt{\text{area of } P}}{\sqrt{2}3^{\frac{5}{4}}} \leq \frac{\sqrt{\|m\|\|l\|}}{\sqrt{2}3^{\frac{5}{4}}} < \frac{d}{5}$.

Since, $r_{E,3}$ is a rotation, we have $\|r_{E,3}(C') - E\| = \|r^2_{E,3}(C') = E\| = \|C' - E\|$, which is less than $d\left(\frac{6}{5} + k'_{\mathbf{h}} + k' + k'_l\right)$. So,

$$\begin{aligned}\|r_{E,3}(C') - C_0\| \leq \|r_{E,3}(C') - E\| + \|E - C_0\| &\leq d\left(\frac{6}{5} + k'_{\mathbf{h}} + k' + k'_l\right) + \frac{d}{5} \\ &= d\left(\frac{7}{5} + k'_{\mathbf{h}} + k' + k'_l\right).\end{aligned}$$

Similarly, $\|r^2_{E,3}(C') - C_0\| \leq d\left(\frac{7}{5} + k'_{\mathbf{h}} + k' + k'_l\right)$. So, by Lemma 6.11, $r_{E,3}(C'), r^2_{E,3}(C') \in \mathcal{C}''_P$. This completes the proof. □

6.3.1 Implementation of the algorithm in SnapPy

We now use Proposition 6.13 to set up a code in SnapPy [9] which will help us find centers of order 3 rotational symmetries of the K_1-circle packing in $\mathcal{E}$ for a SnapPy cusp parallelogram P of the K_1-cusp of a hyperbolic 3-manifold M. We also define a function which detects whether these centers fixes centers of horoballs of the other cusps. We describe the code below. We comment out the explanations of each command.

```
import math
k0=1/math.sqrt(math.sqrt(27))

def intlist(k):
      '''for natural number k, returns the set of integers
      {-k,-k+1,...,k-1,k}'''
      return range(-k,k+1,1)

def cosangle(u,v):
     '''returns absolute value of cosine of the angle between the vectors
     given by complex numbers u and v'''
     return abs(u.real*v.real+u.imag*v.imag)/(abs(u)*abs(v))

def r1(x,y):
    ''' returns r_{x,3}(y) '''
    re=x.real-(y-x).real/2-(y-x).imag*math.sqrt(3)/2
    im=(x.imag-(y-x).imag/2+(y-x).real*math.sqrt(3)/2)*(0+1J)
    return re+im

def r2(x,y):
    '''returns r_{x,3}^2 (y)'''
    re=x.real-(y-x).real/2+(y-x).imag*math.sqrt(3)/2
    im=(x.imag-(y-x).imag/2-(y-x).real*math.sqrt(3)/2)*(0+1J)
    return re+im

def Tri(h,H,v):
    '''returns the pair (x,y) of elements from H such that
    vectors joining h to x and h to y have angle \pi/3 or \pi/6 and
    length of these vectors is less than or equal to k_0* \sqrt(v)'''
    G=[]
    for x in H:
        if 0.005<abs(x-h)<k0*math.sqrt(v)+0.005:
            for y in H:
                if abs(abs(y-h)-abs(x-h))<0.005:
                    if abs(cosangle(x-h,y-h)-0.5)<0.005:
                        G.append((x,y))
    return list(set(G))

def Epi(h,G,d):
    '''returns the centers of triangles with vertices h and the pairs
    from G which lie in the d/5 disk around h'''
    E=[h]
```

```
    for t in G:
        if abs(-2*h+t[0]+t[1])/3<(d/5)+0.005:
            E.append((h+t[0]+t[1])/3)
    return list(set(E))

def include(x,H):
    '''checks whether x belong to H'''
    r=False
    for y in H:
        if abs(x-y)<0.005:
            r=True
            break
    return r

def Cen(x,D,R):
    '''checks if images of the elements of D under r_{x,3} and r_{x,3}^2
    lie in R'''
    r=True
    for y in D:
        if include(r1(x,y),R)==False or include(r2(x,y),R)==False:
            r=False
            break
    return r

def mer(M,i):
    '''returns m, the complex number representing the non-horizontal sides
    of SnapPy cusp parallelogram for cusp i of manifold M'''
    c=M.cusp_neighborhood()
    c.set_displacement(c.reach(i),i)
    return c.translations(i)[0]

def lon(M,i):
    '''returns l, the complex number representing the horizontal sides of
    SnapPy cusp parallelogram for cusp i of manifold M'''
    c=M.cusp_neighborhood()
    c.set_displacement(c.reach(i),i)
    return c.translations(i)[1]

def hei(M,i):
    '''returns the heigh of the cusp parallelogram determined by m and l
    for cusp i of manifold M'''
    return abs(mer(M,i))*math.sqrt(1-pow(cosangle(mer(M,i),lon(M,i)),2))

def d(M,i):
    '''returns the maximum amongst abs(m), abs(l), abs(m+l) and abs(m-l)
    for cusp i of manifold M'''
    m=mer(M,i)
    l=lon(M,i)
    return max(abs(m), abs(l), abs(m+l), abs(m-l))

def k_h_sm(M,i):
     '''returns k_h' for cusp i of manifold M'''
     return math.ceil(((4/3)*d(M,i)+1)/hei(M,i))
```

```
def k_sm(M,i):
    '''return k' for cusp i of maniofold M'''
    m=mer(M,i)
    l=lon(M,i)
    return math.ceil(k_h_sm(M,i)*abs(m)*abs(cosangle(m,l))/abs(l))

def k_l_sm(M,i):
    '''returns k_l' for cusp i of manifold M'''
    l=lon(M,i)
    return math.ceil(((4/3)*d(M,i)+1)/abs(l))

def k_h_la(M,i):
    '''returns k_{h}'' for cusp i of manifold M'''
    return math.ceil((d(M,i)*((12/5)+ k_h_sm(M,i)+k_sm(M,i)+k_l_sm(M,i))+1)/
        hei(M,i))

def k_la(M,i):
    '''return k'' for cusp i of manifold M'''
    m=mer(M,i)
    l=lon(M,i)
    return math.ceil(k_h_la(M,i)*abs(m)*abs(cosangle(m,l))/abs(l))

def k_l_la(M,i):
    '''returns k_l'' for cusp i of manifold M'''
    l=lon(M,i)
    return math.ceil((d(M,i)*((12/5)+k_h_sm(M,i)+k_sm(M,i)+k_l_sm(M,i))+1)/abs
        (l))

def full_horo(M,i):
    '''returns the full sized horoballs whose centers lie in the
    cusp parallelogram for cusp i of manifold M'''
    c=M.cusp_neighborhood()
    c.set_displacement(c.reach(i),i)
    return c.horoballs(cutoff=0.9, which_cusp=i, full_list=True,
        high_precision=False)

def Circ_cen(M,i):
    '''returns the list \mathcal{C}_P containing the centers of the circles
    in the i-circle packing lying in cusp parallelogram P
    for cusp i of manifold M'''
    H=[]
    for x in full_horo(M,i):
        if x['index']==i:
            H.append(x['center'])
    return H

def Circ_cen_trnsltd_large(M,i):
    '''returns the translations \mathcal{C}_P'' of the list \mathcal{C}_P
    from Circ_cen function'''
    H=[]
    for x in Circ_cen(M,i):
        for p in intlist(k_h_la(M,i)):
            for q in intlist(k_la(M,i)+k_l_la(M,i)):
                H.append(x+p*mer(M,i)+q*lon(M,i))
```

```
    return H

def Circ_cen_trnsltd_small(M,i):
    '''returns the translations \mathcal{C}_P' of the list \mathcal{C}_P
    from Circ_cen function'''
    H=[]
    for x in Circ_cen(M,i):
        for p in intlist(k_h_sm(M,i)):
            for q in intlist(k_sm(M,i)+k_l_sm(M,i)):
                H.append(x+p*mer(M,i)+q*lon(M,i))
    return H

def max_vol(M,i):
    '''returns (maximal) cusp volume of cusp i of manifold M'''
    c=M.cusp_neighborhood()
    c.set_displacement(c.reach(i),i)
    return c.volume(i)

def rot(M,i):
    '''returns centers of valid order 3 rotations of i-circle packing
    of manifold M which lies in \mathcal{E}'''
    cen=[]
    dis=d(M,i)
    h=Circ_cen(M,i)[0]
    CS=Circ_cen_trnsltd_small(M,i)
    CL=Circ_cen_trnsltd_large(M,i)
    E=Epi(h,Tri(h,CS,max_vol(M,i)),dis)
    for x in E:
            if Cen(x,CS,CL)==True:
                cen.append(x)
    return cen

def Horo_cen_diff(M,i):
    '''returns enough translations of the centers of horoballs of cusps
    other than i in manifold M'''
    c=M.cusp_neighborhood()
    c.set_displacement(c.reach(i),i)
    h=Circ_cen(M,i)[0]
    H=[]
    for x in c.horoballs(cutoff=0.1,which_cusp=i,full_list=True,
        high_precision=False):
        if x['index']!=i:
            H.append(x['center'])
    G=[]
    for x in H:
        for p in intlist(k_h_sm(M,i)):
            for q in intlist(k_sm(M,i)+k_l_sm(M,i)):
                if abs(x+p*mer(M,i)+q*lon(M,i)-h)<(d(M,i)/5)+0.005:
                    G.append(x+p*mer(M,i)+q*lon(M,i))
    return G

def free_rot(M,i):
      '''returns elements of the output of the rot function,
      i.e., the centers of valid order 3 rotations
```

```
    of i-circle packing of manifold M, which do not fix
    centers of horoballs of other cusps'''
    H_rot=rot(M,i)
    H_free_rot=False
    if len(H_rot)>0:
        H_diff=Horo_cen_diff(M,i)
        for x in H_rot:
            if include(x,H_diff)!=True:
                H_free_rot=True
                break
    return H_free_rot
```

Remark 6.14. *Note that we use this code to rule out cases, i.e. when for cusp i of manifold M , if "free_rot(M, i)" returns "False", we conclude that there is no order* 3 *required symmetry of the i-circle packing. Since Python floating point numbers are not exact, in order to reduce approximation error, we have added "0.005" to the bounds of some of the conditionals in the code.*

Similarly, while getting the full sized horoballs in the cusp parallelogram, we are setting the "cutoff" as 0.9 *instead of* 1 *("cutoff" in SnapPy means lower cutoff of the diameter of the horoballs) to reduce the error of missing out a full sized horoball.*

We also note that in the code above, we set 0.1 *as the cutoff in the definition of the function "Horo_cen_diff()" which returns the centers of a list of horoballs corresponding to cusps other than i. Since we are trying to rule out the cases where the fixed points of the order* 3 *rotational symmetries happen to be centers of horoballs corresponding to cusps different than i, if we take a smaller cutoff in the definition of the function "Horo_cen_diff()", we could (potentially) rule out more cases, but it will increase computation time.*

6.4 Examples

First we enter last section's Python code in SnapPy. Then we define the manifolds from Subsection 6.2.3 in SnapPy [9]:

```
M1=Manifold('L11n354')
M2=Manifold('L10a157')
```

```
M3=Manifold('L8a20')
```

Now we run "rot" and "free_rot" functions in snappy with the manifolds and the corresponding cusps from Subsection 6.2.3 as its arguments (SnapPy [9] labels cusp 0 by red, cusp 1 by blue, cusp 2 by green and so on):

```
rot(M1,0)
rot(M2,2)
rot(M3,0)
free_rot(M1,0)
free_rot(M2,2)
free_rot(M3,0)
```

The first two commands return empty lists, where as the fourth and the fifth return "False", which we would expect from our observation from Subsection 6.2.3. On the other hand, the third command returns the list "[(1.000000000000003+1.7320508075688856j)]" and the last command returns "True". Both of these commands correspond to the red cusp of $L8a20$, whose complement can be identified with tetrahedral manifold $otet10_{00006}$. Later in Section 7.5 (in Case 3 of proof of Theorem 7.4), we argue that the corresponding circle packing of $\mathbb{C}$ even for this case cannot have $(3,3,3)$ wallpaper group of symmetries.

7.0 Tetrahedral links

In this chapter, we will apply our results and the SnapPy code from the previous chapter to certain elements of a family of links called tetrahedral links. This family of links are natural candidates to study in connection with hidden symmetries, which we will explain why.

7.1 Definitions and census paper

A hyperbolic manifold L is called a *tetrahedral manifold* if it can be triangulated into regular ideal hyperbolic tetrahedra. A hyperbolic link whose complement is a tetrahedral manifold is referred as a *tetrahedral link*. For example, figure eight knot is a tetrahedral knot since its complement decomposes into two regular ideal tetrahedra. Fominykh et al. [11] found a census consisting of the orientable tetrahedral manifolds with decomposition into 25 or fewer (regular ideal) tetrahedra and the non-orientable tetrahedral manifolds with decomposition into 21 or fewer (regular ideal) tetrahedra.

7.2 Why study tetrahedral links

All the shape parameters of a regular ideal tetrahedron is $\frac{1+i\sqrt{3}}{2}$. So, the shape field (see Definition 2.29) of a tetrahedral manifold is $\mathbb{Q}(i\sqrt{3})$ which via Theorem 2.30 implies that the invariant trace field is also $\mathbb{Q}(i\sqrt{3})$. Now arguing similarly as in the proof of Theorem 5.7 in Section 5.3, we see the cusp field of a cusp of a tetrahedral manifold is also $\mathbb{Q}(i\sqrt{3})$ as the cusp field contains non-real complex numbers and by virtue of Theorem 2.31 it is contained in the invariant trace field. Now, we know from Theorem 4.7 if Dehn filling on all but one component of a link L produces an infinitely family of geometrically converging hyperbolic knots with hidden symmetries, then the cusp field of the non-filled cusp of L must be $\mathbb{Q}(i)$ or

$\mathbb{Q}(i\sqrt{3})$. Since the cusp field of all the cusps of a tetrahedral link is $\mathbb{Q}(i\sqrt{3})$, tetrahedral links are natural candidates for testing whether we can obtain an infinitely family of geometrically converging hyperbolic knots with hidden symmetries from Dehn filling all but one cusp.

7.3 Tetrahedral link complements and their first homology

Fominykh et al. [11] in their paper gives a list of tetrahedral links. Their list consists of the figure eight knot and 25 tetrahedral links with two or more components. One of these links has 20 and the rest has 12 or fewer (regular ideal) tetrahedra in their triangulation. The number of total links in their orientable tetrahedral census is far bigger and it is not an easy task to find out whether an orientable tetrahedral manifold is a link or not. But, we should note that tetrahedral links can also been seen as links in the integral homology spheres and from the following result from [11] one can easily find out when a cusped hyperbolic 3-manifold is a link complement in an integral homology sphere:

Proposition 7.1 (Lemma 6.1, [11])**.** *A cusped hyperbolic* 3*-manifold* M *is a link complement in an integral homology sphere if and only if the first homology group of* M*,* $H_1(M,\mathbb{Z})$*, is torsion free and* $rank(H_1(M,\mathbb{Z}))$ *is equal to the number of cusps of* M*.*

We use this above proposition to write the following code on SnapPy [9] which can tell us when a cusped hyperbolic 3-manifold in SnapPy is a link complement in an integral homology sphere:

```
def htor(M):
    r=False
    G=M.homology()
    L=G.elementary_divisors()
    if L[0]!=0:
            r=True
    return r
```

```
def linkHS(M):
    r=False
    G=M.homology()
    if htor(M)==False:
        if G.rank()==M.num_cusps():
            r=True
    return r
```

The function "htor" finds out if the homology group of the argument has torsion elements and if the answer is no, it returns "False". Now, "linkHS" function first tests using "htor" function whether the manifold M in the argument has torsion or not. If it does not, then, "linkHS" checks whether the rank of the first homology group of M is equal to the number of the cusps of M. If this answer is yes, then the function "linkHS" returns "True", i.e. M is a link complement in an integral homology sphere by Proposition 7.1.

The orientable tetrahedral census of [11] is embedded in SnapPy [9]. Using the "linkHS" function defined above, the code below forms a list "K" containing all the two or more cusped orientable tetrahedral manifolds with 25 or fewer (regular ideal) tetrahedra in their decomposition which are link complements in integral homology spheres (we imported SnapPy as a Python module for the code below).

```
K=[]
for i in range(1,26):
    for M in snappy.TetrahedralOrientableCuspedCensus(solids=i):
        if linkHS(M)==True:
            if M.num_cusps()>1:
                K.append(M)
```

So, this "K" contains all the tetrahedral links (with two or more components) in the orientable tetrahedral census of [11] (i.e. with 25 or fewer (regular ideal) tetrahedra in their triangulations). One can see (for example by typing "len(K)") that "K" contains 882 elements. Our goal would be to understand whether for each element L of "K", an infinite

family of geometrically converging hyperbolic knots obtained from Dehn filling all but one component of L can have hidden symmetries. We will use Theorem 6.5 to find out whether given L in "K" and a cusp c of L, the c-circle packing of $\mathbb{C}$ can have order 3 rotational symmetries. We will apply our SnapPy code from Subsection 6.3.1 on the elements of "K" for this objective.

7.4 Cusp exchanging symmetries

We first recall from Fact 2.15 that if there is an isometry of a hyperbolic 3-manifold M exchanging two of its cusps c_1 and c_2, then, the members of a geometrically converging family of hyperbolic knots obtained from all cusps of M but c_1 are each isometric to a member of a geometrically converging family of hyperbolic knots obtained from Dehn filling all cusps of M but c_2. Keeping this in mind, we first write a function "cusplist" which determines a maximal list of cusps of its argument "M" with no two elements in the list exchanged by any isometry of "M".

```
def cusplist(M):
    G=M.symmetry_group()
    IG=G.isometries()
    L=range(M.num_cusps())
    K=[]
    for g in IG:
        for i in L:
            if g.cusp_images()[i]>i and g.cusp_images()[g.
               cusp_images()[i]]==i:
                K.append(g.cusp_images()[i])
    return list(set(L)-set(K))
```

We are now ready to run the SnapPy code from Subsection 6.3.1 on the elements of our list of tetrahedral manifolds "K".

7.5 Running the SnapPy code

We recall from the code in Subsection 6.3.1 that the "free_rot" function takes two arguments. For a pair of argument "(M,i)" where "M" is a SnapPy manifold and "i" an integer in $[0, \ldots, n-1]$ where n is the number of cusps of "M", if "free_rot(M,i)" returns "False", then, the symmetry group of the i-circle packing of $\mathbb{C}$ contains no $(3,3,3)$ wallpaper group.

Now, for any $0 \leq m \leq n \leq 881$, if we run the function "compute(m,n)" as below on SnapPy, it should give two lists: "excep_link" and "nice_link".

```
excep_link=[]
nice_link=[]
def compute(m,n):
  for M in K[m:n+1]:
    for i in cusplist(M):
      print(' ')
      print(K.index(M),M,i)
      if free_rot(M,i)==True:
        excep_link.append((K.index(M),M,i))
        print('excep_link list: ', excep_link)
      else:
        nice_link.append((K.index(M),M,i))
        print('nice_link list: ', nice_link)
      print((K.index(M),M,i), ' is not crashing')
  print(' ')
  print('Final excep_link = ', excep_link)
  print(' ')
  print('Final nice_link = ', nice_link)
```

Elements of both "excep_link" and "nice_link" are pairs "(M,i)" where "M" is a member of "K" and "i" is a member of "cusplist(M)". For an "(M,i)" in "nice_link", the symmetry group of i-circle packing of $\mathbb{C}$ does not contain a $(2,3,6)$ or $(3,3,3)$ wallpaper group satisfying

the conditions of Theorem 6.5 whereas for an "(M,i)" in "excep_link" we cannot conclude anything as such for the i-circle packing of $\mathbb{C}$.

Definition 7.2. *If we try to run the above code, SnapPy also crashes for some cases. Keeping this in mind, we define* $Excep_{m,n}$ *to denote the list "Excep_link' that we get for* m *and* n*, where* $0 \leq m \leq n \leq 881$*, plus the "(M,i)" cases for which our SnapPy code crashes for* M *in "K[m:n+1]".*

We run "free_rot" function as described above for first 162 members of "K", i.e. for "K[0:162]" in Python notation (Python list "K[0:162]" does not have any "K[162]" element) and for each cusp the "cusplist" function returns for such a member of "K[0:162]". We list the elements of $Excep_{0,161}$ in the Appendix A. So, the discussion above leads to the following theorem:

Theorem 7.3. *Let* L *be tetrahedral link in "K[0:162]" and* K_0 *a component of* L*. If* $(\mathbb{S}^3 - L, c)$ *does not belong to* $Excep_{0,161}$ *for any cusp* c *of* L *which is symmetric to the cusp corresponding to* K_0*, then a family of geometrically convergent hyperbolic knots obtained from Dehn filling all components of* L *but* K_0 *can have at most finitely many elements with hidden symmetries.*

Using this theorem above, we will now show the following:

Corollary 7.4. *If* L *is one of* 25 *tetrahedral links with more than one component that are listed in Fominykh et. al [11], then for any cusp* c *of* L*, a family of geometrically convergent hyperbolic knots obtained by Dehn filling all cusps of* L *but* c *cannot have infinitely many members with hidden symmetries.*

Proof. The 25 tetrahedral links listed in [11] paper are written down in Appendix B. The index of $otet20_{00570}$ in "K" is 253 and it does not belong to "K[0:162]". If we run "cusplist" function for this manifold on SnapPy, we get "[0,2]". After defining the list "K" and code given in Subsection 6.3.1 on SnapPy, if we run "free_rot(K[253],0)" and "free_rot(K[253],2)", they return "False".

We now check the elements from Fominykh et al. [11] list (see Appendix B) which appear in Appendix A.

Case 1 - cusp 0 of $otet04_{00001}$, which is "K[1]":

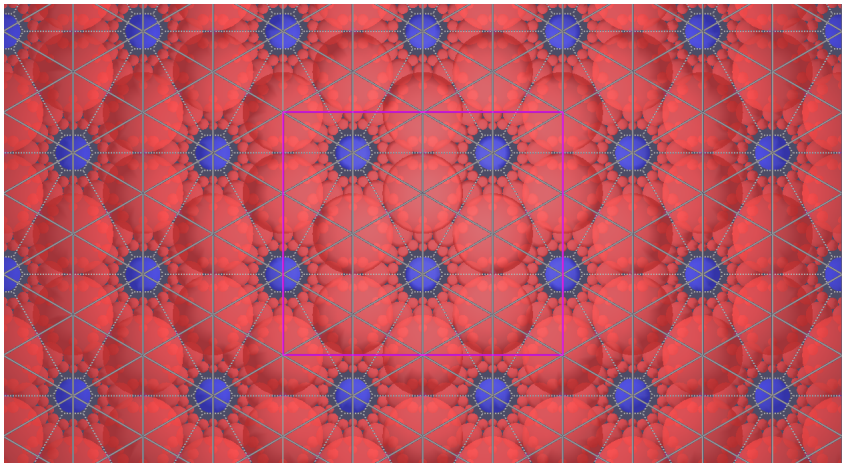

Figure 33: Red cusp maximal packing of $\mathbb{H}^3$ for $otet08_{00002}$ (picture obtained from SnapPy [9])

SnapPy identifies $otet04_{00001}$ with 6_2^2 complement. So, this case is already proven in Theorem 4.11.

Before we proceed with the next cases, we recall that the 0 cusp in SnapPy is labelled red and cusp 1 blue and cusp 2 green.

Case 2 - cusp 0 and 1 of $otet08_{00002}$, which is "K[3]":

Figure 33 and 34 show respectively the red cusp and blue cusp maximal packings of $\mathbb{H}^3$ for this manifold. Note that the cusp area of each of these cusps is $24a$ where $a = \frac{\sqrt{3}}{4}$ and the smallest co-area hexagonal lattice for each of the red cusp and blue cusp circle packings that we see has co-area of $6a$, which is exactly $\frac{1}{4}$ of the cusp area of the red cusp or the blue cusp. But, one can see from the picture that if these hexagonal lattices of co-area $6a$ are subgroups of a $(3, 3, 3)$ wallpaper group W, then W contains an order 3 rotation which fixes the center of a horoball of the other color (see Figure 6), which is not allowed. So, using Theorem 6.5, we can now conclude the result for this case.

Case 3 - cusp 0 of $otet10_{00006}$, which is "K[8]":

Red cusp maximal packing of $\mathbb{H}^3$ for $otet10_{00006}$ is shown in Figure 35. Cusp area of the red cusp is $12a$. But, the smallest co-area hexagonal lattice for the red cusp circle packing has

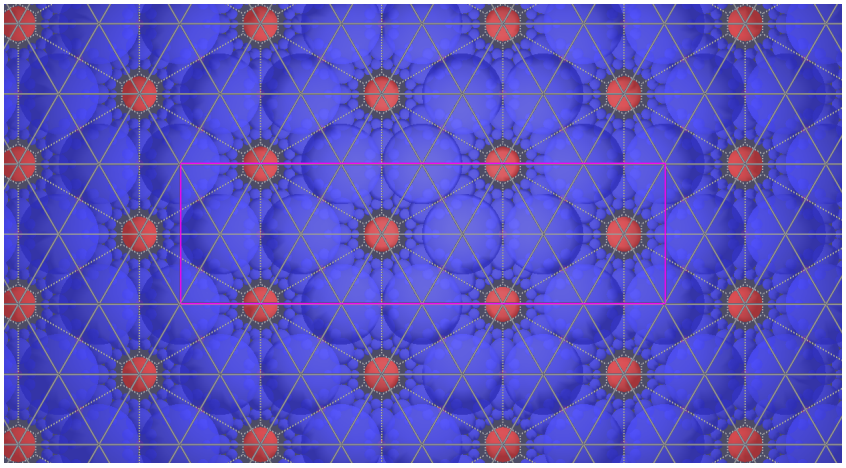

Figure 34: Blue cusp maximal packing of $\mathbb{H}^3$ for $otet08_{00002}$ (picture obtained from SnapPy [9])

co-area $6a$, which is greater than $\frac{12a}{4}$. So, Theorem 6.5 concludes the result for this as well.

Case 4 - cusp 2 of $otet10_{00008}$, which is "K[10]":

Figure 36 depicts the green cusp maximal packing of $\mathbb{H}^3$ for $otet10_{00008}$. Note that the co-area of the smallest co-area hexagonal lattice is $\frac{1}{2}$ of the cusp area of the green cusp. Theorem 6.5 then completes the proof for this case.

Case 5 - cusp 0 of $otet10_{00011}$, which is "K[11]":

We have shown the red cusp maximal packing of $\mathbb{H}^3$ for $otet10_{00011}$ in Figure 37. We can see from this figure that the argument given in Case 3 would apply here as well.

Case 6 - cusp 1 and 2 of $otet10_{00014}$, which is "K[12]":

Figure 38 shows the blue cusp maximal packing and Figure 39 the green cusp maximal packing of $\mathbb{H}^3$ for $otet10_{00014}$. The argument for the blue cusp is similar to that in Case 3 and Case 4. On the other hand, the cusp area of the green cusp is the co-area of the smallest co-area hexagonal lattice in the green cusp circle packing of $\mathbb{C}$. Therefore, Theorem 6.5 implies the result for the green cusp.

Case 7 - cusp 0 of $otet10_{00043}$, which is "K[17]":

One can see from Figure 40, which shows the red cusp maximal packing of $\mathbb{H}^3$ for $otet10_{00043}$,

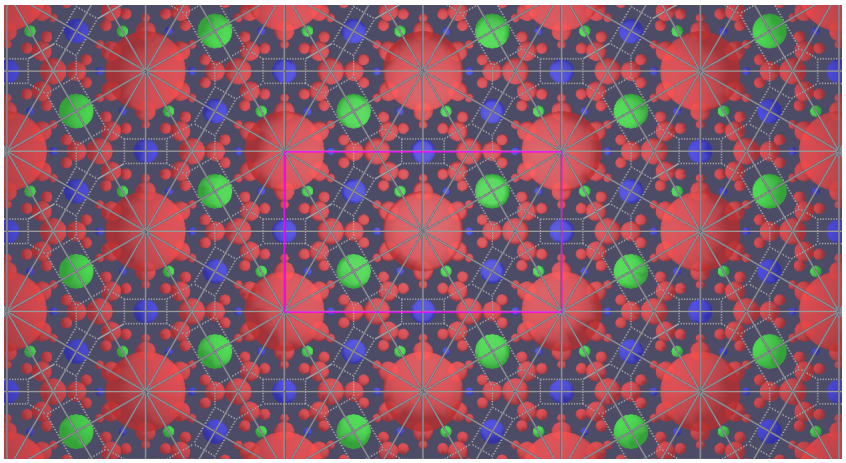

Figure 35: Red cusp maximal packing of $\mathbb{H}^3$ for $otet10_{00006}$ (picture obtained from SnapPy [9])

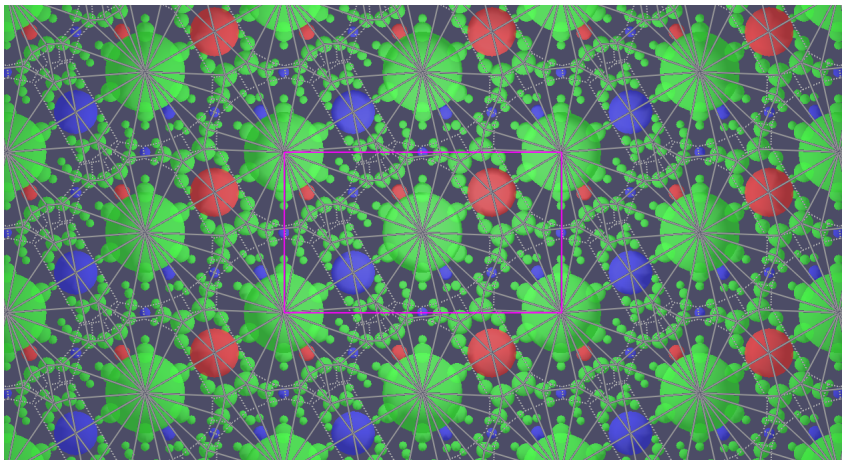

Figure 36: Green cusp maximal packing of $\mathbb{H}^3$ for $otet10_{00008}$ (picture obtained from SnapPy [9])

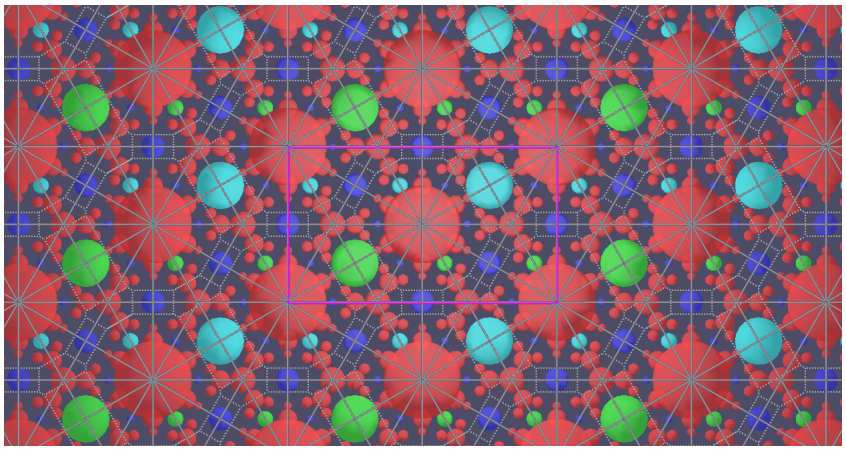

Figure 37: Red cusp maximal packing of $\mathbb{H}^3$ for $otet10_{00011}$(picture obtained from SnapPy [9])

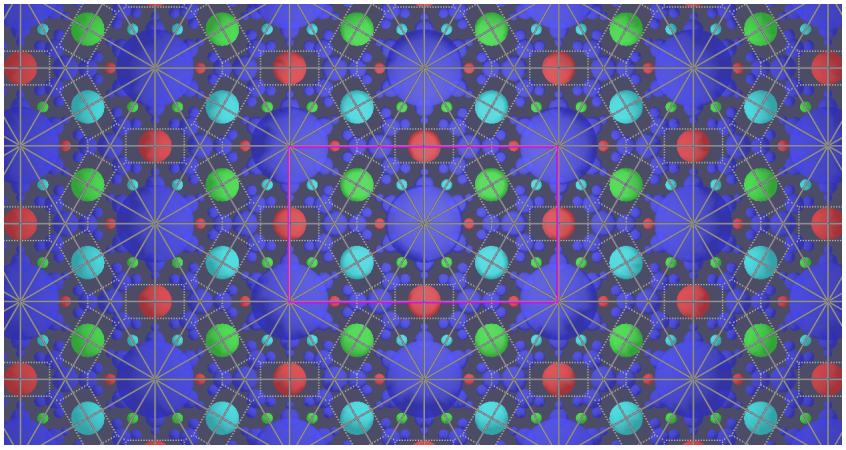

Figure 38: Blue cusp maximal packing of $\mathbb{H}^3$ for $otet10_{00014}$ (picture obtained from SnapPy [9])

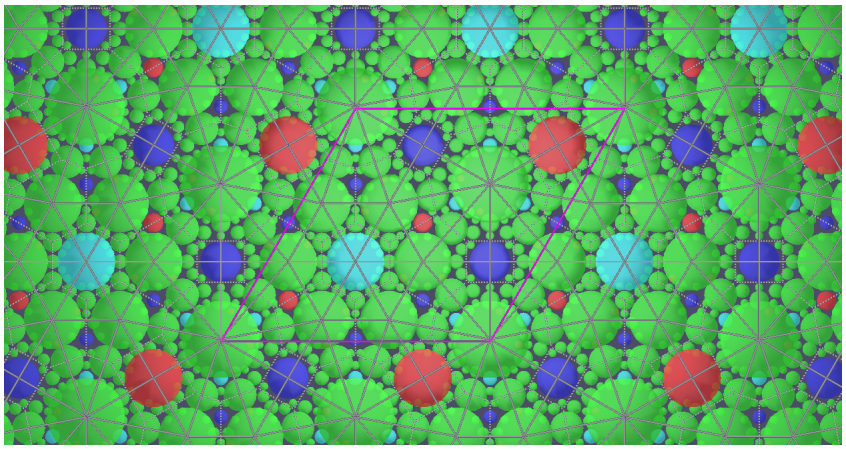

Figure 39: Green cusp maximal packing of $\mathbb{H}^3$ for $otet10_{00014}$ (picture obtained from SnapPy [9])

that we can argue Case 7 similarly as in Case 3.

Case 8 - cusp 0 of $otet12_{00009}$, which is "K[22]":
Red cusp maximal packing of $\mathbb{H}^3$ for $otet12_{00009}$ is shown in Figure 41. We can see from this figure that the cusp area of red cusp is $36a$. On the other hand, if a hexagonal lattice with co-area less than or equal to $9a = \frac{36a}{4}$ is contained in a $(3, 3, 3)$ wallpaper group W, then W has an element fixing a blue or green or light blue horoball. So, by Theorem 6.5 the result also follows for this final case.

Now, since by Theorem 7.3 the result follows for the cases which do not appear in Appendix A, the corollary can be concluded.

□

Remark 7.5. *We note that in addition to* 6_2^2*, the link corresponding to the Berge manifold also belongs to list of* 25 *links from [11] and from [15, Proof of Theorem 6.1](or, [14, Proof of Theorem 1.1]) we already know that the above result is true for the Berge manifold.*

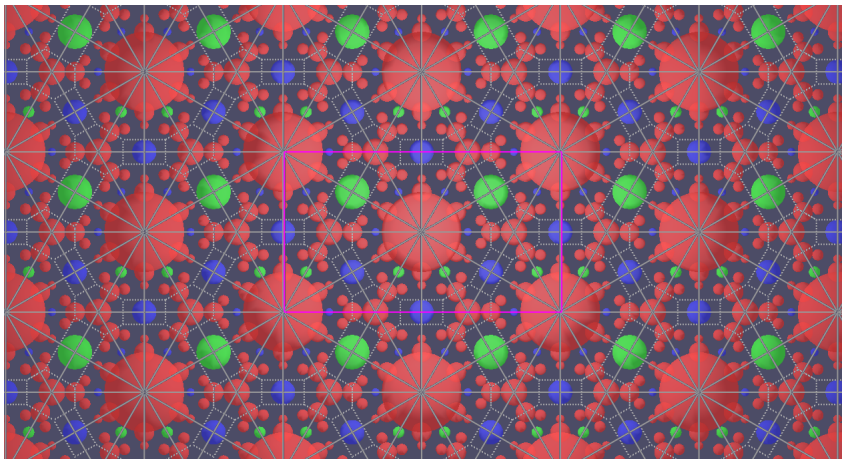

Figure 40: Red cusp maximal packing of $\mathbb{H}^3$ for $otet10_{00043}$ (picture obtained from SnapPy [9])

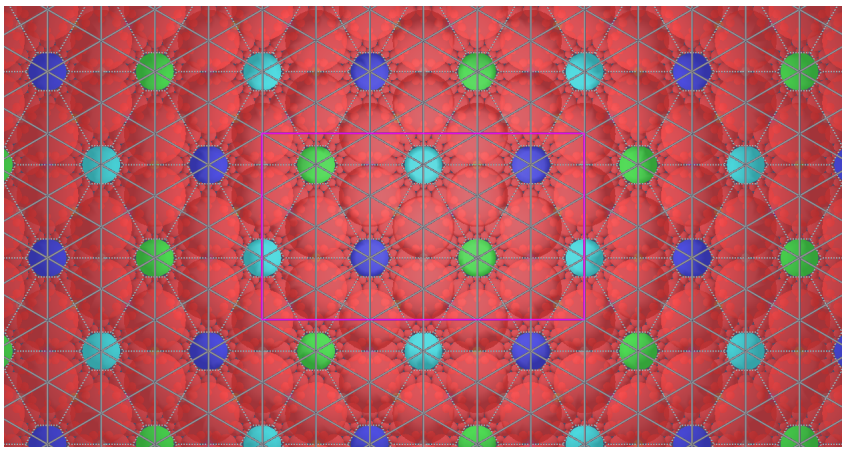

Figure 41: Red cusp maximal packing of $\mathbb{H}^3$ for $otet12_{00009}$ (picture obtained from SnapPy [9])

8.0 Some members of $Excep_{0,161}$

In this chapter, we will discuss some elements of $Excep_{0,161}$. We will use the notation $K_{Excep_{0,161}}$ to denote the elements of "K" which appears as the first component of an element of $Excep_{0,161}$.

In section 8.1, we will discuss some tetrahedral links whose complements belong to $K_{Excep_{0,161}}$ and the horoball packings associated with the corresponding cusps have a $(3,3,3)$ wallpaper group of symmetries. Section 8.2 contains example of a member of $Excep_{0,161}$ for which we don't know whether if the corresponding (tetrahedral) link in the homology sphere is actually a tetrahedral link or not. In section 8.3, we will show an example of a manifold in $K_{Excep_{0,161}}$ for which there is a $(3,3,3)$ wallpaper group of symmetries of the circle packing of $\mathbb{C}$ for the corresponding cusp, but, there is no order 3 symmetry of the corresponding horoball packing of $\mathbb{H}^3$.

8.1 Some exceptional tetrahedral links

8.1.1 Tetrahedral link $L14n63694$

The complement of the link $L14n63694$ can also be identified as $otet20_{00063}$ in the notation of [11]. $otet20_{00063}$ appears as a manifold in $K_{Excep_{0,161}}$. All of $(otet20_{00063}, 0)$, $(otet20_{00063}, 1)$ and $(otet20_{00063}, 2)$ belong to $Excep_{0,161}$. Recall that cusp 0 in SnapPy is labelled red, cusp 1 blue and cusp 2 green. Figure 42 shows the red cusp, the blue cusp and the green cusp maximal packings of $\mathbb{H}^3$. Note that the symmetry groups of both the red cusp and the green cusp circle packings contain $(3,3,3)$ wallpaper groups whose lattice subgroups have co-area exactly $\frac{1}{4}$ of the corresponding cusp area such that no rotations of the wallpaper groups fix the center of a horoball corresponding to a different cusp. On the other hand, in the blue cusp circle packing, co-area of the smallest co-area hexagonal lattice is half of the area of the blue cusp. So, the blue cusp circle packing is not really "exceptional" even

though our code detects it to be.

We should note here that $otet20_{00063}$ has 5 components. Using SnapPy one can check that cusps 1 and 3 are symmetric, so are 2 and 4. Therefore, the "cusplist()" function (see Section 7.4) returns the list "[0,1,2]" for $otet20_{00063}$.

8.1.2 Tetrahedral link $L12a2018$

$otet20_{00061}$ is 5-cusped tetrahedral manifold which can be identified with the complement of the link $L12a2018$. $(otet20_{00061}, 0)$ and $(otet20_{00061}, 1)$ both belong to $Excep_{0,161}$. We picture the red cusp and blue cusp maximal packings of $\mathbb{H}^3$ in Figure 43. Figure 43 shows that the symmetry group of the red cusp circle packing has a $(3, 3, 3)$ wallpaper subgroup, say W, such that the lattice subgroup of W has co-area exactly $\frac{1}{4}$ of the cusp area of the red cusp and no member of W fix the center of a horoball of a different color. On the other hand, in the blue cusp circle packing, smallest co-area that a hexagonal lattice has is half of the area of the blue cusp. So, similarly as in the case above, the blue cusp circle packing is not really "exceptional". We also note from SnapPy [9] that the cusp 1 is symmetric to cusp 3, cusp 2 is symmetric to cusp 4 and $(otet20_{00061}, 2)$ does not belong to $Excep_{0,161}$.

8.1.3 Tetrahedral link $L14n62448$

The tetrahedral manifold $otet20_{00060}$ is isometric to the complement of the 4-component link $L14n62448$. We see that $(otet20_{00060}, 0)$ and $(otet20_{00060}, 1)$ are contained in $Excep_{0,161}$. The red cusp and blue cusp maximal packings of $\mathbb{H}^3$ for this manifold are shown in Figure 44. We can see from this figure that the symmetry group of red cusp maximal packing contains a $(3, 3, 3)$ wallpaper group, the co-area of whose lattice subgroup is $\frac{1}{4}$ of the cusp area of the red cusp. Also, this wallpaper group has no rotational symmetry which fixes center of a different colored horoball. Blue cusp circle packing on the other hand as in the two cases above is not truly "exceptional" since the co-area of the smallest co-area hexagonal lattice is half of the area of the blue cusp. We note, "cusplist()" function returns "[0,1,2]" for this manifold and $Excep_{0,161}$ does not contain $(otet20_{00060}, 2)$. One can check from SnapPy that cusps 1 and 3 are symmetric.

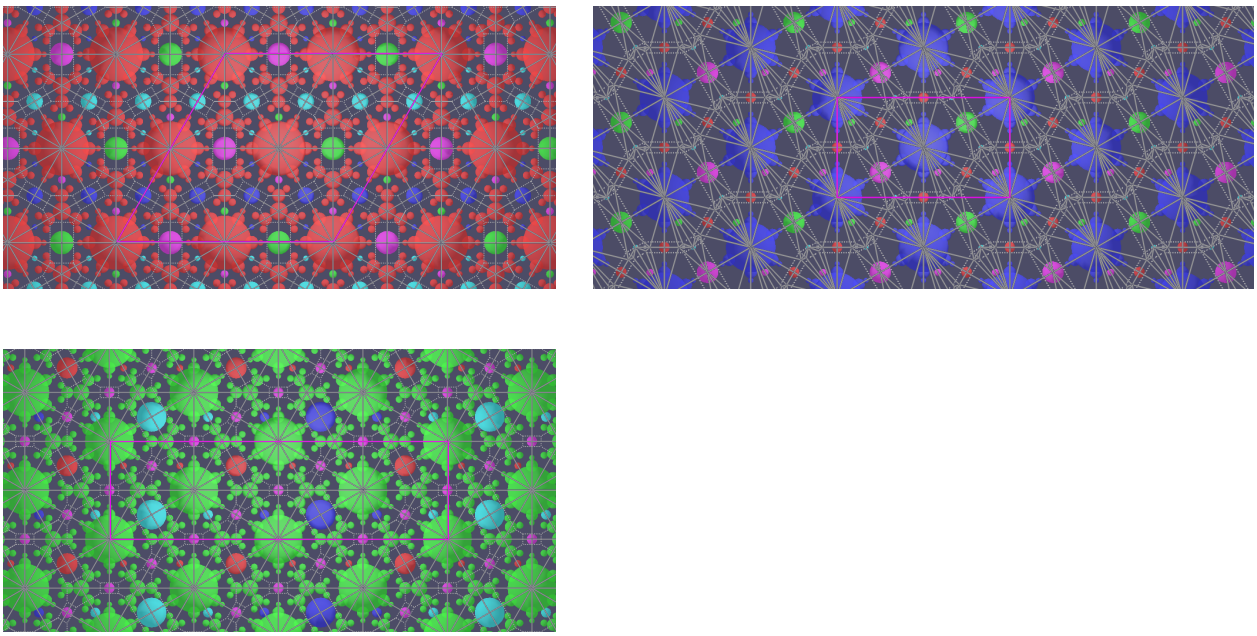

Figure 42: Top left: Red cusp maximal packing of $\mathbb{H}^3$ for $otet20_{00063}$, Top right: Blue cusp maximal packing of $\mathbb{H}^3$ for $otet20_{00063}$, Bottom: Green cusp maximal packing of $\mathbb{H}^3$ for $otet20_{00063}$ (pictures obtained from SnapPy [9])

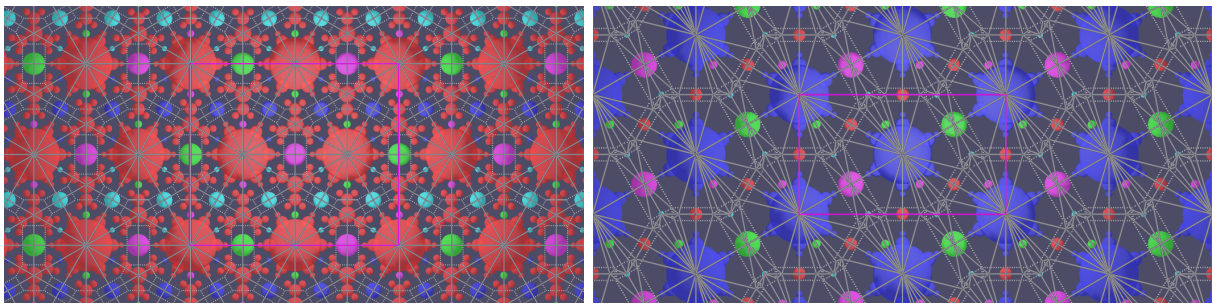

Figure 43: Left: Red cusp maximal packing of $\mathbb{H}^3$ for $otet20_{00061}$, Right: Blue cusp maximal packing of $\mathbb{H}^3$ for $otet20_{00061}$ (pictures obtained from SnapPy [9])

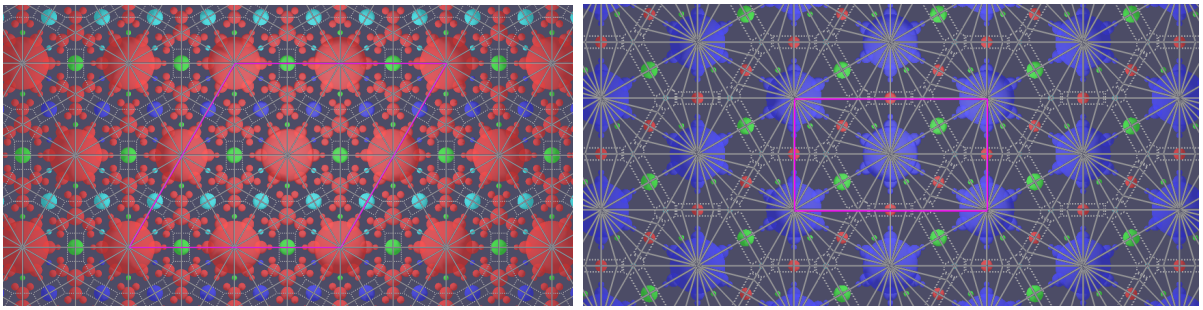

Figure 44: Left: Red cusp maximal packing of $\mathbb{H}^3$ for $otet20_{00060}$, Right:Blue cusp maximal packing of $\mathbb{H}^3$ for $otet20_{00060}$ (pictures obtained from SnapPy [9])

8.2 Tetrahedral manifold $otet20_{00049}$

We now discuss the tetrahedral manifold $otet20_{00049}$ which belongs to $K_{Excep_{0,161}}$ such that for all of its cusps, the "free_rot()" function from Subsection 6.3.1 would return "True". But, we don't know whether this manifold is isometric to a link complement or not. $otet20_{00049}$ is a 4-cusped manifold. SnapPy tells that cusps 1 and 2 are symmetric as are cusps 0 and 3. So, "cusplist()" returns "[0,1]" for this manifold. We picture red cusp and blue cusp maximal packings of $\mathbb{H}^3$ in Figure 45. We see that the symmetry groups of each of these packings have $(3, 3, 3)$ wallpaper subgroups none of whose elements fix the center of a horoball of a different color and their lattice subgroups have co-area $\frac{1}{4}$ of the corresponding cusp area.

8.3 Tetrahedral manifold $otet20_{00062}$

In Figure 46, we show the green cusp maximal packing of $\mathbb{H}^3$ for the tetrahedral manifold $otet20_{00062}$. Note that the green cusp circle packing of $\mathbb{C}$ has a $(3, 3, 3)$ wallpaper group of symmetries none of which fix a center of a different colored horoball such that the lattice subgroup has co-area $\frac{1}{4}$ of the cusp area of the green cusp. But, none of the order 3 elements of this wallpaper group is actually a symmetry of the green cusp maximal packing of $\mathbb{H}^3$,

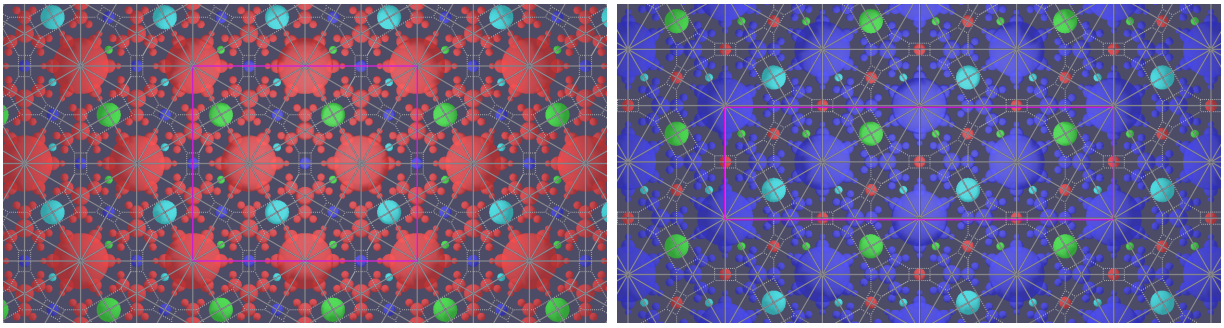

Figure 45: Left: Red cusp maximal packing of $\mathbb{H}^3$ for $otet20_{00049}$, Right: Blue cusp maximal packing of $\mathbb{H}^3$ for $otet20_{00049}$ (pictures obtained from SnapPy [9])

since for each of them there is some smaller (Euclidean) sized green horoball which they do not send to a green horoball of the same (Euclidean) size. So, even though $(otet20_{00062}, 2)$ belongs to $Excep_{0,161}$, we can conclude by Fact 6.8 that a geometrically convergent family of hyperbolic knots obtained by Dehn filling all but green cusp of $otet20_{00062}$ can only have finitely many elements with hidden symmetries. We also remark that a similar conclusion can be made for the other cusps of $otet20_{00062}$ as for any $i \neq 2$ in the "cusplist(otet20_00062)", $(otet20_{00062}, i)$ does not belong to $Excep_{0,161}$.

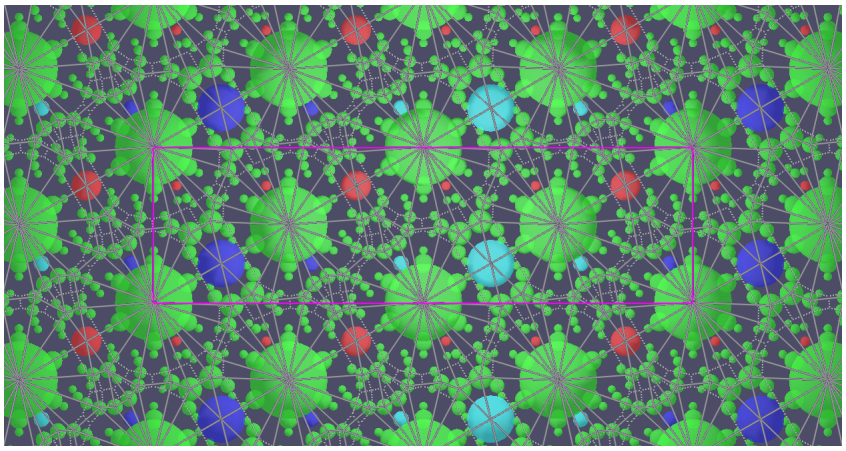

Figure 46: Green cusp maximal packing of $\mathbb{H}^3$ for $otet20_{00062}$ (picture obtained from SnapPy [9])

Appendix A $Excep_{0,161}$

We will write the elements in the following format: (i, M, j) where i is the index of manifold M in "K" and j is the cusp of M. Description of M from SnapPy also shows how many cusps it has by the number of $(0, 0)$ that appear at the end of M. $(0, 0)$ in SnapPy means that the corresponding cusp is unfilled.

A.1 Cases where SnapPy code crashes

1. $(28, otet14_{00004}(0,0)(0,0)(0,0), 1)$
2. $(97, otet18_{00026}(0,0)(0,0)(0,0), 2)$
3. $(116, otet18_{00074}(0,0)(0,0)(0,0), 0)$
4. $(117, otet18_{00076}(0,0)(0,0)(0,0), 1)$
5. $(138, otet18_{00127}(0,0)(0,0)(0,0)(0,0), 3)$

A.2 Cases for which "free_rot()" function returns "True"

1. $(1, otet04_{00001}(0,0)(0,0), 0)$
2. $(3, otet08_{00002}(0,0)(0,0), 0)$
3. $(3, otet08_{00002}(0,0)(0,0), 1)$
4. $(4, otet08_{00003}(0,0)(0,0), 0)$
5. $(8, otet10_{00006}(0,0)(0,0)(0,0), 0)$
6. $(10, otet10_{00008}(0,0)(0,0)(0,0), 2)$
7. $(11, otet10_{00011}(0,0)(0,0)(0,0)(0,0), 0)$
8. $(12, otet10_{00014}(0,0)(0,0)(0,0)(0,0), 1)$
9. $(12, otet10_{00014}(0,0)(0,0)(0,0)(0,0), 2)$
10. $(17, otet10_{00043}(0,0)(0,0)(0,0), 0)$

11. $(22, otet12_{00009}(0,0)(0,0)(0,0)(0,0), 0)$
12. $(39, otet14_{00027}(0,0)(0,0)(0,0)(0,0), 2)$
13. $(40, otet14_{00029}(0,0)(0,0)(0,0)(0,0), 2)$
14. $(58, otet16_{00013}(0,0)(0,0), 0)$
15. $(58, otet16_{00013}(0,0)(0,0), 1)$
16. $(69, otet16_{00053}(0,0)(0,0)(0,0)(0,0), 3)$
17. $(74, otet16_{00058}(0,0)(0,0), 0)$
18. $(74, otet16_{00058}(0,0)(0,0), 1)$
19. $(79, otet16_{00090}(0,0)(0,0), 0)$
20. $(83, otet18_{00003}(0,0)(0,0)(0,0)(0,0), 3)$
21. $(89, otet18_{00012}(0,0)(0,0)(0,0)(0,0), 3)$
22. $(98, otet18_{00028}(0,0)(0,0)(0,0)(0,0), 0)$
23. $(98, otet18_{00028}(0,0)(0,0)(0,0)(0,0), 1)$
24. $(104, otet18_{00044}(0,0)(0,0)(0,0)(0,0), 3)$
25. $(127, otet18_{00104}(0,0)(0,0)(0,0)(0,0), 0)$
26. $(137, otet18_{00126}(0,0)(0,0)(0,0)(0,0), 3)$
27. $(139, otet18_{00130}(0,0)(0,0)(0,0)(0,0), 3)$
28. $(140, otet18_{00131}(0,0)(0,0)(0,0)(0,0), 3)$
29. $(143, otet18_{00151}(0,0)(0,0)(0,0)(0,0), 3)$
30. $(145, otet18_{00171}(0,0)(0,0)(0,0)(0,0)(0,0)(0,0), 0)$
31. $(148, otet20_{00037}(0,0)(0,0)(0,0)(0,0), 3)$
32. $(149, otet20_{00038}(0,0)(0,0)(0,0)(0,0)(0,0), 1)$
33. $(149, otet20_{00038}(0,0)(0,0)(0,0)(0,0)(0,0), 4)$
34. $(150, otet20_{00039}(0,0)(0,0)(0,0)(0,0)(0,0)(0,0), 1)$
35. $(156, otet20_{00049}(0,0)(0,0)(0,0)(0,0), 0)$
36. $(156, otet20_{00049}(0,0)(0,0)(0,0)(0,0), 1)$
37. $(157, otet20_{00059}(0,0)(0,0)(0,0)(0,0), 0)$
38. $(157, otet20_{00059}(0,0)(0,0)(0,0)(0,0), 1)$
39. $(158, otet20_{00060}(0,0)(0,0)(0,0)(0,0), 0)$
40. $(158, otet20_{00060}(0,0)(0,0)(0,0)(0,0), 1)$

41. $(159, otet20_{00061}(0,0)(0,0)(0,0)(0,0)(0,0), 0)$
42. $(159, otet20_{00061}(0,0)(0,0)(0,0)(0,0)(0,0), 1)$
43. $(160, otet20_{00062}(0,0)(0,0)(0,0)(0,0), 2)$
44. $(161, otet20_{00063}(0,0)(0,0)(0,0)(0,0)(0,0), 0)$
45. $(161, otet20_{00063}(0,0)(0,0)(0,0)(0,0)(0,0), 1)$
46. $(161, otet20_{00063}(0,0)(0,0)(0,0)(0,0)(0,0), 2)$

Appendix B List of tetrahedral links with more than one cusp from Fominykh et al. paper [11] and their indices in "K"

Elements below are written in (i, M) form, where i is the index of M in "K".

1. $(0, otet04_{00000}(0,0)(0,0))$
2. $(1, otet04_{00001}(0,0)(0,0))$
3. $(2, otet08_{00001}(0,0)(0,0))$
4. $(3, otet08_{00002}(0,0)(0,0))$
5. $(5, otet08_{00005}(0,0)(0,0))$
6. $(6, otet08_{00009}(0,0)(0,0))$
7. $(7, otet10_{00003}(0,0)(0,0))$
8. $(8, otet10_{00006}(0,0)(0,0)(0,0))$
9. $(9, otet10_{00007}(0,0)(0,0))$
10. $(10, otet10_{00008}(0,0)(0,0)(0,0))$
11. $(11, otet10_{00011}(0,0)(0,0)(0,0)(0,0))$
12. $(12, otet10_{00014}(0,0)(0,0)(0,0)(0,0))$
13. $(13, otet10_{00025}(0,0)(0,0)(0,0))$
14. $(14, otet10_{00027}(0,0)(0,0)(0,0)(0,0)(0,0))$
15. $(15, otet10_{00028}(0,0)(0,0)(0,0)(0,0))$
16. $(16, otet10_{00042}(0,0)(0,0)(0,0)$
17. $(17, otet10_{00043}(0,0)(0,0)(0,0))$
18. $(18, otet12_{00001}(0,0)(0,0)(0,0))$
19. $(19, otet12_{00005}(0,0)(0,0))$
20. $(20, otet12_{00006}(0,0)(0,0)(0,0))$
21. $(21, otet12_{00007}(0,0)(0,0)(0,0))$
22. $(22, otet12_{00009}(0,0)(0,0)(0,0)(0,0))$
23. $(23, otet12_{00010}(0,0)(0,0)(0,0))$
24. $(24, otet12_{00018}(0,0)(0,0)(0,0))$
25. $(253, otet20_{00570}(0,0)(0,0)(0,0)(0,0)(0,0)(0,0)(0,0))$

Bibliography

[1] I. R. Aitchison and J. H. Rubinstein. Combinatorial cubings, cusps, and the dodecahedral knots. In *Topology '90 (Columbus, OH, 1990)*, volume 1 of *Ohio State Univ. Math. Res. Inst. Publ.*, pages 17–26. de Gruyter, Berlin, 1992.

[2] Riccardo Benedetti and Carlo Petronio. *Lectures on hyperbolic geometry*. Universitext. Springer-Verlag, Berlin, 1992.

[3] Michel Boileau, Steven Boyer, Radu Cebanu, and Genevieve S. Walsh. Knot commensurability and the Berge conjecture. *Geom. Topol.*, 16(2):625–664, 2012.

[4] Benjamin A. Burton. The Pachner graph and the simplification of 3-sphere triangulations. In *Computational geometry (SCG'11)*, pages 153–162. ACM, New York, 2011.

[5] Benjamin A. Burton, Ryan Budney, William Pettersson, et al. Regina: Software for low-dimensional topology. `http://regina-normal.github.io/`, 1999–2021.

[6] R. D. Canary, D. B. A. Epstein, and P. L. Green. Notes on notes of Thurston [mr0903850]. In *Fundamentals of hyperbolic geometry: selected expositions*, volume 328 of *London Math. Soc. Lecture Note Ser.*, pages 1–115. Cambridge Univ. Press, Cambridge, 2006. With a new foreword by Canary.

[7] Eric Chesebro, Jason DeBlois, Neil R Hoffman, Christian Millichap, Priyadip Mondal, and William Worden. Dehn surgery and hyperbolic knot complements without hidden symmetries. Preprint. arXiv:2009.14765, 2020.

[8] Eric Chesebro, Jason DeBlois, and Priyadip Mondal. Generic hyperbolic knot complements without hidden symmetries. Preprint. arXiv:1910.04712, 2019.

[9] Marc Culler, Nathan M. Dunfield, Matthias Goerner, and Jeffrey R. Weeks. SnapPy, a computer program for studying the geometry and topology of 3-manifolds. Available at `http://snappy.computop.org`.

[10] William D. Dunbar and G. Robert Meyerhoff. Volumes of hyperbolic 3-orbifolds. *Indiana Univ. Math. J.*, 43(2):611–637, 1994.

[11] Evgeny Fominykh, Stavros Garoufalidis, Matthias Goerner, Vladimir Tarkaev, and Andrei Vesnin. A census of tetrahedral hyperbolic manifolds. *Exp. Math.*, 25(4):466–481, 2016.

[12] M. Gromov. Almost flat manifolds. *J. Differential Geometry*, 13(2):231–241, 1978.

[13] Allen Hatcher. Hyperbolic structures of arithmetic type on some link complements. *J. London Math. Soc. (2)*, 27(2):345–355, 1983.

[14] Neil Hoffman. Commensurability classes containing three knot complements. *Algebr. Geom. Topol.*, 10(2):663–677, 2010.

[15] Neil R. Hoffman. Small knot complements, exceptional surgeries and hidden symmetries. *Algebr. Geom. Topol.*, 14(6):3227–3258, 2014.

[16] Neil R Hoffman. Cusp types of quotients of hyperbolic knot complements. Preprint. arXiv:2001.05066, 2020.

[17] Wolfram Research, Inc. Mathematica, Version 12.0. Champaign, IL, 2019.

[18] Melissa L. Macasieb and Thomas W. Mattman. Commensurability classes of $(-2, 3, n)$ pretzel knot complements. *Algebr. Geom. Topol.*, 8(3):1833–1853, 2008.

[19] Colin Maclachlan and Alan W. Reid. *The arithmetic of hyperbolic 3-manifolds*, volume 219 of *Graduate Texts in Mathematics*. Springer-Verlag, New York, 2003.

[20] A. Marden. *Outer circles*. Cambridge University Press, Cambridge, 2007. An introduction to hyperbolic 3-manifolds.

[21] Christian Millichap. Mutations and short geodesics in hyperbolic 3-manifolds. *Comm. Anal. Geom.*, 25(3):625–683, 2017.

[22] Christian Millichap and William Worden. Hidden symmetries and commensurability of 2-bridge link complements. *Pacific J. Math.*, 285(2):453–484, 2016.

[23] Walter D. Neumann and Alan W. Reid. Arithmetic of hyperbolic manifolds. In *Topology '90 (Columbus, OH, 1990)*, volume 1 of *Ohio State Univ. Math. Res. Inst. Publ.*, pages 273–310. de Gruyter, Berlin, 1992.

[24] Walter D. Neumann and Alan W. Reid. Rigidity of cusps in deformations of hyperbolic 3-orbifolds. *Math. Ann.*, 295(2):223–237, 1993.

[25] Walter D. Neumann and Don Zagier. Volumes of hyperbolic three-manifolds. *Topology*, 24(3):307–332, 1985.

[26] Grisha Perelman. The entropy formula for the Ricci flow and its geometric applications. *arXiv Mathematics e-prints*, page math/0211159, November 2002.

[27] Grisha Perelman. Finite extinction time for the solutions to the Ricci flow on certain three-manifolds. *arXiv Mathematics e-prints*, page math/0307245, July 2003.

[28] Grisha Perelman. Ricci flow with surgery on three-manifolds. *arXiv Mathematics e-prints*, page math/0303109, March 2003.

[29] Jessica S. Purcell. *Hyperbolic knot theory*, volume 209 of *Graduate Studies in Mathematics*. American Mathematical Society, Providence, RI, [2020] ©2020.

[30] John G. Ratcliffe. *Foundations of hyperbolic manifolds*, volume 149 of *Graduate Texts in Mathematics*. Springer, New York, second edition, 2006.

[31] Alan W. Reid. A note on trace-fields of Kleinian groups. *Bull. London Math. Soc.*, 22(4):349–352, 1990.

[32] Alan W. Reid. Arithmeticity of knot complements. *J. London Math. Soc. (2)*, 43(1):171–184, 1991.

[33] Alan W. Reid and Genevieve S. Walsh. Commensurability classes of 2-bridge knot complements. *Algebr. Geom. Topol.*, 8(2):1031–1057, 2008.

[34] Robert Riley. A quadratic parabolic group. *Math. Proc. Cambridge Philos. Soc.*, 77:281–288, 1975.

[35] Dale Rolfsen. *Knots and links*, volume 7 of *Mathematics Lecture Series*. Publish or Perish, Inc., Houston, TX, 1990. Corrected reprint of the 1976 original.

[36] Makoto Sakuma and Jeffrey Weeks. Examples of canonical decompositions of hyperbolic link complements. *Japan. J. Math. (N.S.)*, 21(2):393–439, 1995.

[37] R. L. E. Schwarzenberger. The 17 plane symmetry groups. *Math. Gaz.*, 58:123–131, 1974.

[38] Peter Scott. The geometries of 3-manifolds. *Bull. London Math. Soc.*, 15(5):401–487, 1983.

[39] W. P. Thurston. The geometry and topology of 3-manifolds. mimeographed lecture notes, 1979.

[40] William P. Thurston. Three-dimensional manifolds, Kleinian groups and hyperbolic geometry. *Bull. Amer. Math. Soc. (N.S.)*, 6(3):357–381, 1982.

[41] Robert J. Zimmer. *Ergodic theory and semisimple groups*, volume 81 of *Monographs in Mathematics*. Birkhäuser Verlag, Basel, 1984.